Oil & Natural Gas Technology

DOE Award No.: DE-FC26-04NT-42264

Final Report

Explorer-II: Wireless Self-powered Visual and NDE Robotic Inspection System for Live Gas Distribution Mains

Submitted by:
Carnegie Mellon University
5000 Forbes Avenue
Pittsburgh, PA 15213

Prepared for:
United States Department of Energy
National Energy Technology Laboratory

September 30th, 2008

Office of Fossil Energy

Final Report
submitted to
The Department of Energy (DoE)
National Energy Technology Laboratory (NETL)

under

Contract # DE-FC26-04-NT42264

for

FINAL REPORT

Reporting Period:
10-01-2004 to 09-30-2008

compiled as part of the project titled

Explorer-II:

Wireless Self-powered Visual and NDE Robotic Inspection System for Live Gas Distribution Mains

Document Number: REP-GOV-DOE-080930

Date of Submission:
September 30th, 2008

submitted by

Carnegie Mellon University
The Robotics Institute - REC
#10 on 40th Street
Pittsburgh, PA 15201
(412) 268-2000

Administrative Contact:
Susan Burkett
Technical Contact:
Hagen Schempf, Ph.D.

DISCLAIMER

This report was prepared as an account of work co-sponsored by an agency of the United States Government. Neither the United States Government nor any agency thereof, nor any of their employees, makes any warranty, express or implied, or assumes any legal liability or responsibility for the accuracy, completeness, or usefulness of the information, apparatus, product, or process disclosed, or represents that its use would not infringe privately owned rights. Reference herein to any specific commercial product, process, or service by trade name, trademark, manufacturer, or otherwise does not necessarily constitute or imply its endorsement, recommendation, or favoring by the United States Government or any agency thereof. The views and opinions of authors expressed herein do not necessarily state or reflect those of the United States Government or any agency thereof.

This report represents an identical account of work partially co-sponsored by the Northeast Gas Association (NGA). Neither NGA, members of NGA, nor any other party acting on behalf of any of them:

(a) makes any warranty or representation, express or implied, with respect to the accuracy, completeness, or usefulness of the information contained in this report, or that the use of any information, apparatus, method, or process disclosed in this report may not infringe privately owned rights; or

(b) assumes any liability with respect to the use of, or for damages resulting from the use of, any information, apparatus, method, or process disclosed in this report.

I. EXECUTIVE SUMMARY

Carnegie Mellon University (CMU) under contract from Department of Energy/National Energy Technology Laboratory (DoE/NETL) and co-funding from the Northeast Gas Association (NGA), has completed the overall system design, field-trial and Magnetic FLux Leakage (MFL) sensor evaluation program for the next-generation ***Explorer-II*** (X-II) live gas main Non-destructive Evaluation (NDE) and visual inspection robot platform. The design is based on the Explorer-I prototype which was built and field-tested under a prior (also DoE- and NGA co-funded) program, and served as the validation that self-powered robots under wireless control could access and navigate live natural gas distribution mains (see Figure I):

Figure I : Prototype of Explorer-I (X-I) and field-trial settings, to serve as basis for the completed X-II program

The X-II system design (~8 ft. and 66 lbs.) was heavily based on the X-I design, yet was substantially expanded to allow the addition of NDE sensor systems (while retaining its visual inspection capability), making it a modular system, and expanding its ability to operate at pressures up to 750 psig (high-pressure and unpiggable steel-pipe distribution mains). A new electronics architecture and on-board software kernel were added to again improve system performance. A locating sonde system was integrated to allow for absolute position-referencing during inspection (coupled with external differential GPS) and emergency-locating. The power system was upgraded to utilize lithium-based battery-cells for an increase in mission-time. The resulting robot-train system with CAD renderings of the individual modules, is depicted in Figure II:

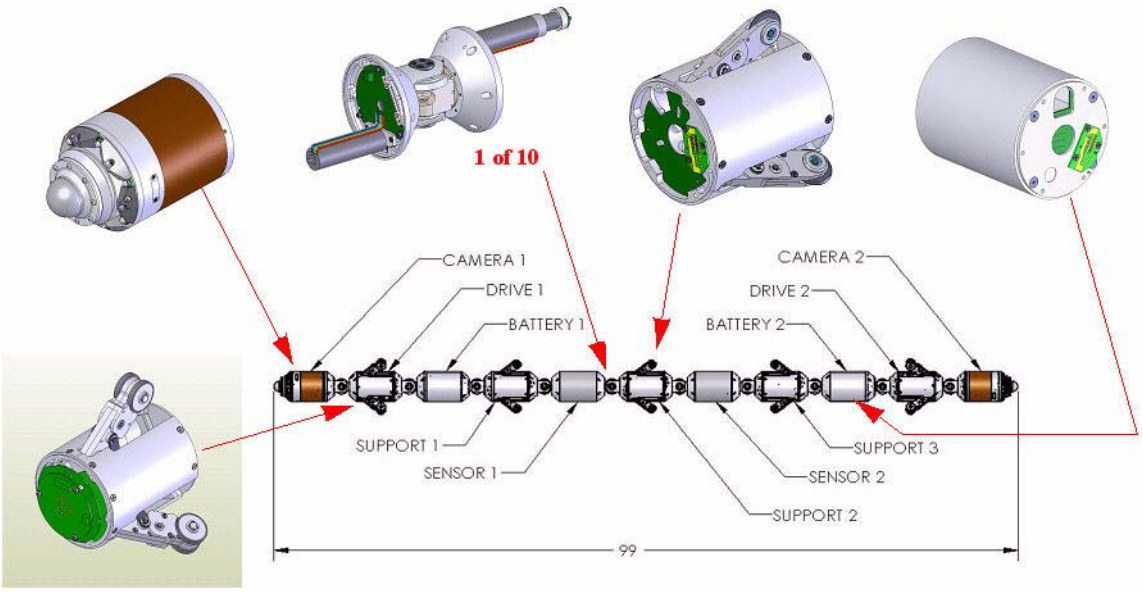

Figure II : Overall image of the Explorer-II (X-II) robot and its main modules.

The system architecture now relies on a dual set of end camera-modules to house the 32-bit processors (Single-Board Computer or SBC) as well as the imaging and wireless (off-board) and CAN-based (on-board) communication hardware and software systems (as well as the sonde-coil and -electronics). The drive-module (2 ea.) are still responsible for bracing (and centering) to drive in push/pull fashion the robot train into and through the pipes and obstacles. The steering modules and their arrangement, still allow the robot to configure itself to perform any-angle (up to 90 deg) turns in any orientation (incl. vertical), and enable the live launching and recovery of the system using custom fittings and a (to be developed) launch-chamber/-tube. The battery modules are used to power the system, by providing power to the robot's bus. The support modules perform the functions of centration for the rest of the train as well as odometry pickups using incremental encoding schemes. The electronics architecture is baed on a distributed (8-bit) microprocessor architecture (at least 1 in ea. module) communicating to a (one of two) 32-bit SBC, which manages all video-processing, posture and motion control as well as CAN and wireless communications. The operator controls the entire system from an off-board (laptop) controller, which is in constant wireless communication with the robot train in the pipe. The sensor modules collect data and forward it to the robot operator computer (via the CAN-wireless communications chain), who then transfers it to a dedicated NDE data-storage and post-processing computer for further (real-time or off-line) analysis.

The prototype robot system was built and tested indoors and outdoors, outfitted with a Remote-Field Eddy Current (RFEC) sensor integrated as its main NDE sensor modality. An angled launcher, allowing for live launching and retrieval, was also built to suit custom angled launch-fittings from TDW. The prototype vehicle and launcher systems are depicted in Figure III.

Figure III : Prototype X-II platform, launcher fitting, GUI and test-setup developed under the X-II program

The complete system, including the in-pipe robot train, launcher, integrated NDE-sensor and real-time video and control console and NDE-data collection and -processing and real-time display, were demonstrated to all sponsors prior to proceeding into final field-trials - the individual components and setting for said acceptance demonstration are depicted in Figure IV.

Figure IV : X-II system acceptance demonstration and evaluation prior to release for field-trial testing

The launcher-tube was also used to verify that the vehicle system is capable of operating in high-pressure environments, and is safely deployable using proper evacuating/purging techniques for operation in the potentially explosive natural gas environment. The test-setting and environment for safety-certification of the X-II robot platform and the launch and recovery procedures, is shown in Figure V.

Figure V : Safety testing of X-II platform and launch/recovery procedures in pressurized (750 psig) natural gas with a participating utility at a pumping station

Field-trials were successfully carried out in a live steel pipeline in Northwestern Pennsylvania. The robot was launched and recovered multiple times, travelling thousands of feet and communicating in real time with video and command-and-control (C&C) data under remote operator control from a laptop, with NDE sensor-data streaming to a second computer for storage, display and post-processing. Representative images of the activities and systems used in the week-long field-trial are depicted in Figure VI.

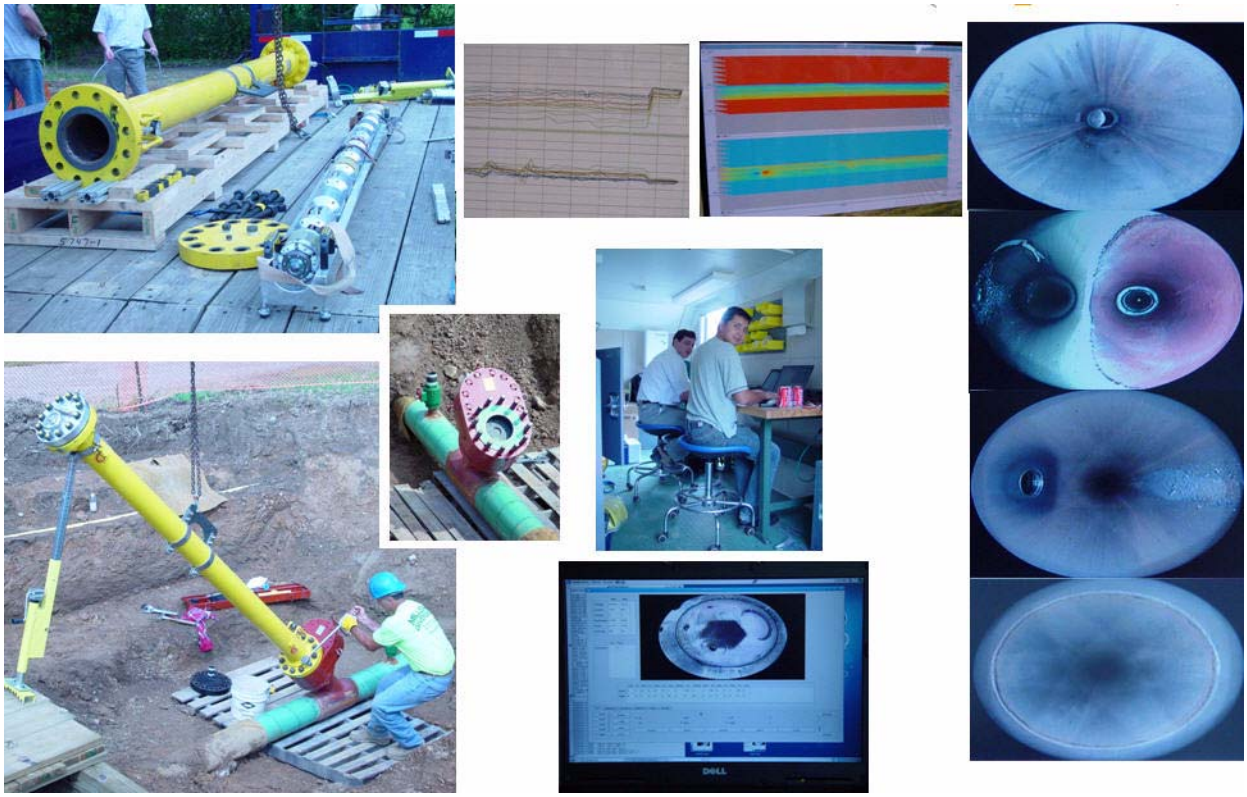

Figure VI : X-II field-trial evaluation in live natural gas pipeline in Northwestern Pennsylvania

CMU also evaluated the ability of the X-II design to be able to integrate an MFL sensor, by adding additional drive-/battery-/steering- and support-modules to extend the X-II train. The extended platform (see Figure VII), was upgraded in terms of its configuration and control software,

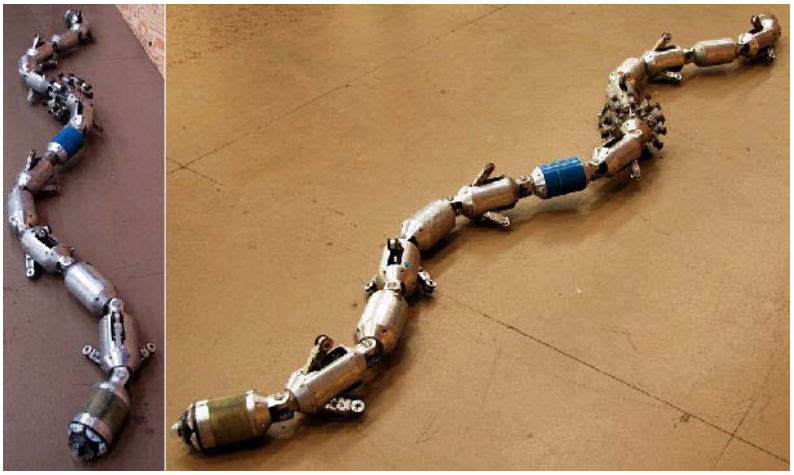

Figure VII : X-II prototype train in extended configuration with additional drive/battery/steering/support modules and MFL mock-up to allow for the deployment of an MFL sensor

GUI scripting and its ability to be field-configured with different sensor-types and less/more/ replacement modules. The MFL sensor prototype mock-up was built (see Figure VIII),

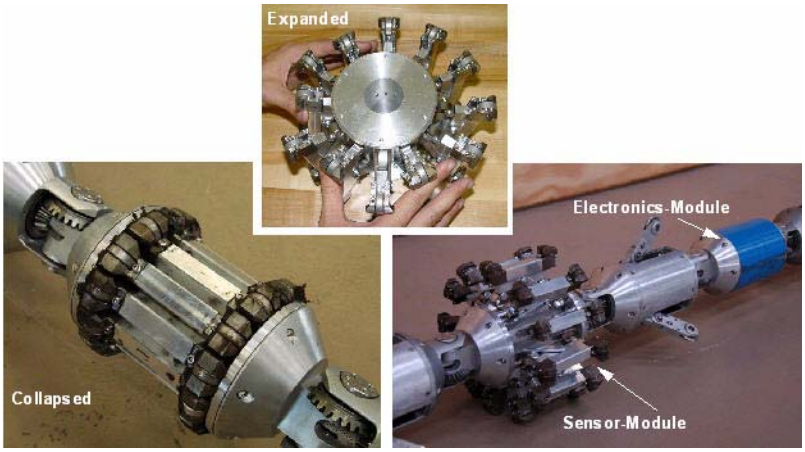

Figure VIII : MFL sensor mock-up as a stand-alone and integrated into the extended X-II robot train

and proven to successfully provide design guidelines for future commercial units in terms of the magnetic flux-field, magnetic shoe design (poles, etc.) as well as the articulation and suspension system(s). Most noticeably, it was proven that if key design guidelines are successfully implemented, that there will be no need for magnet-shunting (as is done in larger MFL sensors carried by the TIGRE robot system), and that 'magnetic anchoring' during obstacle traverse (launcher cutout, elbow and T-turns) should not be an issue.

The conclusions drawn from the results of this R&D and field-trial program are multi-fold. For one, it was shown that modular designs for NDE inspection robots are viable and that such systems can successfully and safely inspect live gas pipelines and provide user feedback in the form of video and wall-thickness data in real time. The design inherent to X-II allows for ready reconfiguration of the robot train and the modular exchange of sensor-types and field-replacement of faulty units, to provide a flexible and cost-effective tool for companies to offer inspection services to gas utilities to help them meet DoT-mandated inspection and safety regulations (transmission and distribution mains in the future). The prototype was shown to be rugged and capable of inspecting live mains, with single operator real-time control and communications of video/data, while operating safely during all phases of the deployment, including launching and recovery. Furthermore, CMU went so far as to show the X-II design to also be capable of alternate sensor-modality usage, proving that X-II is capable of handling an RFEC as well as an MFL sensor for NDE inspection of live gas pipelines.

Based on the results of the program, CMU has also developed recommendations for future activities related to both the platform, deployment and future sensor integration. The X-II platform, now that the technology has been licensed to NGA, should be reproduced for commercial application using improved materials and upgraded components only viable in larger scale production (gearing, etc.). Additional features and testing is also recommended to evaluate further real-world conditions encountered during field trials, including drive-upgrades, obstacle-types, antenna-housing, etc. It is presumed that a commercial inspection provider (sublicensee to NGA), would also improve on the execution and cleanliness of any field-installed fittings (launcher, weldolet, etc.), to further improve on the reliability of the system operation, which directly impacts the commercial bottomline. Future sensor developments for the MFL modality are recommended with clear guidelines for the design, testing and integration of the same provided herein.

TABLE OF CONTENTS

LIST OF FIGURES

LIST OF TABLES

LIST OF ACRONYMS

I. INTRODUCTION

1.0 Overview

1.1 Setting the Stage

Gas distribution utilities nationwide continually search for new and improved means to maintain, upgrade and efficiently operate their underground natural gas distribution and delivery system. To do so, these utilities use a substantial array of technologies to monitor, inspect, repair, rehabilitate and replace their underground mains. With these mains ageing rapidly, the biggest need in the industry is to perform in-situ inspection using a vast array of inspection sensors, so as to ascertain the state of the main prior to making decisions as to what maintenance steps to take. Performing such inspections under live conditions, with minimal excavation and without considerations as to pipe-internal layout, has been an unattainable goal with existing technologies. This goal is now becoming reality with Explorer.

1.2 Vision

The vision that utility companies have of how to maintain and manage their gas distribution network, is based mainly on their short- and long-term needs, and the state of technology and its potential to offer novel solutions in the near to mid future. The vision centers heavily on information of the state of the network, both in terms of structure (pipe-integrity, corrosion, cracks, leaks, etc.), as well as process properties (pressure, flow, humidity, etc.). A major part of the management plan relies on having sufficient high-density in-situ data of the pipe-internals, so as to be able to ascertain parameters such as leak-paths, water-intrusion, corrosion and cracking, etc. Such data is typically only available after a local inspection survey is performed, either visually via a camera, or through other pipe-structure sensor systems (MFL, UT, eddy-current, etc.). Based sometimes on this, but mostly on no concrete data, managers have to make a decision as to whether to repair, reline or replace (typically with plastic) their mains. Their need thus for comprehensive, detailed, real-time data as to the internal state of a line, would be immensely helpful to them to make a decision as to what course of action to take.

The vision that would make this need a reality, centers around a sensor-probe, capable of single and low-cost pipe-access and traverse of live gas mains of varying pipe-sizes, during 24 hour operations, without any human tending. This system would provide continuous data, initially purely visual, to a central control location, where data could be viewed live or off-line. Over time this (or more) unit(s) would have traversed most of the network and amassed a complete record of the system for operators to review. Such a system should ideally be capable of operating autonomously, rely on its own power and communicate its data back live for storage, viewing and post-processing.

Even though this might seem to be an unattainable vision if assumed to be required in its entirety, the utilities are eager to even utilize technology that extends their current inspection-cost, -time and -range, beyond what is currently in use within the field. Utilizing this concession, and surveying the technical state-of-the-art, it would thus seem that the need for systems capable of accessing the underground network from a single point and travelling on their own, untethered and without requiring topside tending but relaying data in real time, constitutes a major step towards realizing at least the up-front portion of the detailed vision.

1.3 Motivation

The use of untethered inspection systems is expected to radically improve gas line inspection and repair. More and more piping needs to be inspected due to the age of the existing urban gas-pipeline distribution network. Currently, little to no internal inspection is performed on a line that is known or assumed to be leaking in one or more locations, unless a major leak is found, warranting immediate action. The operating company has to make a decision as to whether to spot- or section-repair the line, reline it or completely dig it up and replace it - these decisions are typically made based on in-situ evidentiary data (maps, historical repairs, leak surveys, corrosion data, etc.) to help the operator make a safe and cost-effective decision. Due to logistical and financial considerations, repairs and line replacement is only performed in the case of a section of pipeline known to be leaking in multiple locations. Most of the time though, the decision to replace and/or reline an existing gasline is not always supported by physical evidence that the line to be replaced actually needs to be replaced along its entire length, rather than just in certain stretches or maybe even only in certain spots.

The overall assessment and repair process can thus be extremely costly without the ability to judge the most cost-effective repair approach. In the US alone, over $650 million per year is spent to repair leaks of all types. Giving the utilities the tools needed to make the decisions for cost-effective repair-method selection would have a drastic impact on their operations. Possible savings are hard to estimate, but if one assumes that up to 50% of the currently section-replaced/relined or completely replaced pipelines could have been repaired with the next-'cheapest' repair method, savings may be on the order of 25% to 50% over conventional replacement techniques, saving the gas industry tens of millions of dollars annually.

The ability to have continuous video footage of the condition within miles of piping of any distribution network, provides the information to the maintenance division of any utility to decide upon the location, repair-method and scheduling of repairs (if any). Such a system would be able to detect: (i) water infiltration, (ii) accumulated debris, (iii) abandoned and live service connections, (iv) locate main reducing fittings and offsets, (v) validate the location (counting joints and reset-measuring and adding pipe-lengths) and path of main (by use of a sonde), (vi) provide a visual evaluation of pipe-internal condition (primarily for corrosion-detection in cast-iron gas-mains).

The availability of such a long-range and easily deployable tool will greatly enhance the diagnostic and maintenance budgeting for existing gas operators (i.e. as a job-planning tool), with the potential to save large costs in terms of providing the data to make decisions as to which repair/ replacement method (spot/local/complete-line replacement/relining) to utilize. In addition, such a system could also be used as an emergency maintenance tool, by assisting in (i) the location of water infiltration into a low pressure gas main (thus eliminating or reducing the duration of costly main-outages), (ii) the location of cracked cast-iron gas mains and damaged steel mains, and (iii) the location of water pools and obstructions due to the presence of foreign material in the pipe.

Since the system is insensitive to which material the pipe is made of, it is actually applicable to 100% of the ferrous (excluding plastic pipe) pipeline market, in sizes bigger than 4 inches - this excludes only the feeds between these lines running under the streets/sidewalks and each individual residence (typically 1-2” ID). In the future, additional corrosion-detection and corrosion-loss measurement sensors could be added to give an even more detailed picture of the non-visible piping-condition within the network if so desired and technically and operationally feasible.

2.0 Relationship to Prior Work

CMU continued its in-pipe robotic system program through the development of Explorer-II (X-II), which is based on the previous Explorer (X-I) design [13]. ***X-II*** represents a leap in the capabilities of Explorer-I (see Figure IX for Explorer-I prototype image), which was also co-funded by DoE, NGA and NASA. The intent was to develop a generic platform capable of carrying a variety of interchangeable sensor modules, to perform self-powered wireless-controlled inspections of gas mains at up to transmission-line pressures (< 750 psig).

Figure IX : Explorer-I (X-I) system prototype served as a baseline platform and design for the enhanced Explorer-II (X-II) platform design and prototype

The principle of operation is similar to that of Explorer-I: launch the system in a no-blow condition into a live gas main using OEM fittings with a custom launcher (see Figure X for pre-prototype fitting-access hardware with staged locomotor), traverse a set distance of pipe while performing NDE and visual cataloging measurements - all of it under self-powered and remote teleoperated wireless control from the surface utilizing (an) in-pipe antenna(e).

The design being implemented, as detailed by the design and prototype details provided in this final report, relies on the powered wheel-arms, capable of deploying into varied-diameter pipe sizes, with turning and climbing capabilities (primarily for launch and recovery). In order to accommodate visual as well as visual-plus-NDE inspection modalities, the modules were designed for in-the-field modular exchange (mechanical and electrical interconnections), with additional modules to provide power (battery-module) and self-centering ability (support-module).

Figure X : X-I prototype in vertical launcher used for medium-pressure (< 125 psig) deployments

Note that due to the nature of launching and inspection in varied pipe-diameters, the sensor-module will require articulation for the sensor-head(s), indicating an involved sensor-module design and increased controller and data-acquisition complexity.

II. BACKGROUND

US gas companies spend over $300 million annually detecting and repairing gas leaks in urban and suburban settings. The current approach is one of above ground leak detection and pinpointing, followed by excavation, repair and restoration. The major cost incurred is typically that of digging and restoring the excavation site. If a tool was available that could provide real-time and long-term inspection capabilities in order to allow for rapid and pre-planned inspections and repairs wherever needed, national utilities would be able to better manage and allocate their operating and repair budgets, potentially reducing costly emergency repairs.

1.0 Prior Art

In the area of in-pipe inspection systems, there are many examples of prior-art robotic systems for use in underground piping (transmission-pipeline pigs excluded). Most of them however are focussed on water- and sewer-lines, and meant for inspection, repair and rehabilitation (Pearpoint, Beaver, KA-TE, etc.). As such, they are mostly tethered, utilizing cameras and specialized tooling, etc. (see Figure XI).

Figure XI : Prior art in-pipe inspection systems

Three of the more notable exceptions are the autonomous *Kurt I* system from GMD (Germany) used for sewer monitoring (not commercial nor hardened), the (albeit tethered) cast-iron pipe joint-sealing robot (*CISBOT*; ConEd), which is deployed through a bolt-on fitting and injects anaerobic

sealant into the leaking jute-stuffed joint, and *GRISLEE (GTI, CMU & MTI)*, a coiled-tubing tether deployed inspection, marking and in-situ spot-repair system. These systems are shown in Figure XII:

Figure XII : Tethered gasmain (CISBOT - right; GRISLEE - bottom) and untethered autonomous (Kurt I) robots developed to date by industry and researchers

A more in-detail treatise on the prior art in this and related fields, can be found in Section IX. APPENDICES on page 26.

2.0 Explorer-I System Background

The Northeast Gas Association (NGA) and its NYSEARCH research-arm, DoE (current) and NASA (past), funded a program at Carnegie Mellon University's (CMU) Robotics Institute (RI) to develop an advanced remote and robotic inspection system, capable of multi-mile long-duration travel inside live gas mains for in-situ assessment and pipe-network cataloging.

Under this program, CMU has developed ***Explorer***, a real-time remotely controllable, modular visual inspection robot system for the in-situ inspection and imaging of live 6- and 8-inch diameter distribution gas-mains (see Figure XIII for an image of the prototype in a test network setting). ***Explorer*** is capable of locomoting through straight pipe segments and sharp bends, elbows, Ys and Ts, using a combination of its on-board driving-arms and steering-joints. The system is sealed and purged (and thus can safely operate in natural gas environments) and capable of negotiating wet and partially-filled (water, mud, etc.) pipes.

Figure XIII : Explorer-I (X-I) - Pipe Inspection System

The architecture of the robot is simple and symmetric. A 7-element articulated body-design houses a mirror-image arrangement of locomotion, battery-, support and computing electronics in purged and pressurized housings (see Figure XIV). Each module is connected to the next through an articulated joint; the joints connecting the locomotor-module(s) to the rest of the 'train', are pitch-roll joints, while the remaining (four) joints are only pitch-joints. This allows the locomotor-modules to articulate in any direction, with subsequent rotation-plane alignment of the remaining joints to enact a turn in any plane. The system is capable of multi-mile travel inside pipes using custom on-board battery-packs, which can use any desired chemistry depending on desired range and cost.

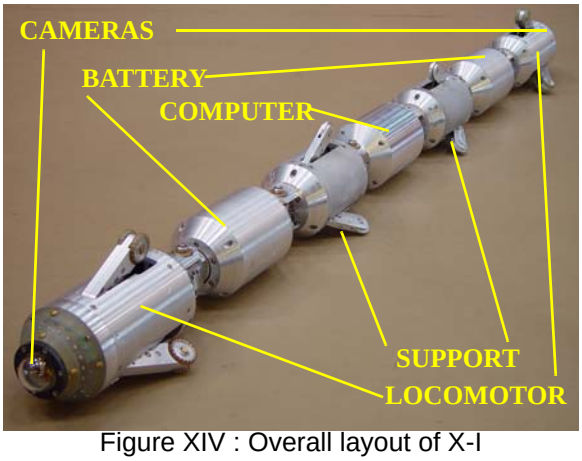

Figure XIV : Overall layout of X-I

The locomotor-module contains the forward-looking mini fish-eye camera, -lens and -lighting elements, as well as dual drive actuators. These actuators allow for the deployment/retraction of a set of three ‘arms’, at the end of which are a set of custom-molded wheels used for pulling/pushing the train through the pipe; sustained speeds of up to 4 in/sec. are achievable. The battery-module(s) contain custom battery packs to allow for a full 10-hour mission with all systems consuming maximum power. The support modules also have extendable ‘arms’, but the wheels at their ends are passive and are used for accurate displacement-encoding. The computer-module contains the custom-packaged 32-bit low-power (< 1 Watt) processor and support hardware for control and communications, as well as power-conversion and -conditioning.

3.0 Field-trial Results for Explorer-I (X-I)

Besides continual functionality-testing in a purposes-built pipe network at CMU, the *Explorer* robot system was fielded into a live 8-inch low-pressure cast-iron main (operated by Consolidated Edison of New York) installed in 1893. An excavation was made and a one-sided IPSCO-fitting and a purgeable/pressurizeable see-thru launch-tube installed. The robot was launched and recovered multiple times during the multi-day test-period (see Figure XVI on page 8).

Figure XV : Live-access launching hardware systems

On average, over a typical 6-hr. (cautious) deployment period (incl. launching and retrieval), the system was able to travel more than 3,000 linear feet, and made several T-turns in the main. Wireless range was the limiting factor, reducing the total maximum distance travel the system is capable of on a single battery charge. Features in the pipe such as taps (mapped and unmapped ones) with associated filings and debris (incl. beer-bottle caps from the original installation-days) were clearly visible (see Figure XVII on page 8). Overall the performance of the system clearly met every criteria it had been designed for, representing a milestone in both the robotics and gas-utility industry. This was the first successful deployment of a fully tetherless and wireless remote-control inspection tool into a live underground gas distribution main.

Figure XVI : Live CI (low-pressure) New York Field-Trial setting

Figure XVII : Operator Interface & visible features (tap, bottle-caps, wheel-tracks)

The third field deployment of *Explorer-I* was held in a live 8-inch high pressure main located in the SUNY campus in Brockport, New York, in the service territory of Rochester Gas & Electric, where a 1979-vintage 8-in 60 psig main was to be inspected (see Figure XVIII).

Figure XVIII : *Explorer-I* live deployment in a medium-pressure steel main

The main ran westward from the point where the launcher was installed for more than half-a-mile straight, while in the other directions about 75 feet away there were two back-to-back elbows (one 90-degree and one 70-degree) followed by a long straight segment. The field trial lasted a total of 4 days, during which four launching and four retrieval procedures were performed. The robot covered a total distance in excess of 6,000 feet. During its travel in the pipe it performed eight successful elbow turns. It traveled more than 1/2 mile in one direction from a single hole in one run, leaving ample battery-power. A number of mapped and unmapped features (Ts and even an unmapped main connection) were verified. The high pressure fitting and launcher worked well, with launching and recovery shown to take 30 minutes each, including all safety steps. Installation of the launcher and antenna was shown to take 30 and 15 minutes respectively. The operator interface was demonstrated to be user friendly and a remote display for monitoring and evaluation was also determined to be a viable option.

Many system improvements were suggested as part of these initial field-trials, such as: (a) manual control of the system during launching and retrieval, as well as obstacle-handling (still requires a good deal of training and finesse), despite the pre-computed scripts and on-board automation), and (b) improved lighting for mid-range (1 - 3 feet ahead) distances in front of the robot.

III. SYSTEM DESIGN

This section addresses the design of the current X-II system, based on the requirements and system specifications, as well as the mechanical/electrical and software elements of the robot train and the interface requirements for the sensor-module(s).

1.0 Requirements and Specifications

1.1 Performance Requirements

The X-II performance requirements are similar yet have been expanded over those for the X-I from the previous development. Primarily, the system was now required to operate at pressures up to 750 psig and be able to carry different NDE sensors. All other requirements were similar to those formulated for X-I, yet were fine-tuned based on the experimental and field-trial results from the previous phase. The complete high-level list of requirements can be summarized as follows (see Table 1-1):

- Access live pipe through angled fitting (not vertical)
- Operate in 6 to/or 8 inch CI/ST pipe in horizontal, sloped, elbowed, T'ed & vertical sections
- Operate at up to 750 psig and (minimal) flows
- Integrate an NDE-sensor from TBD; Specify generic electro-mechanical & software interface
- Minimize length and weight
- Operate on sequential daily shift(s)
- Inspect at speed (4 in/sec) & range (2,500 ft.+) while minimizing down-/recharge-time
- Provide wireless interface and GUI similar to X-I, including NDE-data transfer port

Table 1-1 : High-level performance requirements listing

These requirements were then used to drive the generation of the system specifications, which are detailed in the next section.

1.2 Robot Train Specifications

Based on the performance requirements agreed-to by all parties, an evolving set of system specifications was drafted, which in final form was summarized and is listed in Table 1-2 on page 11.

- **Physical**
  - Length: 99” (~ 8.3’)
  - Weight: 63.5#
  - # Modules: 11
  - Drive (2), Support (3), Battery (2), Camera (2), Sensor (2)
  - Interconnecting Steering-Modules: 10 (Roll=2; Pitch=10)
  - Power: Li-Polymer Custom packs with safety charge/discharge circuitry
  - Electronics: Multi-8-bit processors with dual 32-bit embedded CPUs
  - Bus: Internal Power- & CAN (2.0b) Data-Bus; External WB-link
  - NDE-Sensor: RFEC or UT
  - Feedback: Odometer, Angle, Inclination, Position (Sonde)
- **Operational**
  - Endurance/Range: 3,500 ft. RT; 6,000 ft. one-way over 8 hrs.
  - Launcher: Weld-on angled pipe-section(s) w. valve and full-bore cutout
  - Comms & Control: Wireless & GUI w. joystick
  - Real-time video & multi-mode NDE data-transfer
  - Safety: Open electronics-/battery-volumes with evacuation/purge in launcher

Table 1-2 : Robot-train system specifications listing

These specifications are reflective of the design-parameters for the X-II system design, which are detailed on a by-module basis in the next major section.

2.0 Prototype Tractor Design

2.1 Overview

The overall design layout can be summarized to state that the complete system is expected to weigh around 65 pounds and measure about 8 feet in length. The overall assembly of the system and its individual modules is as depicted in Figure XIX:

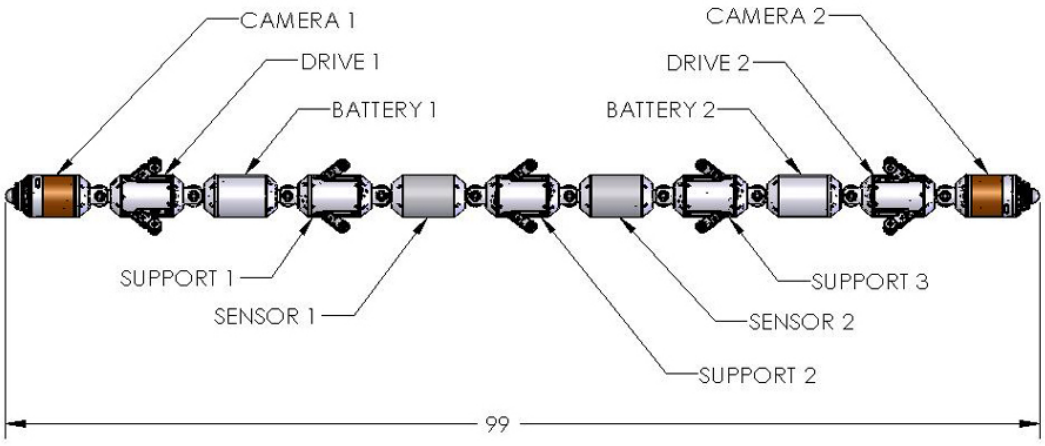

Figure XIX : Overall X-II robot train layout with module identification

Notice the symmetry as well as the retention of drive- and support-modules. The camera-modules

are now separate and distinct, and given that X-II has provision for 2 separate sensor-modules, required the addition of an extra support-module.

The weight-breakdown is as shown in Table 1-3.

Qty	Module	Weight	Total
2	Camera	3.3 Lb	6.6 Lb
2	Drive	4.4 Lb	8.8 Lb
2	Battery	4.6 Lb	9.2 Lb
3	Support	2.9 Lb	8.7 Lb
2	Sensor	3.5 Lb	7.0 Lb
2	Steering (pitch only)	2.1 Lb	4.2 Lb
6	Steering (pitch only, high torque)	2.2 Lb	13.2 Lb
2	Steering (pitch & roll)	2.9 Lb	5.8 Lb
		Total Weight	63.5 Lb

Table 1-3 : X-II weight breakdown (design-estimate)

2.2 Reconfigurability due to Modularity

The modularity of X-II allows for multiple configurations in the field. This feature is advantageous, when an inspection might require a first live video-run to make sure the line is able to be inspected (blockages, etc.), by using a smaller, lighter and faster to deploy/retrieve camera-platform, or when sensors that are smaller and require longer range allowing for more battery modules need to be deployed. Figure XX shows such different potential configurations field-personnel have the option to deploy.

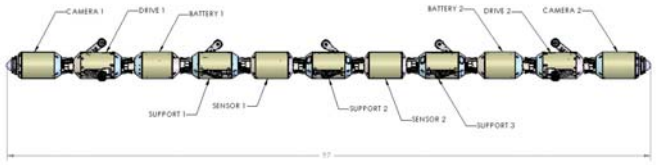

• X-II with 2 Sensor Modules

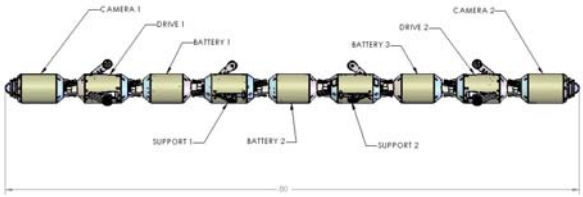

• X-II w/out Sensor Mod.s
Long Range Inspect.

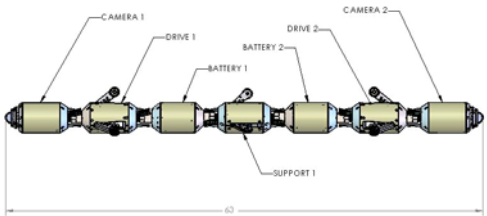

• X-II without Sensor Modules
Base Range Inspector

Figure XX : Modularity of X-II affords the use of different configurations in the field

The main elements of the design, including the separate modules, as well as the electronics and software for this system, are detailed in the sub-sections below.

2.3 Camera-Module Design

2.3.1 Overall Assembly

The nose- or camera-module was designed to integrate computing, wireless communication, video-sensing and lighting and emergency-locator systems into a single monolithic module. The resulting design is shown in Figure XXI.

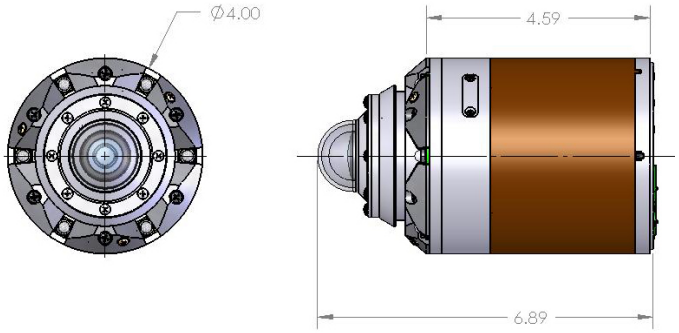

Figure XXI : Overall nose-module CAD image

The main elements, including the modular inter-connect board, the locating-sonde coil and the forward LEDs, charging contacts and the fisheye camera-dome, are all visible in Figure XXII.

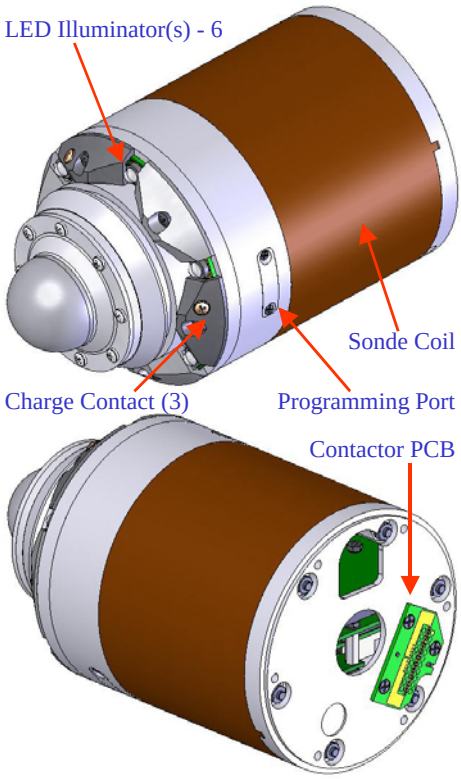

Figure XXII : Overall multi-angle view of the forward/rearward nose- or camera-module

This module contains the main elements of the imaging (fisheye lens) and video system (640 x 480 NTSC analog imager) as well as the digitization hardware (MPEG4 hardware compression with 15 to 30 frames/sec.) and illumination system (6 white LEDs under PWM control). Both of the 32-bit SBCs reside in this module, running all the high-level planning, control and communication tasks. The SBC is interfaced to the remainder of the robot over a common power and CAN-base communication bus. Supported buses include SPI, CAN, USB and 802.3-based wired ethernet for inter-SBC-communications. In addition, the custom wireless antenna and RF control and power-stages are integrated into the nose-cone and electronics.

2.3.2 Locating Sonde

An additional requirement in X-II was the capability to locate the system underground during operations and in case of system failure requiring extrication. This method had to be based on an absolute measurement and left only the use of electro-magnetics (EM) based sonde system as an option. After a survey and review of existing systems was carried out, a miniaturized sonde system was commissioned from an OEM, allowing the electronics to be tailored to the space available in the front camera-module, and embedding a novel doughnut-coil into the external structural element of the module. The individual components (in CAD) as well as the COTS antenna and locating equipment are shown in Figure XXIII on page 14:

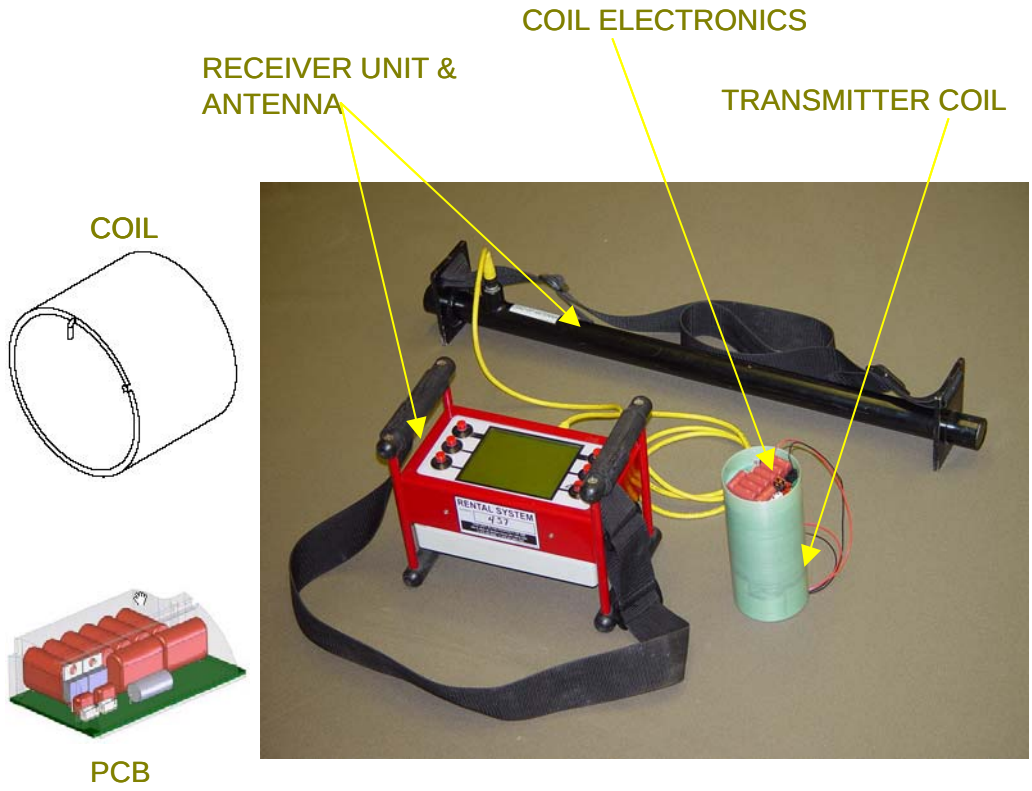

Figure XXIII : Locating sonde coil and PCB design, as well as COTS locating equipment

The sonde design was tested with a standard coil in a buried pipe and found to result in 30 to 40 feet on-/off- pipe-axis detection ranges utilizing the proper combination of gain/sensitivity and operating mode.

2.4 Steering-Module Design

The steering module design is similar to that used in X-I, but with marked electronics improvements including the exclusive us of DC servomotors as an example. The steering joint includes the ability to roll and pitch any so-designed joint using motors and custom gearing and control electronics. The setup of the joints is based on allowing the ends of the train to roll, while all other joints only pitch - implying that as in X-I, roll-joints are only located at the end of the train. Notice that the design is very similar to that from X-I, in that a motor with a gear-train either drives a set of bevel gears (pitch) or a ring-gear (roll) - absolute position is detected using multi-turn potentiometers or a geared potentiometer (roll). Unlike in X-I, these modules are designed to be mechanically and electrically exchangeable through the use of a common mechanical mounting interface, and a pass-through power- and communication bus (see connector blocks in Figure XXIV). All common control and communications electronics are contained on separate PCBs on either side of the conical frustums of this module.

The common steering joint design resulting from this design effort is shown in Figure XXIV on page 15.

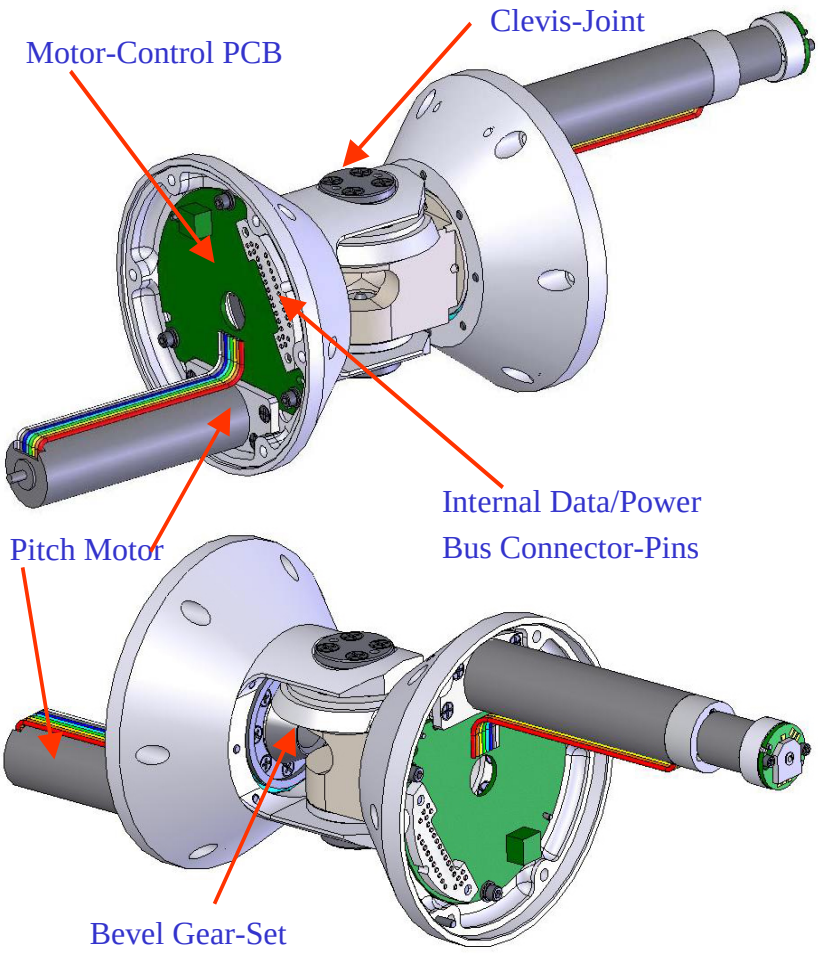

Figure XXIV : Multiple end-views of the roll- and pitch steering module

2.5 Drive-Module Design

The drive-module, just like with X-I, includes the ability to center and brace the module inside the pipe and allow for the driving of the legged arm-wheels. All the required mechanical elements and electrical PCBs and subsystems were integrated into a final design reflected by the design shown in Figure XXV.

The module utilizes the same ball-screw custom-gear design to expand/collapse a set of three drive-legs, where each drive-leg contains a gear-train to rotate a set of drive-wheels. The legs brace the module against the internal pipe-walls and by driving the wheel pulls/pushes the robot-train through the pipe.

A three-bar linkage with a compliant link allows for a suspension and variable pipe-diameter accommodation. In addition, this design now also includes a set of strain-gauge beams to measure the contact forces so as to ensure proper contact-force within allowable tolerances for the mechanism and the pipe-walls. A set of custom PCBs provide the motor-control and multi-drop CAN bus interface for the module; a custom interconnect PCB allows for power and data signals to be passed along the spine-bus of the robot train.

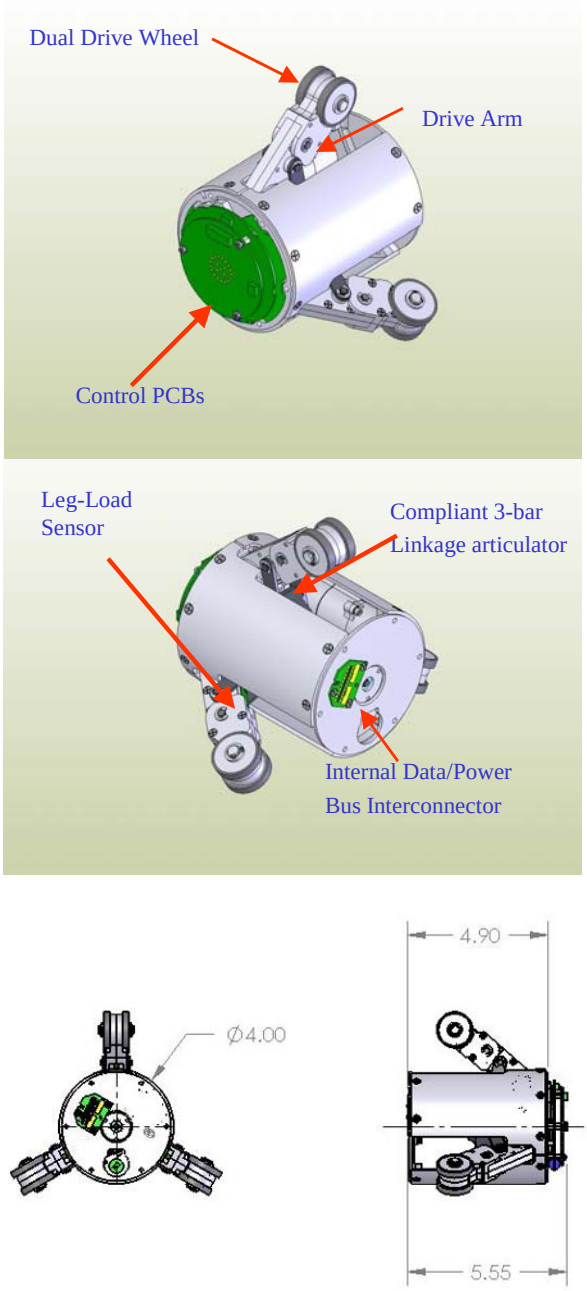

Figure XXV : Multi-view CAD rendering of drive-module design

2.6 Support-Module Design

The support module was designed to provide the necessary centration and passive encoding for position determination. An overall design assembly view is shown in Figure XXVI.

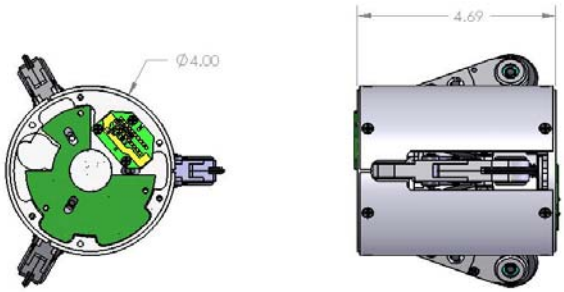

Figure XXVI : Support Module Overview Design

The design is similar to the drive-module in terms of the leg articulation, but in this case the arm is devoid of any geartrain, and only holds a passive wheel. Said wheel has multiple magnets on its circumference face which are monitored by hall-sensors to detect direction and extent of rotation. This principle allows for the odometry feature necessary for NDE data-encoding.

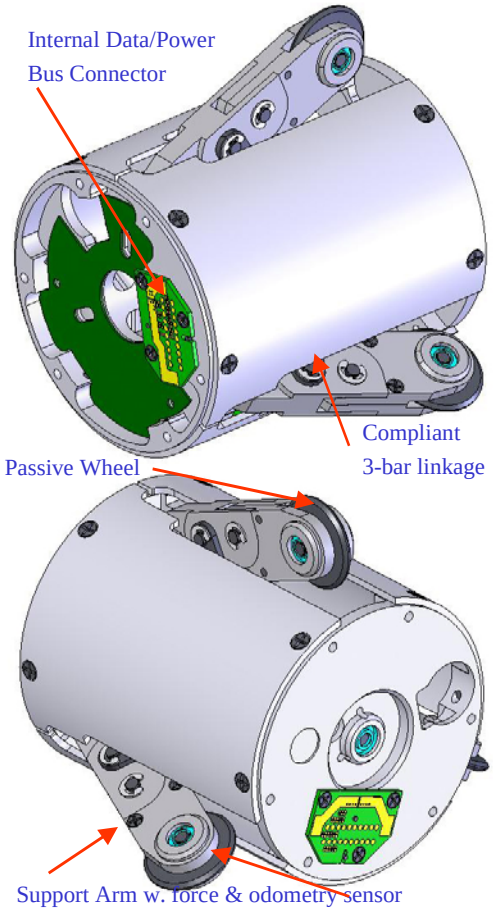

Figure XXVII : Multi-view CAD rendering of the support-module

All local control is enabled through a custom PCB with motor controls and CAN bus interface. Preloading of the arms (up to 80 lbs) is monitored through a set of strain gauge beams in each leg. All power and data is passed through and connected to adjacent modules through the use of a custom interconnect PCB.

2.7 Battery-Module Design

The battery module is sized akin to all other modules in the train (see inset image in Figure XXVIII).

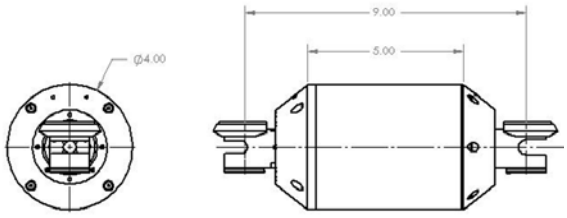

Figure XXVIII : Overall design of the battery module

The battery-module design revolves around the use of lithium-based battery-cells combined into packs to provide 26 VDC and up to 15 A-hrs. of energy to the robot for a meaningful 8-hr. mission. The battery-module contains safety electronics and

voltage converters to allow monitoring of charge and discharge. An image of the layout of the module is shown in Figure XXIX.

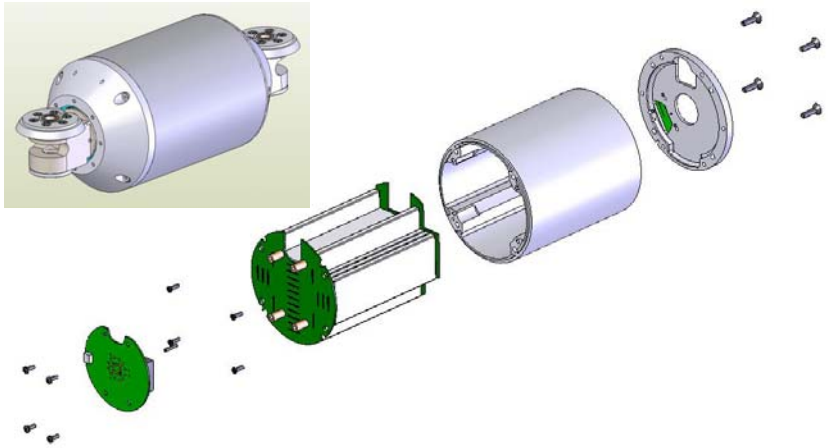

Figure XXIX : Exploded and rendered views of the battery module design

All control (charge and discharge), power-conversion and bus-interconnects (both power and data over CAN-bus) are provided though custom-designed PCBs and interconnects to allow the interfacing of adjacent modules.

2.8 Electronics Architecture Design

The electronics architecture for the platform and overall system was also developed and can be summarized as shown in Figure XXX below:

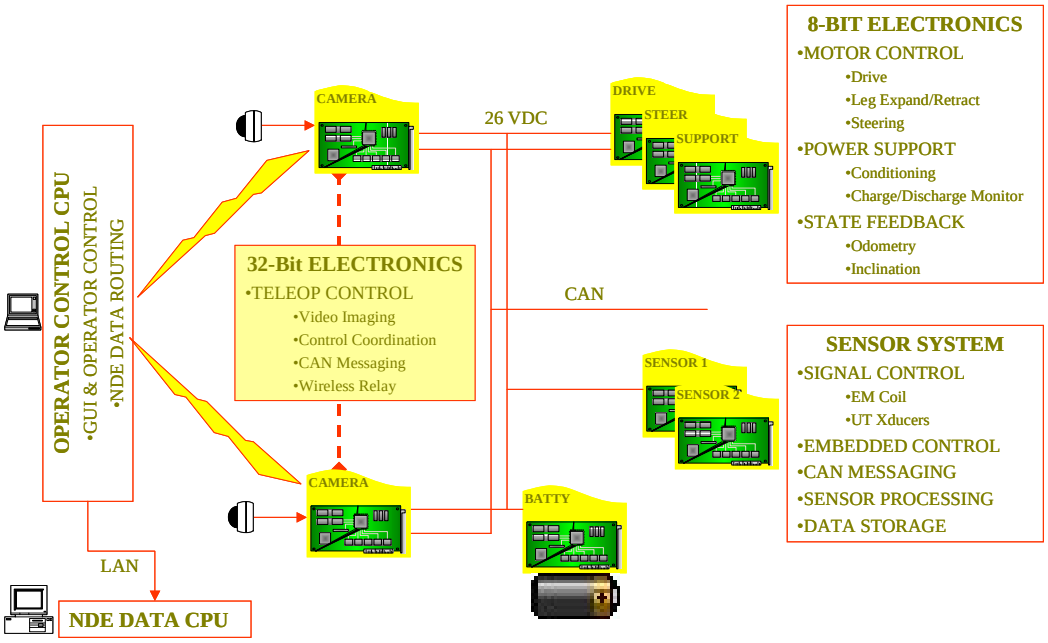

Figure XXX : Overall Explorer-II (X-II) electronics architecture

The design calls for an off-board Operator Control CPU, which communicates over custom antenna hardware using customized wireless protocols to the robot unit's camera-module 32-bit SBC. All commands and data are passed in this fashion to and from the operator. The robot's SBC handles all control and communications and video digitization tasks, as well as CAN-bus and power-bus control. A set of distributed 8-bit multiprocessors on different modules, provide all the power-support and motor-control as well as feedback and control message parsing. A set of (up to 2) sensor modules are responsible for all data-collection and -relaying over the CAN bus. All NDE-data is passed over the CAN bus to the 32-bit SBC, and over the wireless to the control CPU at the operator, from where it is forwarded over ethernet to the data-collection and -processing computer.

2.9 Software Architecture Design

The software design mirrors the distributed multi-processor electronics architecture. Each module's 8-bit processor is in charge of control and messaging running separate tasks via real-time kernel. The 32-bit SBC coordinates them all, running tasks that are responsible for video-processing, posture-control, communications, safety- and health-management and off-board communications and other house-keeping tasks. The 32-bit SBC operates under a reduced-build Linux Operating System (OS), and due to its duplication (one in each camera-module) allows for splitting of the video-processing and communication tasks at will, based on a wired-ethernet peer-to-peer setup with a master/slave configuration (also implies system redundancy and antenna-gain diversity communications). A graphical rendition of the software architecture for the platform and overall system are shown in Figure XXXI on page 20.

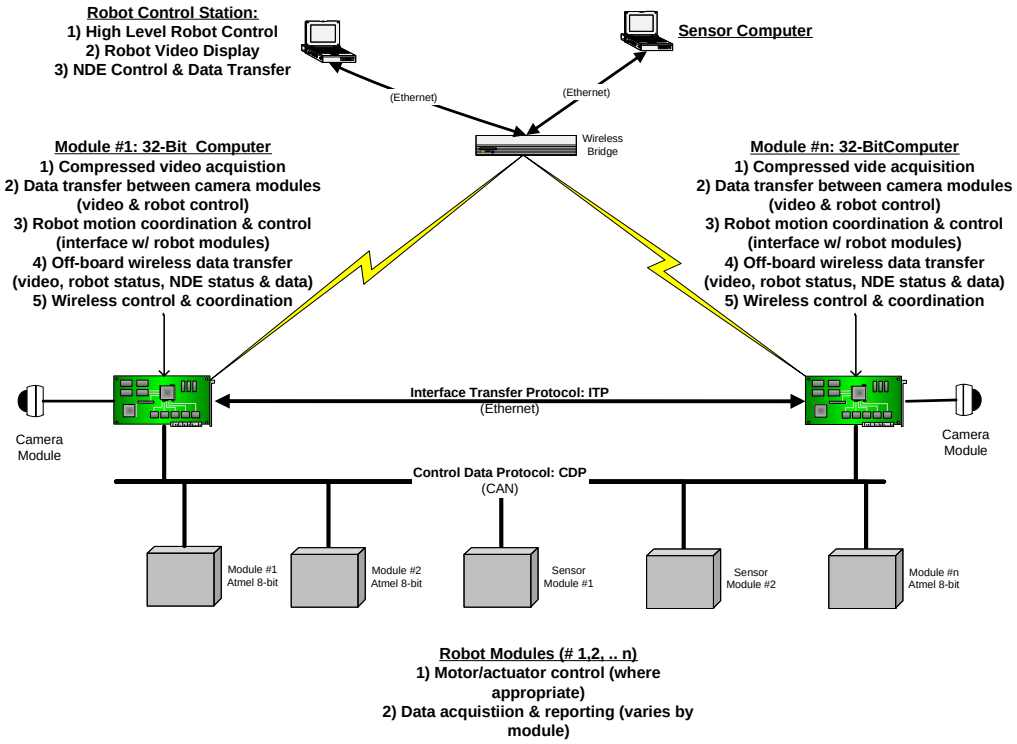

Figure XXXI : X-II robot platform software architecture

3.0 Launcher & Antenna Design

4.0 Launcher Design

The use of an angled launcher design was preferable (for reasons of deployment-speed, technical feasibility, operational and design simplicity and reduced development and capital costs), rather than vertical (as was used in X-I). The launcher design is based on the selection of OEM fittings, which were supplied by TDW (see Figure XXXIII). A preliminary layout of the launcher-setup is shown in the inset image of Figure XXXII.

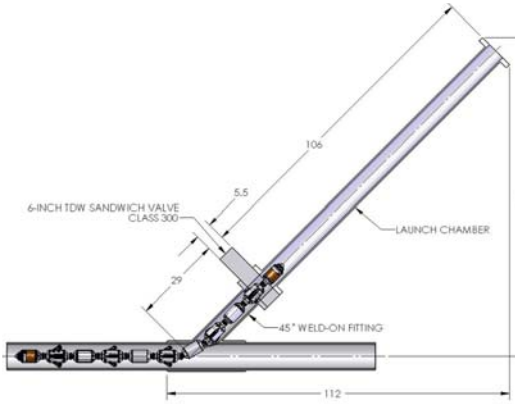

Figure XXXII : Angled launcher configuration for Explorer-II

The important characteristics relate to the distances between the pipe-centerline and the individual fitting-, valve- and launch-tube flanges. the launch-tube has to be long enough to accommodate the robot and some additional length to allow for checkout (sensor, driving, etc.) before the system is launched. The angled fitting has to provide sufficient length to allow the robot to center in the fitting and provide driving traction to allow the robot to span the gate-valve body as no traction will be possible inside the valve. These requirements are all reflected in the layout design shown in Figure XXXII.

Figure XXXIII : TDW's custom-made angled weld-on fitting and shell (left) and gate-valve (right)

The launcher design was completed based on the selection of the TDW fittings and valve (Figure XXXIII). The launcher consisted of two main parts: launch-tube and endcap. The launch-tube was fabricated out of thick-wall drawn steel-pipe with 600# flanges welded onto it on both ends. The tube was certified for ultimate pressure of 1,000 psig. A manual valve and pressure-gauge at the valve-end of the tube allow for purging operations with nitrogen, and monitoring of line and purge/vent pressures during launch and recovery.

The endcap was made of aluminum in a multi-stage design. The need to retain and communicate with the robot while in the angled (re-launch) position, required the integration of a holding mechanism and a remote antenna. The retention approach used a hand-crank with a worm-gear cam actuator to engage/retract tongs into the recess of the RF-transparent nose at the ends of the robot. This allows the robot to be held in the pipe

(fully vertically, including under full traction force of the drive-modules) for safe holding and transportation. A conically shaped plastic frustum on the underside of the endcap ensures the robot self-centers itself when it is retrieved as it drives into the launch-tube and into the endcap. so as to ensure that the latching mechanism grabs the front-nose of the train properly. This is to avoid a run-away after the motors are turned off, when gravity forces might pull the robot down the tube towards the gate-valve.

The same antenna that is designed into the nose-modules(s) of the robot train is also embedded on the underside of the endcap, with a coaxial penetrator atop the endcap, to allow for communications with the robot when it is in the launcher (and even to a few hundred feet in the pie as long as the gate-valve remains open). A quick-disconnect check-valved fitting and pressure-gauged-release (silenced) allow for the controlled feeding and release of nitrogen (for purging) and natural gas (during venting).

A layout of the launcher-design is shown in Figure XXXIV, including the endcap.

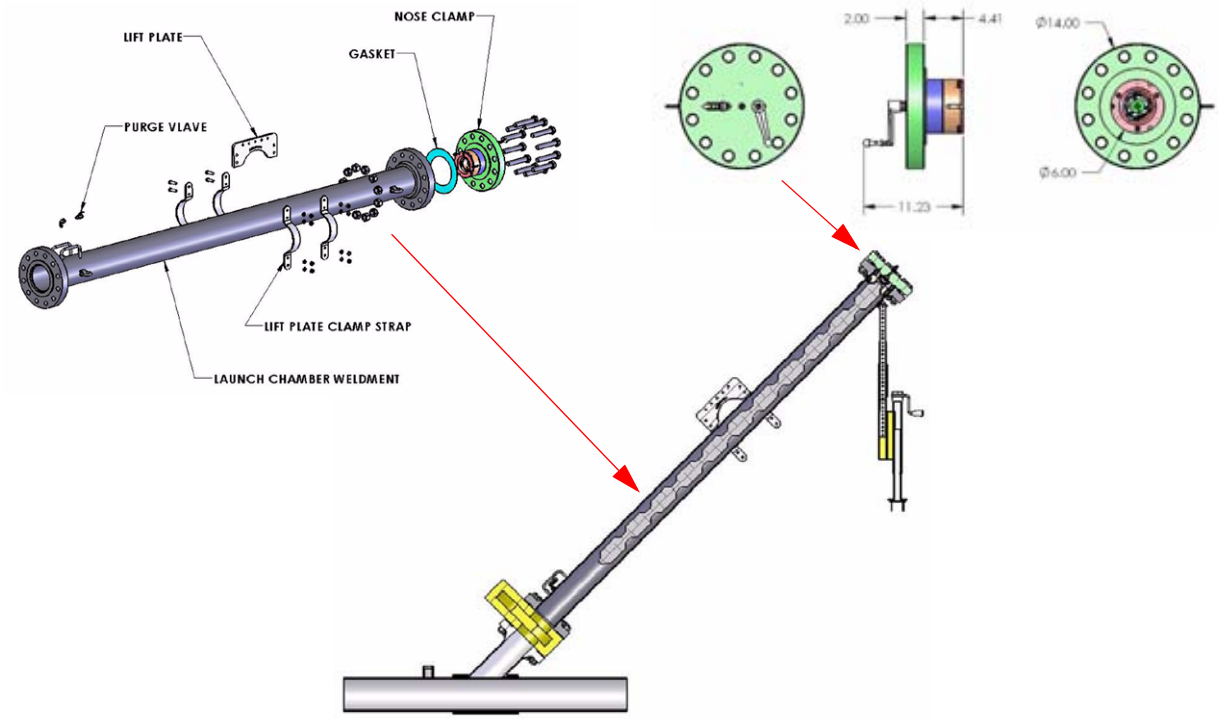

Figure XXXIV : Launcher tube and endcap design for live-pipe access for Explorer-II

4.1 Remote Antenna

In order to allow long-distance travel and operations after the gate-valve is closed on the launcher, a separate no-blow installable antenna is required. CMU used, with minimal adaptations, a design developed for a similar application, by Automatika, Inc. (ATK) in Pittsburgh, PA, which was itself funded by the Northeast Gas Association (NGA) under separate cover for multiple gas pipeline sensing, communication and robotics projects.

The design utilizes a custom-developed (ATK-proprietary) PCB-based antennae, housed in a fitting with sealed coaxial penetration and adapted with a rotary alignment feature, capable of using a standard 1.75-inch weldolet (TDW-provided) to penetrate into the internal void of the pipe. This allows the pipe to be used as a waveguide between the robot nose-module antenna and this fixed antenna. An environmental sealing cap allows the system to operate in any weather, including full submersion should it rain during deployments and the excavation fill with water.

An image depicting the location, main components and assembled views, with cross-sections is shown in Figure XXXV.

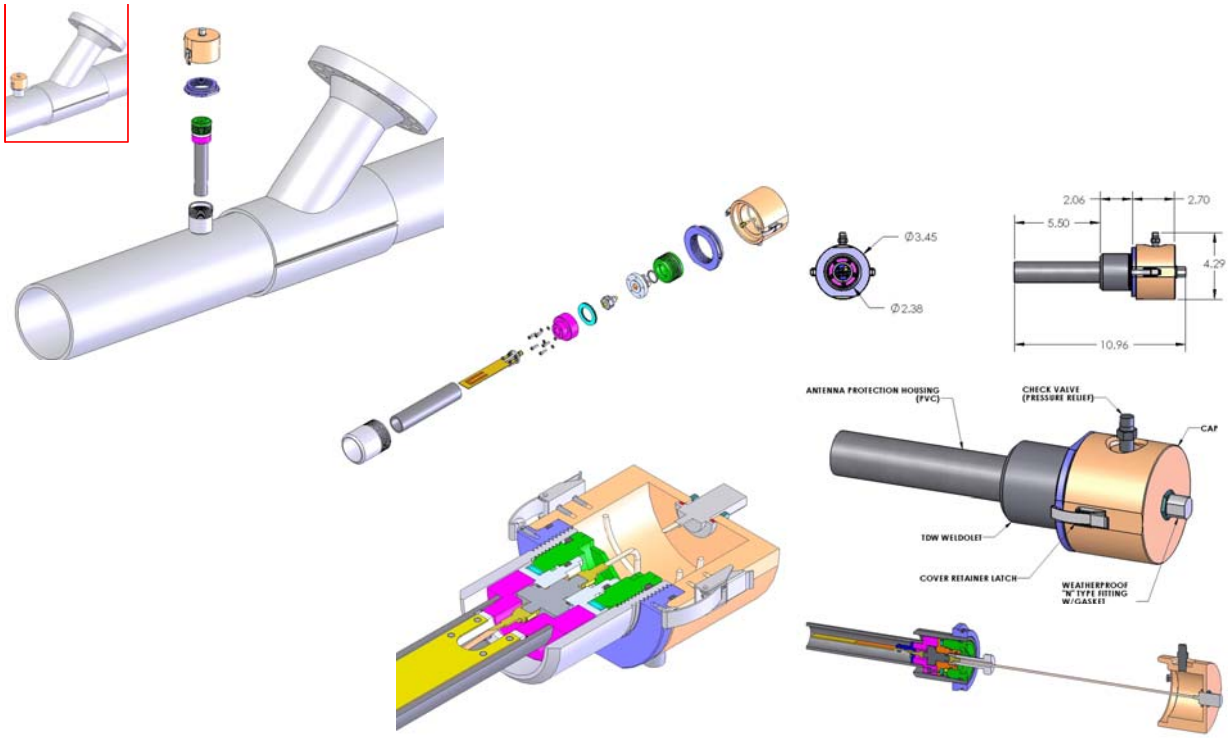

Figure XXXV : Configuration, layout and exploded/cross-section views of the ATK-proprietary stationary in-line communications antenna

5.0 Alternate Sensor Train Configuration

The default sensor configuration originally considered for X-II, implied the use of a Remote-Field-Eddy-Current (RFEC) sensor, under development by SwRI under DoT funding [33][34][35][36]. However, the interfaces between the robot-train and the sensor-module(s) was defined generically to allow for other future sensor integration. Towards that end, CMU was chartered to evaluate platform performance and impact for such a potential future sensor design, if an MFL sensor was to be used. An MFL is substantially different sensor, in that it uses permanent magnets to magnetically saturate the pipe-wall, and co-located hall-effect sensors to measure magnetic field-variations (from fully saturated) present due to wall-loss, cracks, etc.[1].

The main difference between an RFEC and MFL sensor, is that the latter had magnetic drag that causes hysteretic losses, requiring higher drag-forces, which impact traction drive designs. Furthermore, the constraints of live launching and elbow/obstacle navigation with essentially a high-strength magnet-loaded module had to be understood not only from the energetic standpoint (energy required for a particular mission), but also whether magnetic attraction forces required the use of any kind of shunting device(s) used for larger in-pipe exploration robots [37]. This is of interest to robot- and sensor-designers, as it impacts required tractive and steering forces not only during launching/recovery operations[2], but also during turning operations in elbows or miters, where the magnets can get ‘stuck’ to the pipe, impeding progress due to effective ‘magnetic anchoring’.

CMU engaged in an effort to gather data to better bound the design space should an MFL sensor-development be undertaken by a third party. Towards that end CMU focussed on several main engineering efforts:

1. developing a longer train X-II by adding two more drive- and battery-modules (plus support and steering modules) so as to expand the platform design to allow for carrying an MFL sensor, and
2. expansion and generalization of the configuration, communication, distributed control and planning software for n-module robot-train configurations, and
3. development of a mock-up MFL sensor with permanent magnets to simulate the drag and tractive forces of an MFL carried by the higher-traction platform.

This section addresses the configuration and design efforts related to these efforts, with prototype descriptions and experimental data provided later in the document.

5.1 Configuration Design

As mentioned previously, CMU expanded its platform train (or tractor) design to include the additional modules for drive, steering, battery and steering, to effectively lengthen the platform so as to

-provide additional drive modules for increased traction-force
-add additional energy capacity to the train to not impact mission duration, and

1. Dents and ovalities are unlikely to be detected. Depending on what kind of MFL is used (axial or transverse), only certain directional cracks can be detected presuming sufficient resolution. See references
2. so as to not effectively get magnetically ‘anchored’ to the edge of the pipe-wall

-provide the needed support- and steering-modules to retain the platforms ability to locomote and steer through pipes, obstacles and launchers, and
-retain the dual-sensor module configuration with one module reserved for sensor-electronics and the second module reserved for the MFL sensor itself.

The final design-configuration for the X-II-MFL robot train, is shown in Figure XXXVI (the red modules are identified as the two MFL-related modules without regard to the actual design of the modules themselves):

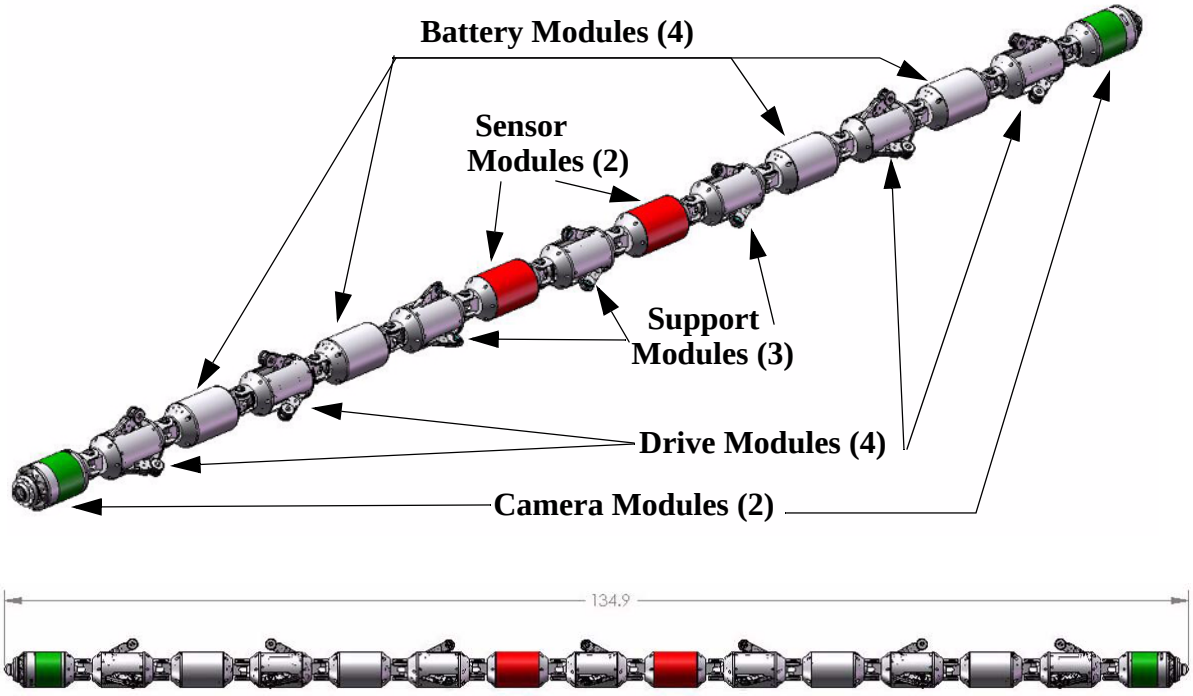

Figure XXXVI : Configuration of the X-II platform configured with additional drive, support, steering and battery modules for deployment of an MFL sensor-module

The length of the robot has increased, but it has retained its modularity and overall configuration to allow it to be launched/retrieved as well as make sharp 90-degree bends in elbows and mitered pipes. The design of the modules required for lengthening the train are identical to those described earlier, with the only difference lying in their arrangement and orientation (compare Figure XXXVI with Figure XIX on page 11).

5.2 Mock MFL Sensor[1]

The mock MFL sensor module was designed around the same-sized sensor-module dimensions provided for the RFEC (size, weight, etc.). The implementation was carried out with simplicity and cost-effectiveness in mind, allowing for manual reconfiguration in between data collection runs, rather than remotely-controlled actuation. Towards that end, the MFL was designed around a maximal number of magnetic shoes arrayed around the cylindrical sensor body, utilizing

1. CMU subcontracted the MFL mock-up design to allow it to concentrate on the platform train and the generic software effort.

suspensioned shoes with internal magnets, to allow the system to compensate for sag and obstacle turning, while keeping the shoes circumferentially and axially constrained (free to move radially only). The sensor-shoes could be arranged in a collapsed (bolt-on) configuration, or spring-loaded expanded configuration with swing-arms, as depicted in Figure XXXVII:

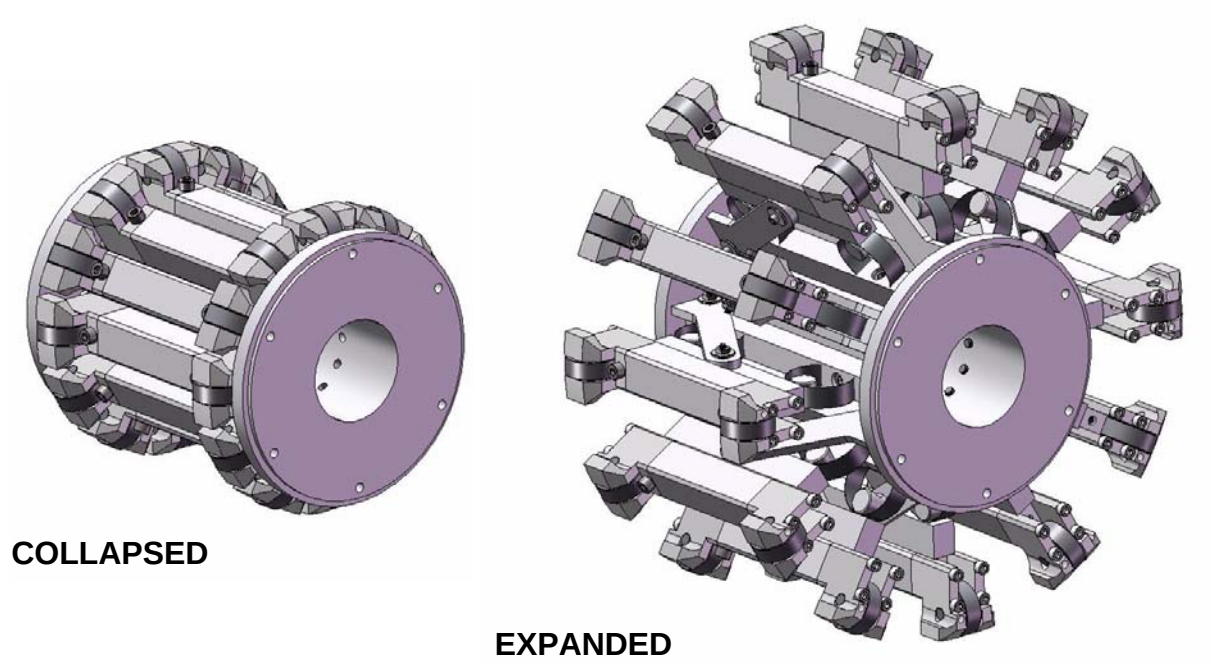

Figure XXXVII : Mock-up MFL sensor module with magnet-shoes in the collapsed and expanded configurations

The magnet-shoe itself, as depicted in Figure XXXVII,

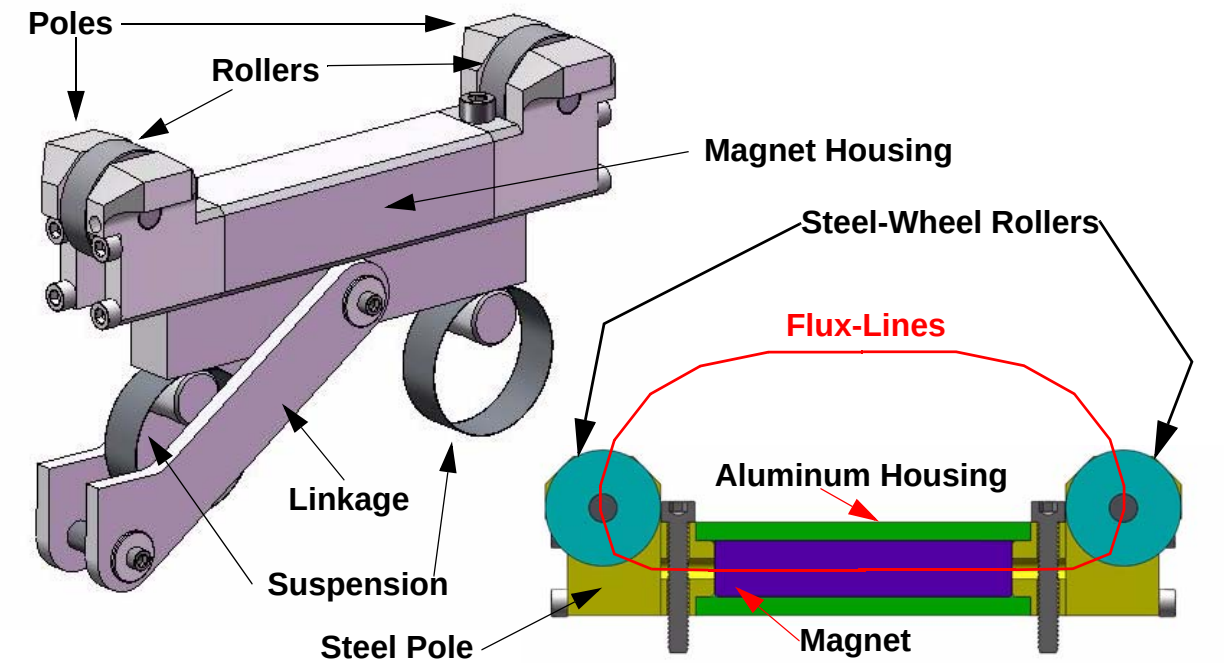

Figure XXXVIII : Design of the magnet-shoe, depicting the magnetic circuit generated by the magnet and

steel poles and rollers, as well as the housing and the suspension

shows how the permanent magnet's poles were coupled with steel poles and a stand-off steel knife-edged roller-wheel, to guarantee stand-off distance and rolling-friction during sensing operations. The interesting part of this design is that the bulk (> 90%) magnetic flux-lines are forced to flow from the N-S poles of the magnet through the steel-couplings into the poles and then across the air-gap into the pipe-wall, with a guaranteed stand-off enforced by the roller-wheels. This is a critical feature that will be shown to be important during launch/recovery and turning maneuvers, where the space between the poles may/will come into contact with pipe-edges. Maintaining minimal flux in that area (area along the structure connecting the two poles with roller-wheels) will reduce the magnetic attraction forces and guarantee passage of that location with minimal effort and without chance of getting magnetically anchored. The magnet shoe is housed in a non-ferrous structure (aluminum) and allowed to move radially by two pinned swing-arms and supported by a coiled leaf-spring to allow for 'flotation' across uneven internal pipe surfaces.

Even though the magnets were selected to be the strongest available (Neodymium-Iron-Boron), CMU does not claim that its mock MFL design was analyzed with FEA methods, nor is CMU an MFL design-specialty house. However, we believe that the design guidelines reflected in this shoe-design are critical to the success of the MFL being carried in/through/out of a live pipe successfully. the details of the actual magnet material, magnetization levels and FEA of the shoe-design are left to third-party sensor-developers with the know-how to guarantee full pipe-wall saturation with the MFL-generated magnetic field.

5.3 Software Architecture Upgrade and Expansion

5.3.1 Overview

Explorer II (X-II) has been designed from the ground up as a highly modular platform (see Figure XXXIX). High modularity of its mechanical, electrical and software systems make X-II a versatile and extremely flexible platform for gas pipeline exploration. This section describes the software features that enable quick changes in configuration (addition of 4 modules to the standard configuration to accommodate the MFL-sensor), without any loss in functionality.

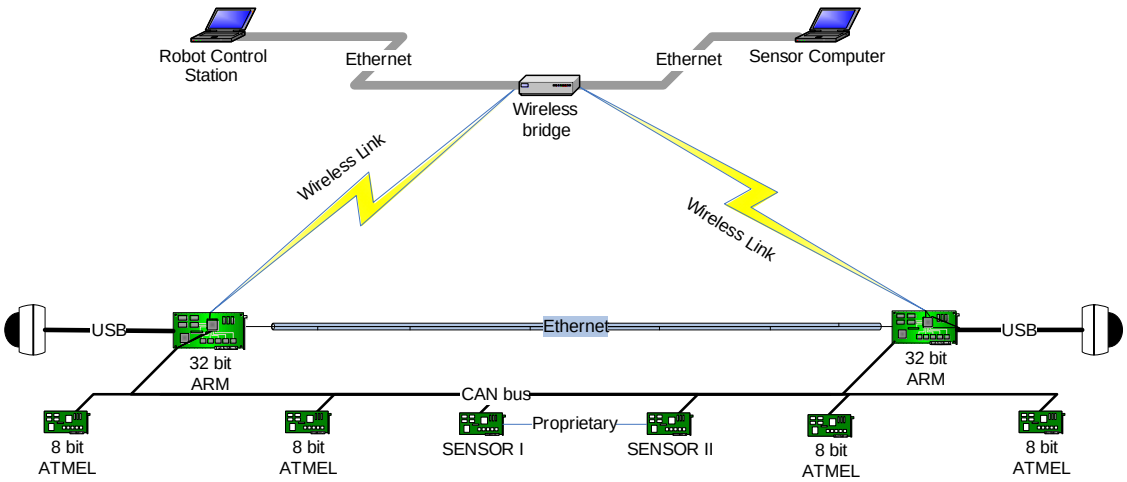

Figure XXXIX : Modular electrical and power/data bus design of X-II

Mechanically, the robot can be built up from 4 types of modules -- cylindrical enclosures with

electronics and function-specific peripherals -- and from steering units, which connect the main modules and enable the robot's actuation.Figure XL depicts the modularity by showing the process of removing a set of modules from the train and allowing its reconnection into a shortened functioning train. This is advantageous for transportation, field-repair as well as re-configuration for alternate sensor configurations.

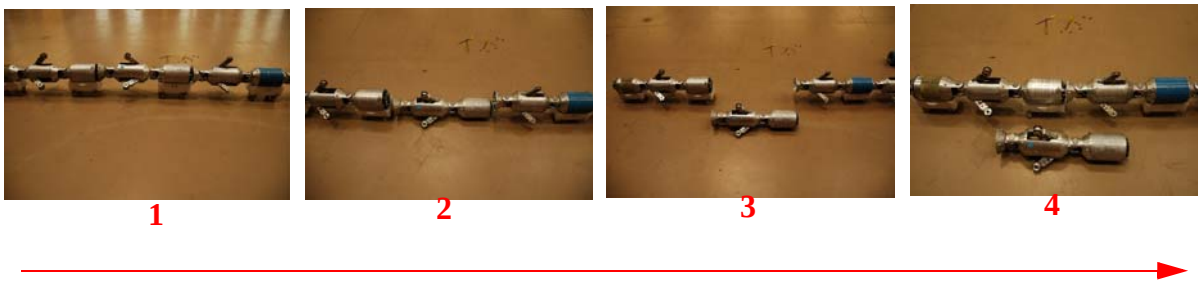

Figure XL : Example sequence of modular element removal to add/remove/replace a single drive-, dual steering- and single battery-module

5.3.2 Software Modularity Upgrade

5.3.2.1 Electromechanical control tier (ATMELs)

Explorer's mechanical systems are controlled by ATMEL microcontrollers distributed across the robot, one per module. There are 4 types of ATMEL-based control boards in direct correspondence to the 4 module types. Each board type has been designed to work with a particular set of sensors and actuators. It is convenient to combine sensors and actuators that are used to perform the same function into functional blocks. Table 1-4 maps the functional blocks to module types that implement them.

	Camera (Nose)	Drive	Battery	Support
Steer	1	1	0	2
Roll	0	0	1	0
Drive	0	1	0	0
Deploy	0	1	0	1
Odometry	0	0	0	1
Battery	0	0	1	0
Camera	1	0	0	0
Lights	1	0	0	0
Power	1	0	0	0
Sonde	1	0	0	0

Table 1-4 : Functional block diagram for robot train configuration

In the microcontroller software each of these functional blocks has a corresponding thread that accomplishes IO tasks. These threads are activated for each functional block with a set of parameters stored in the microcontroller's EEPROM. This allows the same code to be installed on all 4 types of boards, with EEPROM settings regulating which threads are activated. For instance, support modules have 2 ***Steer*** functional blocks, therefore 2 steering threads will be activated with different parameters (which motors are being controlled, potentiometer limit and center values, PID coefficients, etc).

Roll and ***Steer*** functional groups on the electromechanical level are identically implemented; therefore they're controlled by the same thread. However, their functions from the perspective of

robot control are decidedly different; hence they are considered distinct functional blocks.

In the fully detailed CAN protocol documentation, these functional blocks correspond directly to "functionalities". The CAN protocol allows addressing these functional blocks directly; in other words, the higher level controller does not need to know which microprocessor controls which actuator – this sort of routing is taken care of by the protocol. Each functional block in the robot must be assigned a unique number ("instance"), which will be specified in the EEPROM of the relevant microcontroller. It is natural to assign these numbers in order of functional block's placement sequence in the train. For example, the message addressed to 2nd ***Lights*** functional block will always be received by the 2nd (and last) camera module, no matter how many modules are in between.

5.3.2.2 Effects of configuration change

The difference between the extended (X-II with the MFL sensor; X-II-MFL) and the standard configuration (X-II with the RFEC sensor; X-II) is that additional two pairs of ***Battery*** and ***Drive*** modules are inserted between ***Battery*** and ***Support*** modules in the standard configuration (see Figure XL on page 28). The additional ***Battery*** modules are equipped with steering instead of roll motors, and the ***Drive*** modules are oriented in the opposite direction of their neighbors. Table 1-5 and Table 1-6 detail the sequence and configuration for each of these trains, with **xM** representing a **M**odule type and **x** representing possible modules, namely **C**amera, **D**rive, **B**attery and **S**upport).

	CM	DM	BM	SM	-	SM	-	SM	BM	DM	CM	Total
Steer	1	1	0	2	0	2	0	2	0	1	1	10
Roll	0	0	1	0	0	0	0	0	1	0	0	2
Deploy	0	1	0	1	0	1	0	1	0	1	0	5
Battery	0	0	1	0	0	0	0	0	1	0	0	2

Table 1-5 : Standard X-II configuration table (RFEC sensor)

	CM	DM	BM	DM	BM	SM	-	SM	-	SM	BM	DM	BM	DM	CM	Total
Steer	1	1	0	1	1	2	0	2	0	2	1	1	0	1	1	14
Roll	0	0	1	0	0	0	0	0	0	0	0	0	1	0	0	2
Deploy	0	1	0	1	0	1	0	1	0	1	0	1	0	1	0	7
Battery	0	0	1	0	1	0	0	0	0	0	1	0	1	0	0	4

Table 1-6 : Extended X-II-MFL configuration (for MFL-sensor)

Supposing additional modules have already been properly calibrated, then all that must be done to make the new configuration operational, involves the following:

1. Reassign instance numbers across the modules.
2. Ensure that drive and steering orientation settings are properly set.

5.3.2.3 Configuration files

EEPROM configuration files have extension .eep and are compiled from usual C-files that only contain global initialized variables and no executable code (detailed in ATMEL software documentation). For instance, Figure XLI on page 30 details a fragment of the front drive module's

CAN configuration block:

```
{   // steer joint
    .mode = 1, // REC
    .id = CDP_CAN_ID(CDP_F_STEER, CDP_I_STEER_DM1, CDP_V_DESIRED, 0),
    .mask = CDP_CAN_MASK,
    .cni = CNI_IN_STEER,
},
{   // drive
    .mode = 1, // REC
    .id = CDP_CAN_ID(CDP_F_DRIVE, CDP_I_DRIVE_DM1, CDP_V_DESIRED, 0),
    .mask = CDP_CAN_MASK,
    .cni = CNI_IN_DRIVE,
},
{   // deploy
    .mode = 1, // REC
   .id = CDP_CAN_ID(CDP_F_DEPLOY, CDP_I_DEPLOY_DM1, CDP_V_DESIRED, 0),
    .mask = CDP_CAN_MASK,
    .cni = CNI_IN_DEPLOY,
},
```

Figure XLI : Software initialization block structure

The three (3) structure initialization blocks in Figure XLI configure three (3) CAN mailboxes to receive Steer, Drive and Deploy commands. The .id field encodes the header of the CAN message the mailbox is configured to receive. Configuration is entirely symbolic – nothing is hard-coded. CDP_F_* constants denote functionality and CDP_V_DESIRED denotes the type of the message (in this case to set the functionality's output). These constants are defined by the protocol and are set in cdp.h, which does not change unless the protocol changes. CDP_I_* constants resolve to the instance number (unique id of a given functionality in the robot) and are set in a different file – map.h – which may vary from configuration to configuration.

In the developed notation, modules are referred to by a two-letter abbreviation (CM, DM, BM or SM) with a number corresponding to its position in the train. Since the original robot (X-II) had a pair (2) of every module type, the number was either 1 or 2. Later, another support module in the middle was added to accommodate two payload modules. That support came to be known as SMA. When four (4) more modules were added in the transition to the expanded X-II-MFL configuration, instead of renaming all the modules, the added modules were given the same number as their closest neighbors with an R on the end (e.g. BM1R or DM2R). Thus the standard configuration has the following instances defined (see Table 1-7):

Steer	Drive	Deploy	Battery

enum {
CDP_I_STEER_CM1,
CDP_I_STEER_DM1,
CDP_I_STEER_SM1F,
CDP_I_STEER_SM1R,
CDP_I_STEER_SMAF,
CDP_I_STEER_SMAR,
CDP_I_STEER_SM2F,
CDP_I_STEER_SM2R,
CDP_I_STEER_DM2,
CDP_I_STEER_CM2,
CDP_I_STEER_N,
};
	enum {
	CDP_I_DRIVE_DM1,
	CDP_I_DRIVE_DM2,
	CDP_I_DRIVE_N,
	};
		enum {
		CDP_I_DEPLOY_DM1,
		CDP_I_DEPLOY_SM1,
		CDP_I_DEPLOY_SMA,
		CDP_I_DEPLOY_SM2,
		CDP_I_DEPLOY_DM2,
		CDP_I_DEPLOY_N,
		};
			enum {
			CDP_I_BATTERY_BM1,
			CDP_I_BATTERY_BM2,
			CDP_I_BATTERY_N,
			};

Table 1-7 : Instance configuration for standard X-II configuration

And the expanded configuration is defined as follows, with additional constants marked in ***RED*** - see Table 1-8).

Steer	Drive	Deploy	Battery

enum {
CDP_I_STEER_CM1,
CDP_I_STEER_DM1,
CDP_I_STEER_DM1R,
CDP_I_STEER_BM1R,
CDP_I_STEER_SM1F,
CDP_I_STEER_SM1R,
CDP_I_STEER_SMAF,
CDP_I_STEER_SMAR,
CDP_I_STEER_SM2F,
CDP_I_STEER_SM2R,
CDP_I_STEER_BM2R,
CDP_I_STEER_DM2R,
CDP_I_STEER_DM2,
CDP_I_STEER_CM2,
CDP_I_STEER_N,
};
	enum {
	CDP_I_DRIVE_DM1,
	CDP_I_DRIVE_DM1R,
	CDP_I_DRIVE_DM2R,
	CDP_I_DRIVE_DM2,
	CDP_I_DRIVE_N,
	};
		enum {
		CDP_I_DEPLOY_DM1,
		CDP_I_DEPLOY_DM1R,
		CDP_I_DEPLOY_SM1,
		CDP_I_DEPLOY_SMA,
		CDP_I_DEPLOY_SM2,
		CDP_I_DEPLOY_DM2R,
		CDP_I_DEPLOY_DM2,
		CDP_I_DEPLOY_N,
		};
			enum {
			CDP_I_BATTERY_BM1,
			CDP_I_BATTERY_BM1R,
			CDP_I_BATTERY_BM2R,
			CDP_I_BATTERY_BM2,
			CDP_I_BATTERY_N,
			};

Table 1-8 : Instance configuration for extended X-II-MFL configuration

Notice that inserting these constants automatically increments those below the inserted one, reassigning the instance numbers. All that is required now is recompiling all the .eep files and updating EEPROM on the modules. CDP_I_*_N constants resolve to the total number of instances for each functionality in the configuration. This information is not useful in the ATMEL code, but is central to the use of the GUI.

5.3.2.4 GUI

GUI software must visibly reflect configuration change. The following components would be affected by change from the standard (X-II) to the expanded (X-II-MFL) configuration:

Controls

1. *Steer (4 additional)*
2. *Deploy (2 additional)*
3. *Drive (2 additional)*

Data reporting:

1. *Battery stats*
2. *Position and PWM signal for Steer and Deploy*

Actual controls – sliders and dials – are generated dynamically according to the number of functional blocks of each type. Currently, these numbers are defined at compile-time (CDP_I_*_N constants) and so changes in configuration requires a recompile. The same is true for Battery and Position/PWM statistics available to the user. Sliders and dials themselves are assigned numeric

IDs in incrementing order, in direct correspondence to instance numbers of the functional blocks on the robot. Once they are instantiated, changes in their state are automatically translated into commands and sent to the robot. No additional code is needed to support the change in configuration.

5.3.2.5 SBC

SBC software acts as an interpreter/retranslator between control tier and the GUI. Reported and desired states of the robot are stored in a shared-memory table, the size of which is initialized according to the CDP_I_*_N constants – therefore change in configuration generally requires a recompile, but not much more.

5.3.2.6 Automation

Automated behaviors are the only ones that require a somewhat significant code change. Currently, the scripts are presented as several 2-dimensional arrays, whose rows correspond to robot state at a particular step. These arrays describe steer state, drive state and deploy state throughout the maneuver. While steer state would be somewhat easy to generate on the fly, since it only involves propagation of a turn through the body of the robot, deploy and drive sequences are harder to generate, since they require information about exact location of deploys in relation to steer joints and whether deploys belong to drive or support modules. Currently, this information is not encoded, and cannot be gleaned from the existing configuration info.

Thus, a change in configuration generally requires preparing a unique set of 2-dimensional arrays for each automated maneuver: turn, launch and unlaunch. Fortunately, this work only needs to be done once, when the configuration is designed., which has been carried out for both the X-II and X-II-MFL configurations.

5.3.3 XML configuration map

The new X-II “extended/expanded” MFL-sensing platform complicates logistics of configuration management in two ways. Firstly, the number of new modules, both active and spare, makes it difficult to manage sets of specific parameters, associated with each electronic board and mechanical assembly. Secondly, a mechanically simple transition from extended to basic platform configuration or vice versa must be reflected in three software components: user interface, motion controller, and module controller, spread over as many as 16 distinct processors. CMU developed the previously-described configuration map mechanism, which solves both the problem of keeping track of specific module parameters and the challenge of synchronizing configuration changes seamlessly over the multiple software layers.

5.3.4 Kinematic model update.

CMU’s original implementation of robot’s kinematics relied on having two drive modules (modules with active drive actuation) in the head and rear of the robot train. Increase in weight and drag associated with extra modules and the anticipated magnetic drag of the MFL-carrying platform required an increase in number of drive modules, and thus in complexity of drive control. CMU implemented changes to the motion controller and its scripts to accommodate any number of drive modules arbitrarily positioned in the drive train (see previous description).

5.3.5 CAN Protocol (Software) Upgrade

CMU developed new functionality to facilitate 8-bit controller code updates. Since both the size and the number of modules in the expanded platform makes manual code update over the entire train a burdensome affair, an in-situ software update mechanism was developed, with a graphical representation of said mechanism shown in Figure XLII.

Each 8-bit board connected to the CAN bus is assigned a unique identifier at the time of assembly and may be commanded to switch into update mode to receive a code update over the CAN network. This functionality in conjunction with the robot configuration map allows software update over the entire robot triggered by the press of a single button.

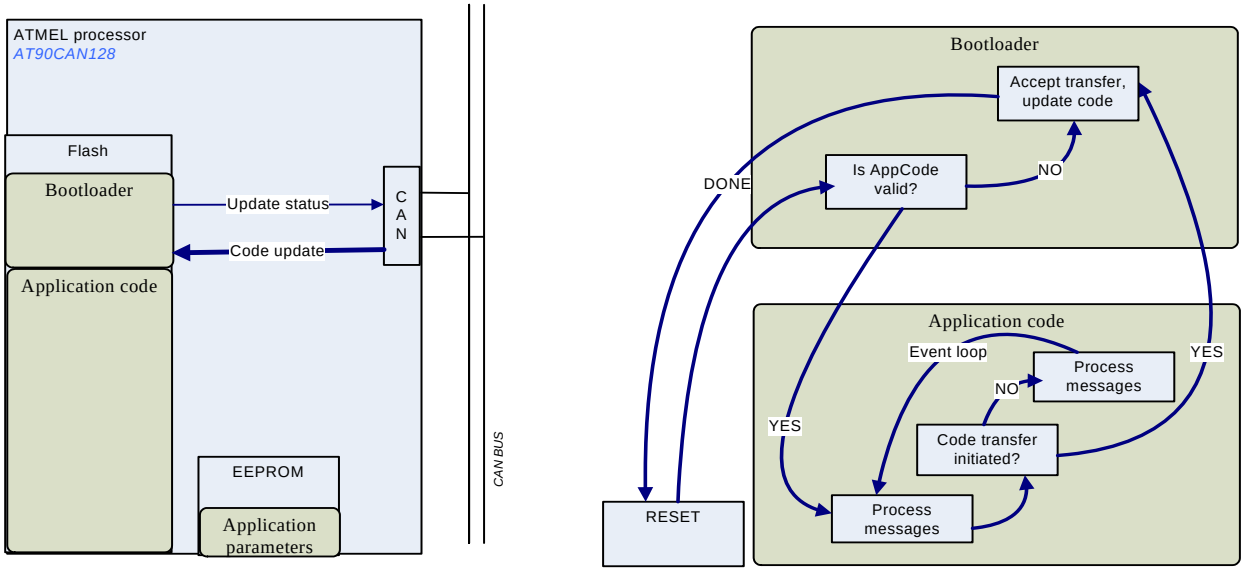

Figure XLII : Software upgrade mechanism for in-situ reprogramming of on-board microcontrollers over the CAN-bus

5.3.6 Augmented CAN protocol

CMU also expanded the CAN Control/Data protocol developed for the original X-II platform to accommodate the increase in number of modules of each type, and to implement transfer of software code and associated handshaking over the CAN bus.

6.0 Sensor-Module Specifications

The sensor module specifications were drafted and finalized and are summarized in key tables and interface drawings related to the mechanical, electrical and software specifications detailed in this section.

6.1 Overall Requirements

The following tabular representation was agreed upon to capture all the main requirements of import to any NDE sensor module requiring to be interfaced to the X-II platform:

PARAMETER	CONSENSUS
# Modules	≤ int(2)
Size	5" L x 4" DIA cylinder
Weight	≤ 10 lbs
Spacing	23 inches
Angular Motion-Range	77^{o} - 80^{o}
System Data on Bus	Inclinometer, system time, odometer
Communications Bus	1 MHz CAN (2.0b)
Protocol	CMU-custom, TTP, 32 bit
Power Bus Specs	26 VDC nominal
Power Draw Specs	Deploy / Retract: 30 W for 2 minutes - (1.2 A @ 24 V dc) Scanning: 24W continuous - (1.0 A @ 24 VDC) Idle: 12W continuous (when not scanning) - (0.2A @ 24 VDC)
Data Storage / Transfer Specs	IDLE: ≤ 50 k bits/sec DATA DUMP: ≤ 450 k bits/sec INTEARCT: ≤ 150 k bits/sec
Sensor-Drag	≤ 1lbf total
Off-board NDE data transfer	Ethernet (802.11)
Inter-module Wiring	4 TP; 28 AWG
Protocol Documentation	**Approved by all**
Vibration Isolation	Standoff & Absorption tolerant
EMI Protection	Motor/Coil EMI to be expected; Isolation responsibility of ea. party
Pass-thru shielding	EMI shielding by Sensor-Providers

Table 1-9 : Sensor Module Interface Specifications

The sensor module specifications cover the number, size and weight of same, as well as their separation and articulation. The system had to operate under different modes with distinct power-draw limitations. Power is off the same robot-bus and communications occur over a CAN bus. Off-board NDE data-transfer between the robot control CPU operated by the operator and the data-operator is over wired/wireless ethernet. Wiring pass-throughs are required and specified in terms of number and gauge. Attention to design is needed due to the potential of non-centricity during operation (up to 0.5"), vibrations during operation and the need to EMI-shield pass-through wiring to avoid noise-introduction.

6.2 Mechanical Interface

The volume and mechanical and wiring interface diagram were clearly defined, as were the interconnections (via pigtail wiring) and are reflected in the image of Figure XLIII:

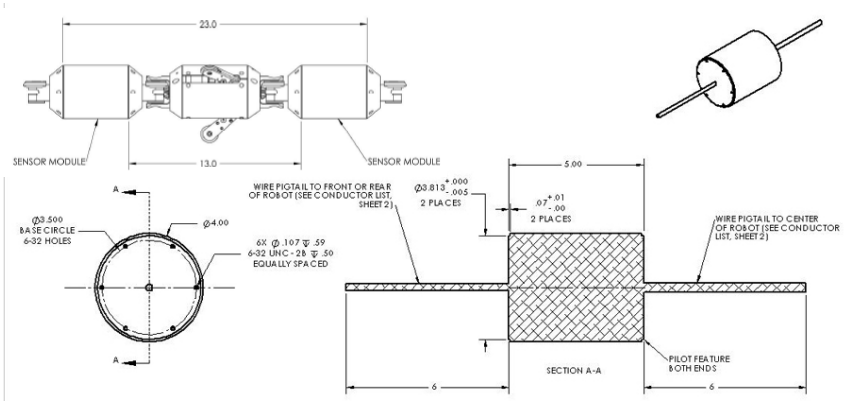

Figure XLIII : Mechanical size and shape specifications for the sensor module

6.3 Sensor Wiring Schematic

The sensor wiring diagram required to be followed by the sensor module was also developed and is depicted in Figure XLIV:

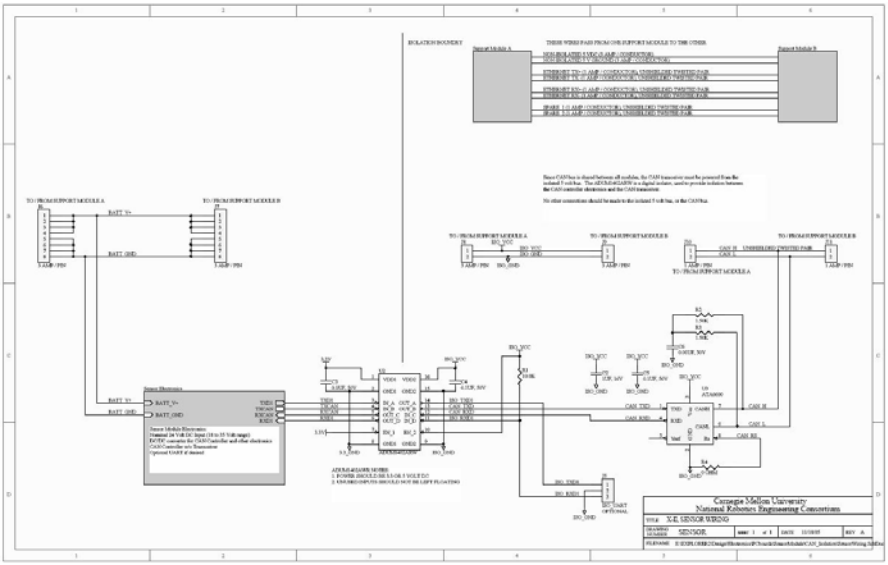

Figure XLIV : Sensor module wiring interface diagram requirements

6.4 CAN Bus Isolation Schematic

In order to avoid any bus-crashes and -hogging', a communication-bus isolation schematic was provided to ensure the availability and up-time of the bus on the robot - it is depicted in Figure XLV:

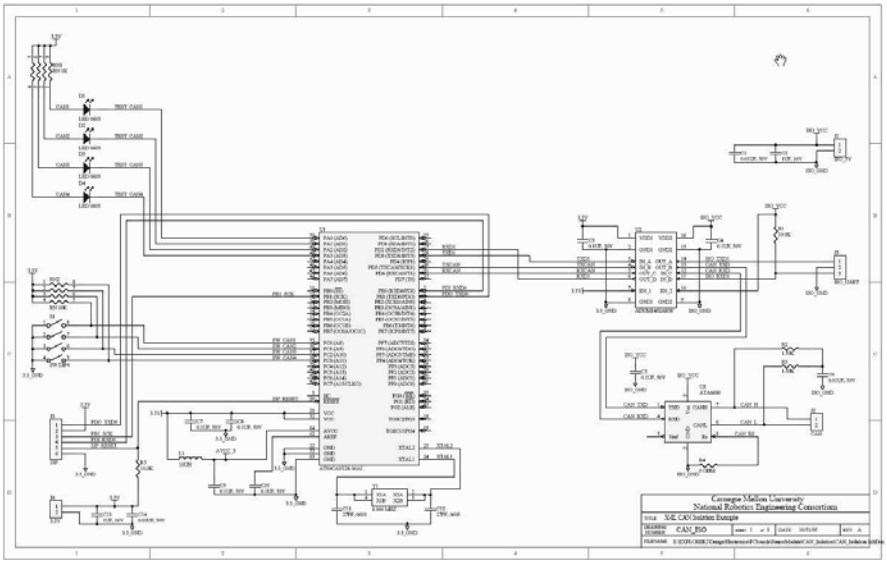

Figure XLV : CAN bus sensor module isolation requirement schematic

IV. PRE-PROTOTYPING & EXPERIMENTATION

As part of the prototype testing activities carried out to support the design phase, CMU engaged in several critical activities in order to reduce technical risk and better guide the design in key areas listed below.

1.0 Pressure Testing

All critical electronic components were tested under pressure in a setup rated to 750 psig, by teaming with an outside contractor. All components, including OEM PCBs were found to be tolerant to those pressures, excluding the video imager, which will have to be housed and pressure-protected. An image of the pressure test setup is shown in Figure XLVI on the right.

Figure XLVI : Pressure test-chamber system

2.0 Computing-System testing

The 32-bit OEM computer was acquired and tested in terms of its main I/O and the OS usability and CAN connectivity and wired/wireless networking hardware. It was discovered that CAN-compatibility 2.0b was not achievable, requiring all systems to be set for 1.1 compatibility. An image of the hardware is shown in Figure XLVII.

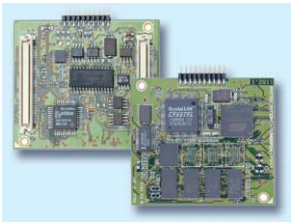

Figure XLVII : 32-bit SBC OEM components used in testing

3.0 Illumination System Testing

A new type of higher-efficiency white LED was tested, using individual units, mounting them to a prototype nose-cone section from X-I and performing illumination (voltage, current LUX, etc.) experiments inside a 6- and 8-inch diameter pipe (see inset Figure XLVIII).

Figure XLVIII : Higher efficiency white LED illuminator test setup

In addition, a prototype LED illumination ring was built and tested in a pipe to ascertain the power, heating and illumination achievable with the new LEDs and system design. An image of the setup is shown to the right in Figure XLIX.

Figure XLIX : Prototype LED illuminator ring and test-camera setup

4.0 Arm Jig

A prototype test-jig for calibrating and testing strain-gauge based leg-force sensors was built and assembled and strain measurements taken to feed into the control algorithms to control bracing and contact forces. An image of the setup is shown on the right in Figure L.

Figure L : Drive-arm strain-gauge and leg-expand/-collapse test-jig

5.0 Prototype Electronics for testing

A suite of preliminary PCBs was built and is undergoing testing for electrical functionality and preliminary software development. Circuits for the nose/camera and drive and steering modules have been developed and are shown in Figure LI.

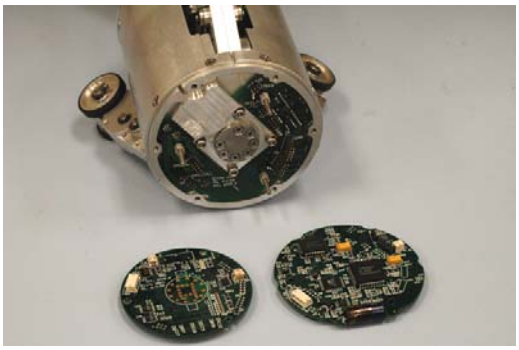

Figure LI : Prototype module control PCBs

6.0 Pre-prototype partial robot train

For more in-depth software and electronics testing, a preliminary drive-, steering and nose-section were built and interfaced to the electronics and bench-top supplies for evaluation and software testing. It was used by developers until the final robot was assembled and readied for software porting, integration and debugging. An image of the setup is shown in the inset image of Figure LII.

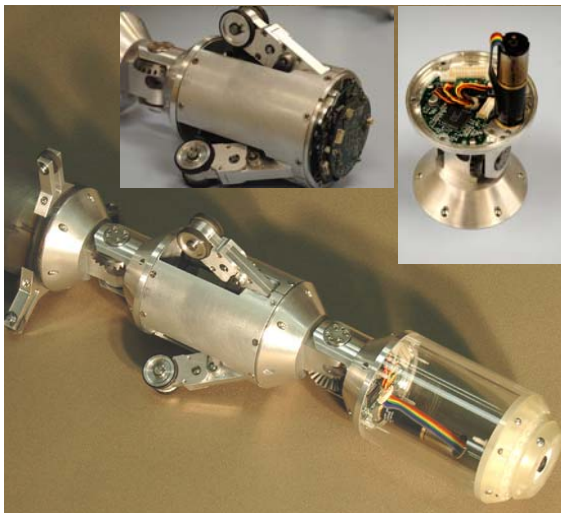

Figure LII : Pre-prototype robot-train section(s) assembly

V. SYSTEM PROTOTYPE

1.0 Locomotor Train

The approved system design, and pre-prototype testing was completed, resulting in the prototyping and assembly of the individual robot modules and the integration of the same into a robot train (with dummy sensor-modules as place-holders).

1.1 Module Assemblies

The main elements of the robot that were built as stand-alone modules, include:

-*Camera-Module*

The nose- or camera-module was built to integrate computing, wireless communication, video-sensing and lighting and emergency-locator systems into a single monolithic module. The resulting prototype is shown in Figure LIII.

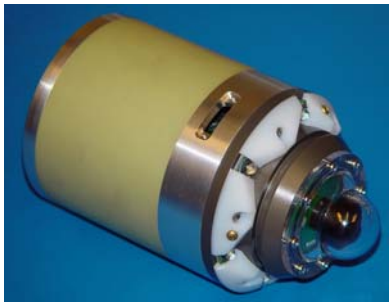

Figure LIII : Prototype Nose-/Camera-module of the X-II prototype tractor/train

-*Steering-Module*

The steering module prototype includes the ability to roll and pitch any so-designed joint using motors and custom gearing and control electronics.

Figure LIV : Prototype Steering-module of the X-II prototype tractor/train

The setup of the joints is based on allowing the ends of the train to roll, while all other joints only pitch. The common steering joint prototype is shown in Figure LIV.

-*Drive-Module*

The drive-module prototype was completed and includes the ability to center and brace the module inside the pipe and allow for the driving of the legged arm-wheels. All the required mechanical elements and electrical PCBs and subsystems were integrated into a final prototype shown in Figure LV.

Figure LV : Prototype Drive-module of the X-II prototype tractor/train

-*Support-Module*

The support module was prototyped as it is needed to provide the necessary centration and passive encoding for position determination. The necessary mechanical and electrical systems were integrated and the resulting integrated module is depicted in Figure LVI.

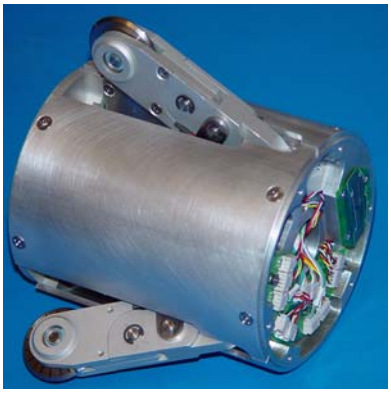

Figure LVI : Prototype Support-module of the X-II prototype tractor/train

-*Battery-Module*

The battery-module prototype is based on the use of lithium-based battery-cells combined into packs to provide 26 VDC and up to 15 Ahrs of energy to the robot for a meaningful 8-hr. mission.

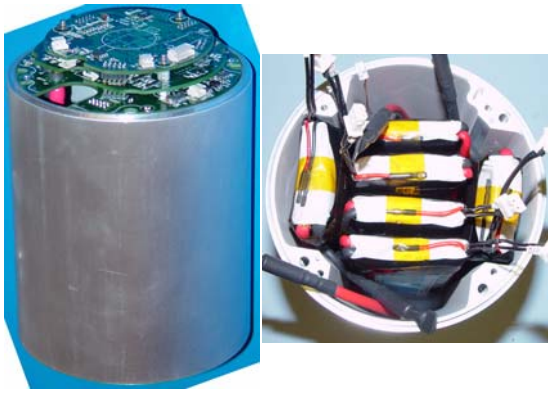

Figure LVII : Prototype Battery-module of the X-II prototype tractor/train

The battery-module also contains safety electronics and voltage converters to allow monitoring of charge and discharge. An image of the prototype of the module is shown in Figure LVII.

1.2 Prototype Train Assembly

The robot modules described in the previous section, were assembled in multi-unit quantity and then coupled in a pre-determined sequence to form the robot train for testing. The train was to utilize stand-in (weighted and sized) 'dummy'-modules to represent the sensor-modules to be provided separately by SwRI.

-*Prototype module assembly*

A complete set of modules to assemble a robot train was built and assembled, including all electro-mechanical (active & passive) components, circuit boards and internal wiring. An image of the complete set of modules (excl. RFEC) is shown in Figure LVIII.

Figure LVIII : Prototype module elements for the X-II robot train/tractor

-*Prototype robot train*

A complete robot train was assembled on the bench, and used to port low-level code and test out all electronic and wire harnessing at the low-level. The SBC software core OS was loaded to test coordinated behaviors and control, as well as wireless communications. The robot runs off its own batteries and performs all communications wirelessly. The prototype was used to enable the development and debugging of turning and obstacle-handling routines in the indoor pipe-network. An image of the complete robot-train assembly is shown in Figure LIX., in both the laboratory and the indoor test-area.

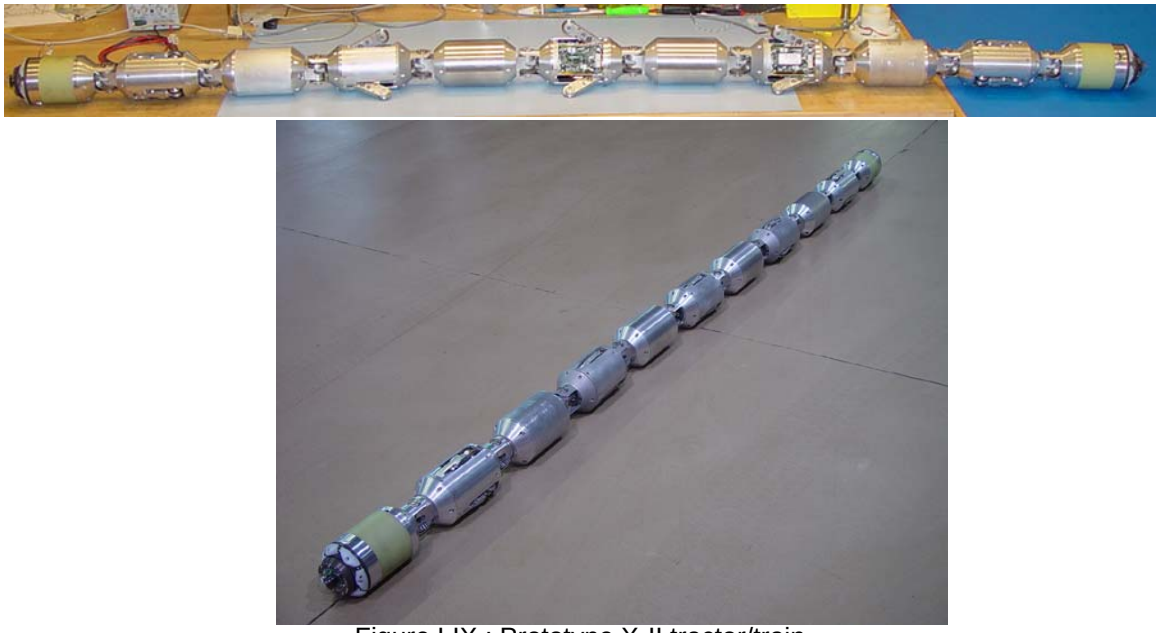

Figure LIX : Prototype X-II tractor/train

1.3 Software Elements

The software elements that were developed and ported to the robot train/tractor and off-board controller, included:

- *8-bit and 32-bit embedded code for the robot microprocessors,*
- *the topside GUI control,*
- *interface software for communications (CAN) between modules,*
- *wireless bi-directional communication protocols,*
- *on-module control and monitoring (motor-controllers and feedback sensing),*
- *32-bit SBC code to orchestrate combined and multi-joint motions to allow the robot train to move and articulate in a coherent fashion.*
- *reliable digital video-stream connection with bi-directional control and status data over the wireless connection to the operator control computer and the GUI.*
- *script-development and testing effort for the indoor and outdoor pipe network.*

1.4 Robot Control GUI

The GUI that was developed, with all its fields and elements, as implemented for the X-II platform is depicted in Figure LX.

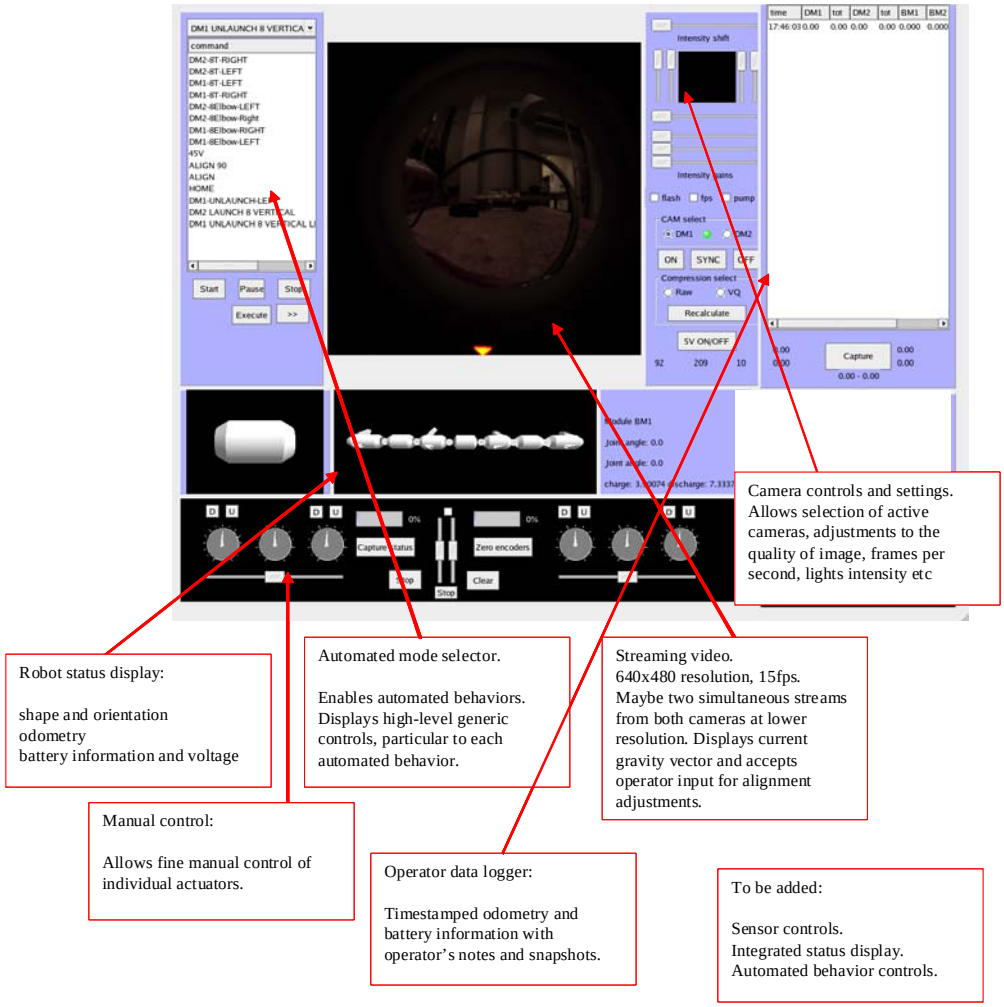

Figure LX : Robot Controller GUI Layout

1.5 Integration of RFEC (SwRI) Sensor

The RFEC sensor was integrated onto the robot train. An image of the two sensor-module sections (detector and exciter), are shown in Figure LXI:

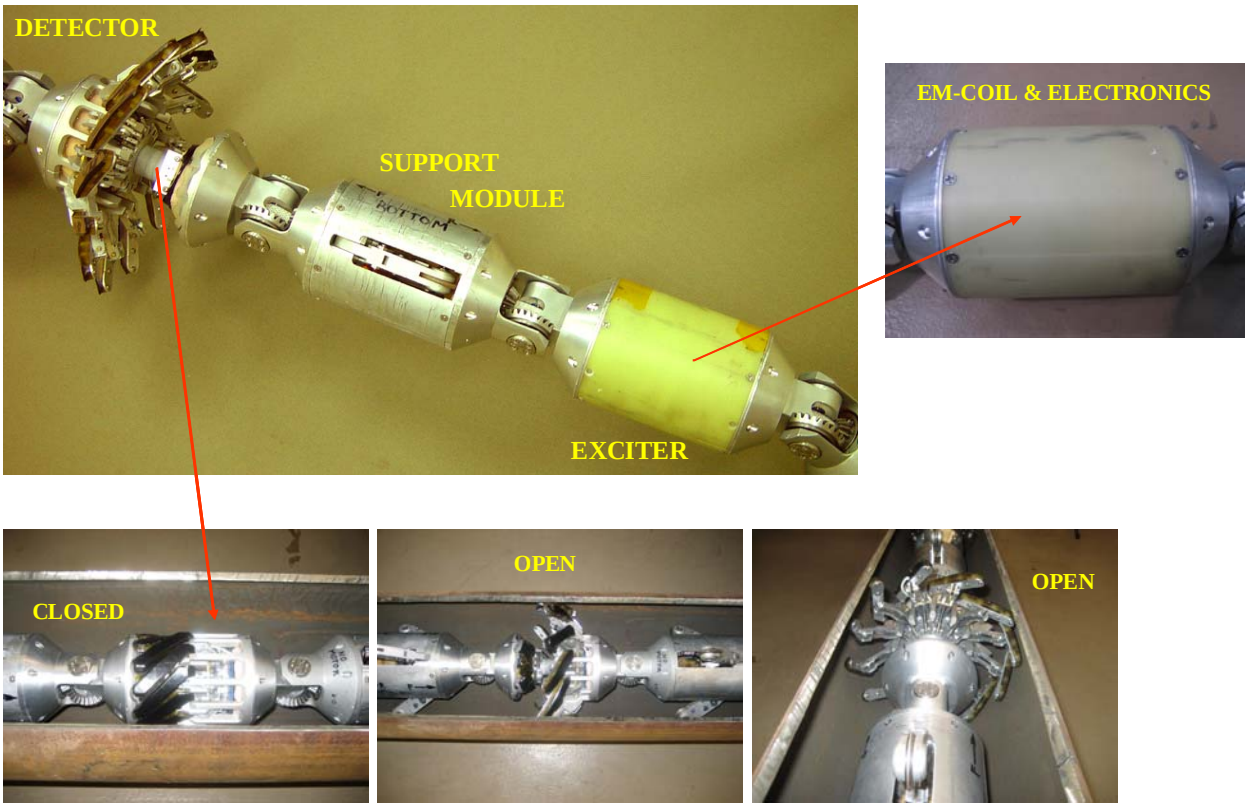

Figure LXI :RFEC sensor module elements: Exciter and Detector in both deployed and closed configurations

Note that the electronics are housed in one of the modules, including the exciter (electro-magnetic coil) and detector. The sensor-elements on the detector are arrayed on deployable shoes (akin to an umbrella), which can be deployed or collapsed on command, resulting in open and deployed configurations as shown in cutaway pipe-views in Figure LXI. More technical detail on this third-party sensor from SwRI, can be found in [33][34][35][36].

2.0 Robot Launcher

The fittings, launcher-tube and endcap were fabricated, tested and assembled. The fittings were welded onto a section of field-perforated pipe and provided to CMU for testing. The gate-valve was installed and the launcher-tube mounted to it, resulting in the indoor test-setup for launch/recovery and pipe-driving (with elbows and Ts and Ys) depicted in an inset image of Figure LXII on page 44; the launcher tube and the fitting and pipe-sections for final launching/recovery testing as well as field-trial use, are also shown in that same figure (Figure LXII).

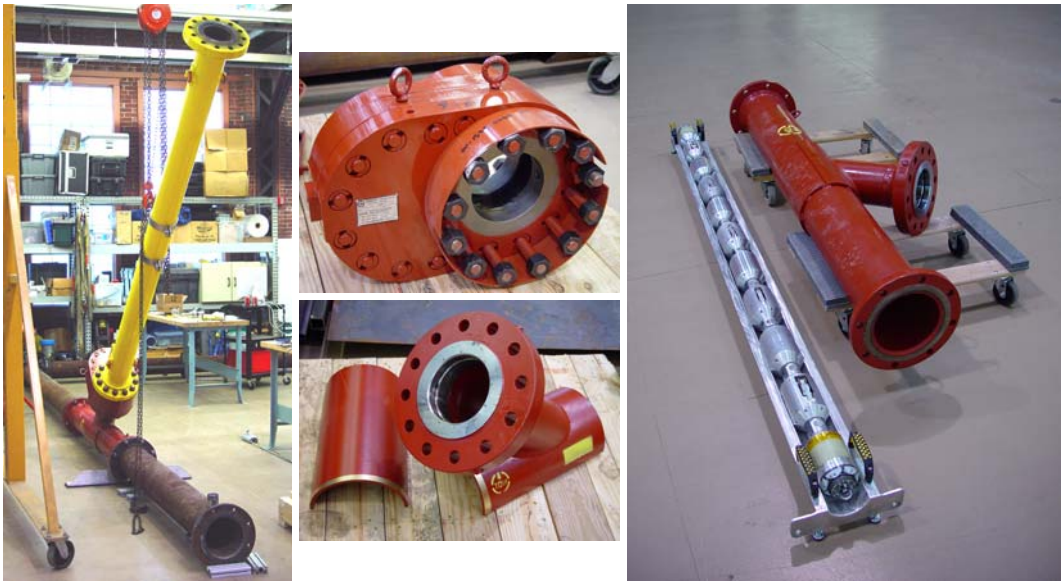

Figure LXII : Launcher tube, fitting, valve and test-section prototypes next to the X-II train/tractor in a launch-tray

3.0 Communications Antenna

The prototype no-blow weldolet installable antenna designed by ATK (including the proprietary alignment-insert and antenna-PCB), were fabricated and used in the indoor and outdoor test-loops. The complete parts and assemblies are depicted in Figure LXIII.

Figure LXIII : Antenna prototype as developed by ATK and adapted for use with X-II

4.0 Alternate Sensing Unit & Platform

CMU, in coordination with its main subcontractor (Automatika, Inc. - ATK), built and integrated both the new MFL mock-up sensor and additional drive/battery/steering/support modules into the extended-length platform. The platform was then utilized to carry out a set of experiments (presented later), to assess the feasibility and develop guidelines for the future development of a field-deployable MFL sensor module. This section will be limited to presenting and detailing the hardware built for both the MFL mock-up as well as the extended robot platform.

4.1 Magnetic Flux Leakage Sensor

The Magnetic FLux Leakage (MFL) module was assembled in both the collapsed-shoes and expanded-shoes configuration and integrated onto the robot train, allowing for all data/power/ network cabling to be passed through the center. The second sensor-module was left in the train and represents the volume for packaging any support electronics. The suspension and centration springs built into the MFL module are visible also in Figure LXIV, which depicts the sensor in its collapsed/expanded configuration and also integrated onto the extended train platform.

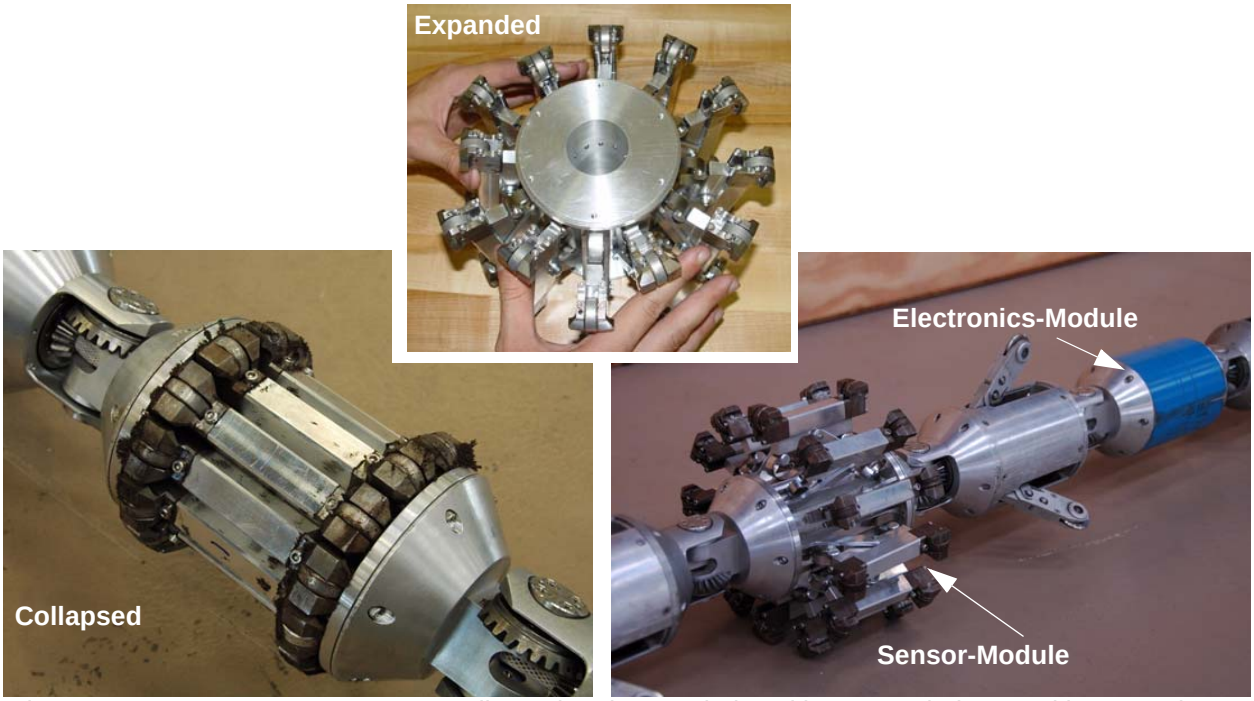

Figure LXIV : Prototype MFL sensor: collapsed and expanded positions; stand-alone and integrated onto robot train (close-up view), including the sensor electronics module (blue cylinder)

The dummy MFL sensor mimics the configuration and magnetic drag effects of a real MFL sensor. Magnetic drag effects are simulated with permanent neodymium magnets mounted in shoes designed to slide along the pipe walls. The dummy sensor has two mechanical configurations – deployed and retracted.

In the retracted state, the shoes are mounted onto the body of the MFL, and in the deployed state, a spring mechanism presses the magnetic shoe against the pipe wall. The MFL needs to be in the retracted state while not sensing to minimize parasitic drag, as well as during turns. The MFL would be deployed during sensing operation, so that the magnetic shoes are pressed against the pipe wall. Figure LXIV on page 45 illustrates the two states in the pipe: to the left, retracted MFL in the turn, and on the right, deployed MFL in the pipe.

The shoes are comprised of three (3) different components. The body of the MFL shoe is constructed out of 6061 aluminum while the outer boots are made of 1215 carbon steel. The purpose of having a non magnetic material encase the magnets in this configuration is to allow magnetic field lines to propagate from the pole of one boot to the other. The MFL was tested with 0, 2, and 4 magnets. Figure LXV depicts the shoe configuration.

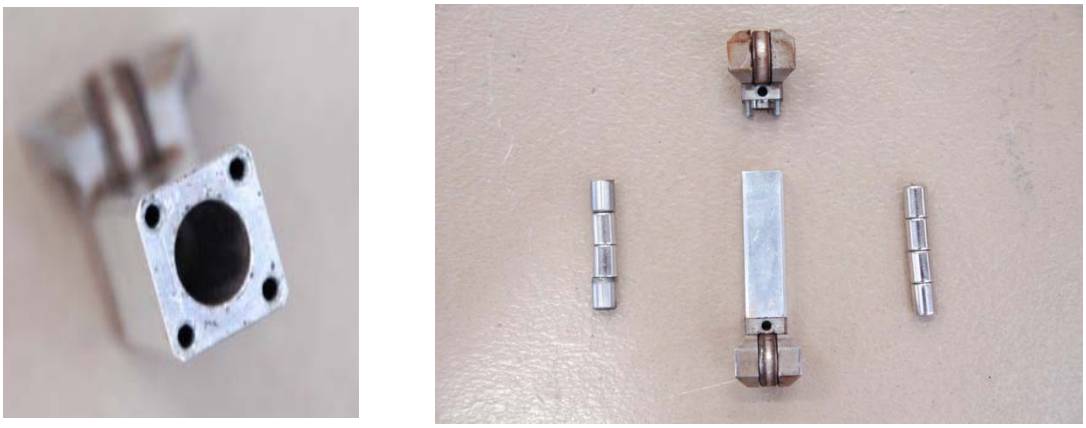

Figure LXV : Magnet show prototype depicting magnet-loading chamber and roller-shoe magnet-poles

On the left side of the shoe is an example of two-magnet population, with two steel pins straddling 2 magnets. The right side of the image shows an example of a four-magnet population. The chamber (left image) must either be fully populated or not at all; this is the reason why two dowel pins are used in the 2 magnet population. It is necessary to have physical contact from boot end to boot end in order to assure proper transmission of magnetic flux.

4.2 Extended X-II-MFL Prototype Train

The additional drive (2), battery (2), support (2) and steering (4) modules are incorporated on both ends of the train (in equal numbers) right after the sensor/camera module. When coupled with the new MFL sensor mock-up module and fully assembled, the final configuration of the robot train resulted as is shown in Figure LXVI. The system continues to retain its symmetry, allowing the use of a more generic controller to develop the scripts to perform obstacle maneuvering (launching, elbows, Ts, Ys, etc.).

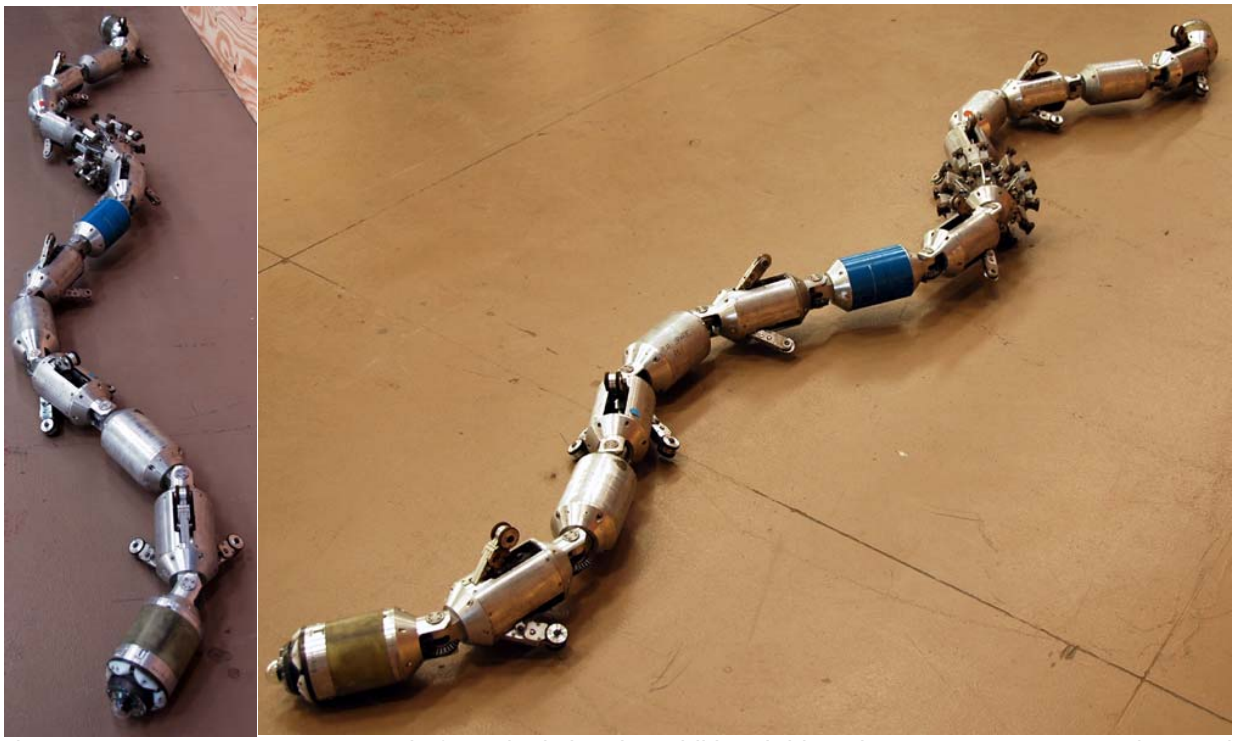

Figure LXVI : Prototype X-II-MFL platform depicting the additional drive-, battery-, support-, steering- and MFL mock-up module(s)

VI. EXPLORER-II: TESTING & VALIDATION

1.0 Laboratory & Outdoor Loop Testing

The X-II prototype system was tested for endurance in the indoor and outdoor test-loops built at CMU (see Figure LXVII). A total of 100 feet indoors and ~600 feet outdoors of 6- and 8-inch pipe was available for testing. Only the indoor setup had the launcher attached to it for ease of all-weather testing.

Figure LXVII : Indoor and outdoor testing facility setups at CMU for X-II endurance testing evaluation

Testing involved launching and recovery of the robot, straight driving, as well as making scripted turns in 90-degree elbows as well as Ts and even Ys - all these elements were cast-iron fittings, attached to flange-welded pipe-sections using bolts and gaskets. None of the pipes were seamlessly welded at the joints in order to allow for ease of assembly and reconfiguration.

The testing was carried out over the period of about 4 months, including several runs with the prototype RFEC sensor - most runs however, due to lack of continuous availability of the RFEC sensor from SwRI, were carried out with the stand-in mock-up sensor-modules (to size and weight). The summary of the test-data based on all the runs, is depicted in Table 1-10 on page 49.

As is apparent from the table, almost 2 miles of pipe-distance was travelled, with 35 out of 41 Ts and elbows having been traversed under computer control, with a smaller number (4 out of 8) of Ys and long-elbows. A total of 80 launches/recoveries (each counted as a single event) was carried out to refine, validate and prove the robustness of the device, procedure and computer-controlled scripts for the robot. This data was presented to the sponsors during the acceptance demonstration, and served as the backup to justify CMU's request, and acceptance by the sponsors to proceed into the field-trial preparation and execution phases of the program.

	Explorer Endurance Runs						
	Feet	Sensor	90 T	90 elbow	45 Y	elbow	Launch
	1600	no	15	15		-	60
	300	sometimes	10	10	4	-	20
	600	yes	-	-	-	-	-
	3000	yes	-	-	-	-	-
	-	no	-	6	-	8	-
	4160	yes	10	10	-	-	-
TOTAL	9660	-	35	41	4	8	80
	Feet	Sensor	90 T	90 elbow	45 Y	45	Launch

Table 1-10 : Endurance test data for X-II by distance, obstacle (and type) and launch/retrievals

2.0 System Acceptance Demonstration of X-II

The complete robot, sensor and GUI systems were demonstrated to the sponsors (DoE, NGA & DoT) on June 7th, 2007. The demonstration consisted of a complete launch, 90-deg elbow and T-turn drive through about 25 feet of 8-in pipe, and a subsequent run in a a corroded pipe to show off the real-time data-collection and display capabilities of the sensored train to the audience on a large visual display. Selected images from the demonstration run are shown in Figure LXVIII:

Figure LXVIII : Selected images from the X-II acceptance demonstration at CMU, depicting the robot, launcher, elbow- and T-turn, as well as sensor-operation and live wireless driving and sensor-data GUI

The review team deemed the demonstration a success and agreed to proceed into the live field testing and demonstration phase, requiring the system be tested in compressed air and then natural gas to pressures of 750 psig, before it would be allowed to be deployed into a live gas main. The results of those tests and trials are detailed in the sections to follow.

3.0 Pressure Testing - Air & Natural Gas

3.1 Pressure-Testing to Design Pressure

The CMU team used the launcher-tube (see Figure LXIX), with specially fabricated endplates for compressed-gas supply, shut-/bleed-off valves and regulators, to test its X-II system for functional operation in 750 psig compressed air. The robot was placed into the launcher, the endplates attached with sealing gaskets, and compressed air fed to the launcher from high-pressure lab-bottles, until 750 psig was reached. The robot's functions (camera, lights, arm-deployments and even short-range driving), were exercised over a period of several hours.

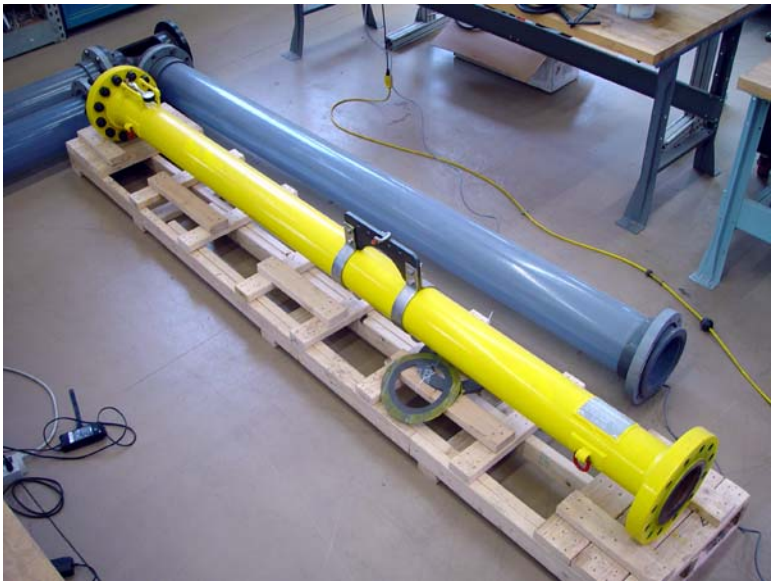

Figure LXIX : Launcher-tube used for pressure testing to 750 psig for air and natural gas

The team was able to thus test the complete robot (incl. the RFEC sensor) in the launcher-tube with pressurized air to 750 psig, without any component failure being evident. Only a camera-upgrade was needed and tuned focussing on the imager to eliminate excessive image de-focussing during pressurization.

No other adverse operational conditions nor defects or flaws were detected during the testing procedure. The robot was then declared ready for identical pressure-testing, but this time in a natural gas environment.

3.2 Pressure and Safety Testing in Natural Gas

The robot and launcher were brought to a natural gas test station in NW PA (Henderson), and with the assistance of National Fuels technicians, the system was pressure and safety-tested (incl. all purging and powering procedures) to 502 psig (limitation of the on-site

gas station pumping equipment) in natural gas without any problems and without losing any functionality nor degrading its performance.

The test proved that the system was not only pressure-tolerant, but also that the procedures of purging and evacuation, coupled with the safety design implementations on the platform, were all effective in allowing the system to operate safely in a potentially dangerous environment, by exercising the maximum exclusion of the oxidizer, namely oxygen-bearing air. Selected images from the NG testing setup are shown in Figure LXX on page 51.

Figure LXX : Test setup of the operational and safety testing for X-II in high-pressure natural gas

4.0 Field-Trials

•Field-Trials in a live field-pipeline

The CMU and SwRI team spent a week in the field in Brookville, PA at a site supplied by National Fuels, Inc. (NFI) to deploy and 'image[1]' a live 8" steel main operating at around 100 psig (see Figure LXXI) - a site-plan is shown in Figure LXXIII on page 53.

Figure LXXI :Explorer-II field-trial team members from CMU, SwRI and NFI

The CMU-supplied fittings and valve were provided to NFI ahead of time for installation and readiness along a rural site along Rte. 28 (see Figure LXXII).

Figure LXXII :Angled live-launch launcher- and antenna-fittings and gate-valve installed on a live buried pipeline

1. both via camera imagery and RFEC sensors

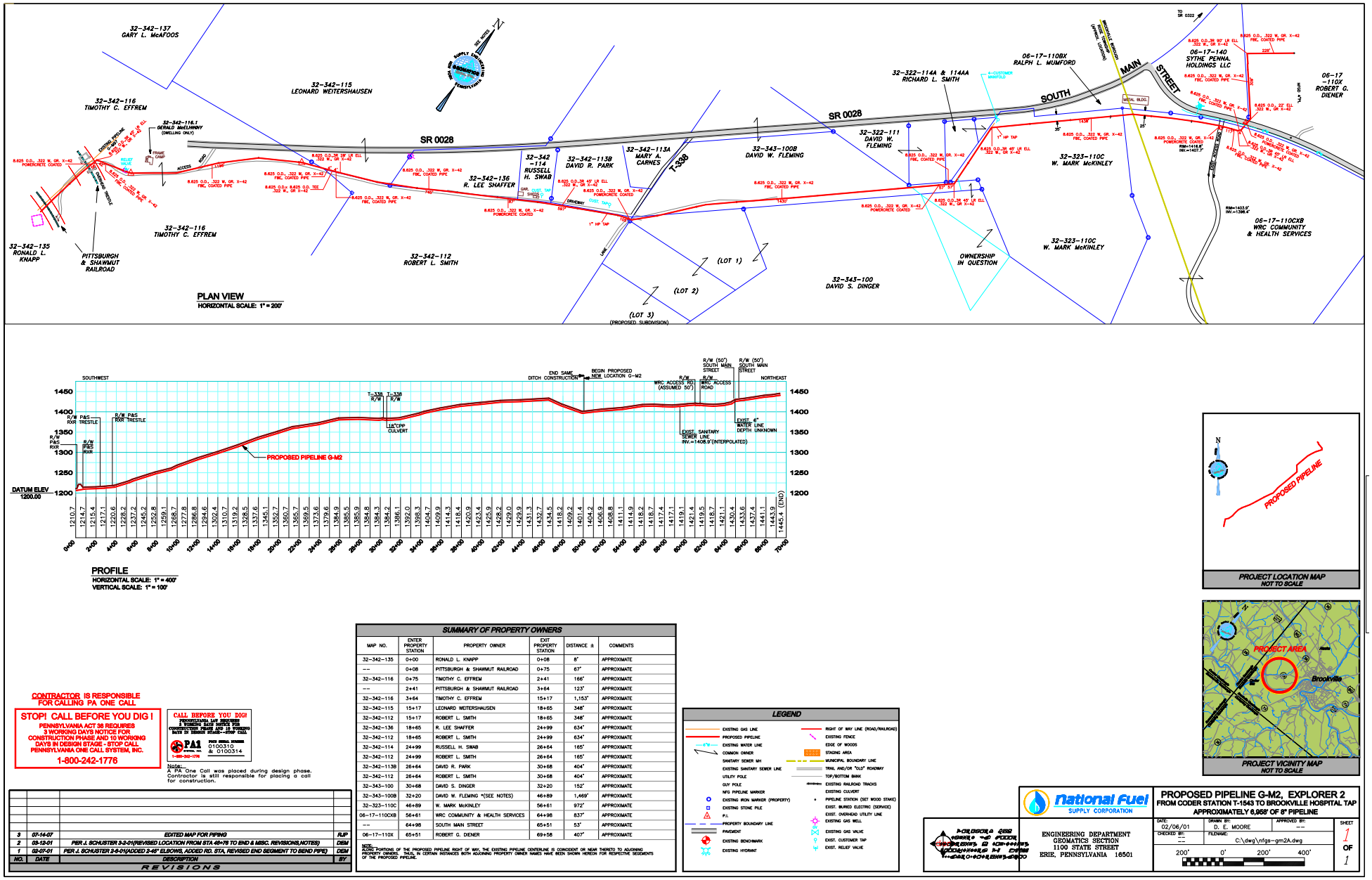

Figure LXXIII : Site-map for field-trial location

The site is located near the intersection of I-80 and Rte.28 near Brookville, PA. The pipeline carries gas along a sloping highway path with a right-of-way burial access path spanning fields, woods, etc.(see Figure LXXIV), with the pipeline located at about 6 feet below grade. The pipeline was excavated and the site prepared, including various antenna access weldolet points along the multi-mile long run available for inspection.

Figure LXXIV :Site of live test-site

The team spent their 1-week trials performing multiple launch-and retrievals, installation/ removal of launchers and antenna-installations/-removals as part of their testing efforts (see Figure LXXV).

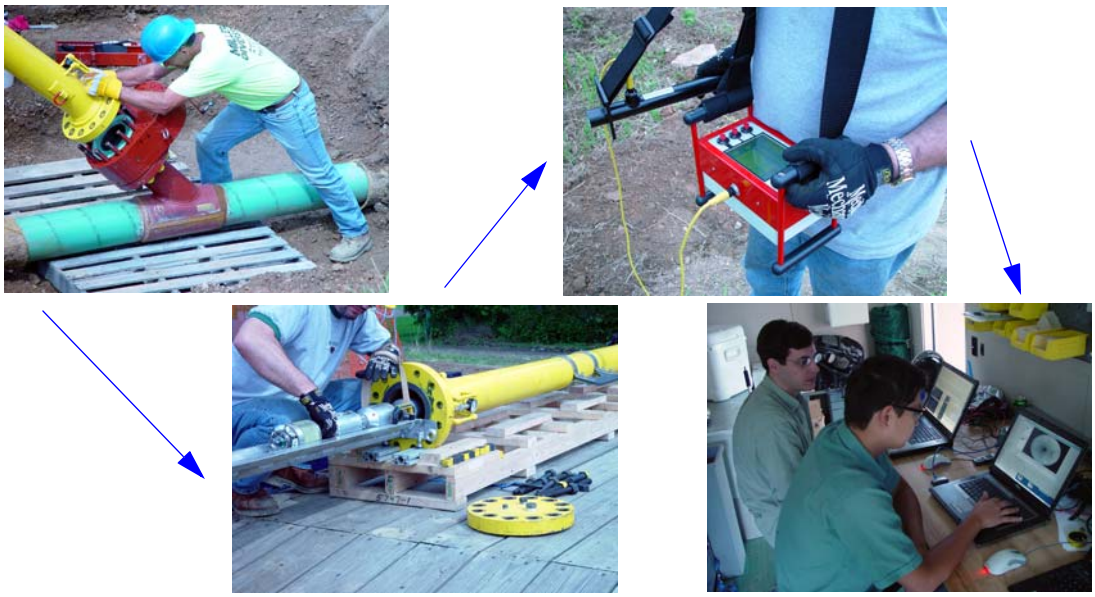

Figure LXXV :Typical daily routine inspection activities

The week was initially spent overcoming both a robot drive-failure (with subsequent retrieval and repair for continued operation), as well as re-installation of flawed antenna-fittings and removal of steel-coupons from the line prior to being able to complete multiple runs during which the robot collected visual as well as sensory-data to provide as a baseline data-set for said pipe-section to NFI for potential submission to DoT.

A few selected images from the field-trial are shown in Figure LXXVI, including the excavation and fitting/launch setup, operators and their GUIs (robot and sensor), as well as imagery from inside the main showing launcher, clean pipe, taps as well as weld-seams.

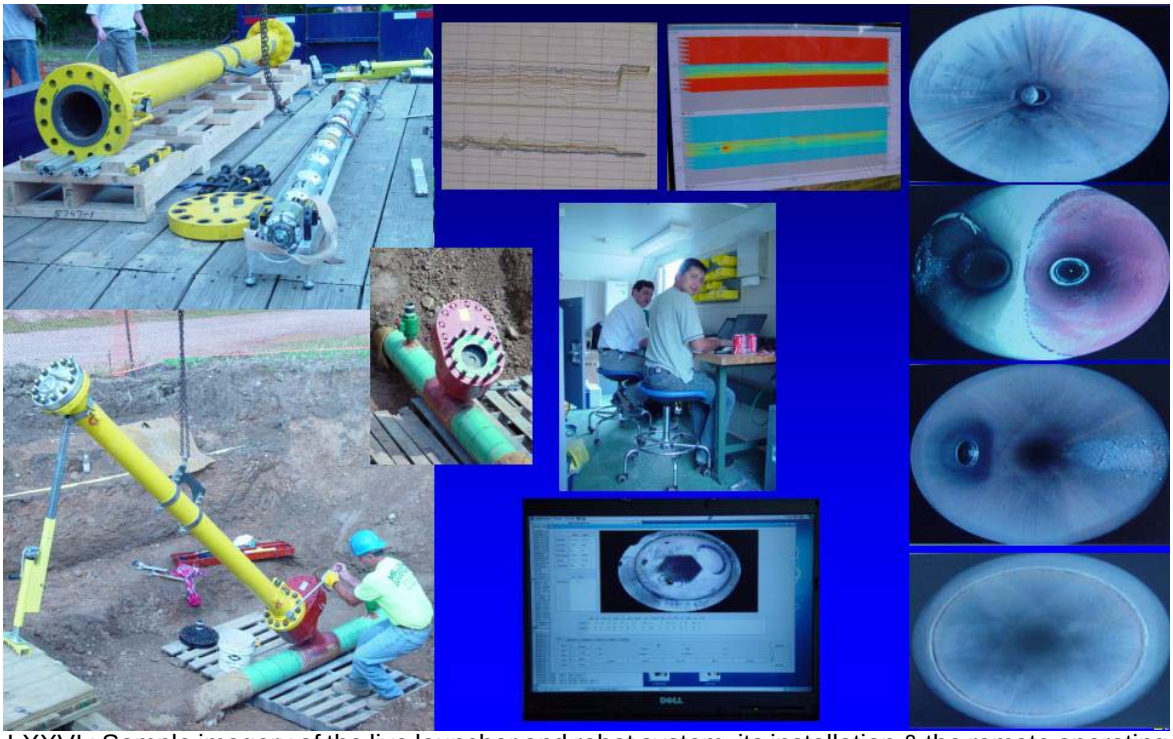

Figure LXXVI : Sample imagery of the live launcher and robot system, its installation & the remote operating room, with live video feedback imagery & RFEC sensor data being transmitted/displayed/ recorded

In addition, a preliminary (uncalibrated) data-set was collected that clearly shows the correlation between imaged features in the pipe (weld, tap, heat-affected zone) as well as a set of sensor data verifying that a section of pipe corresponding to the data was seemingly free of flaws and defects[1].

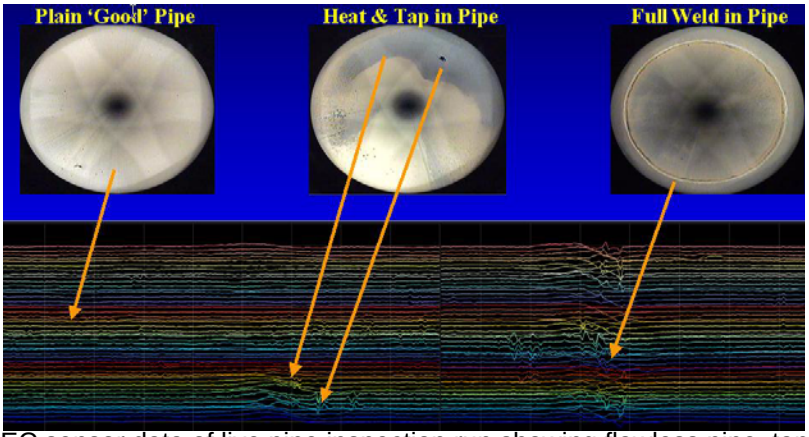

Figure LXXVII :RFEC sensor data of live pipe inspection run showing flawless pipe, taps and heat-zones

1. a final report for the data was to be generated and provided by SwRI to NGA and DoT

The statistics of the runs in the pipeline are summarized below in Table 1-11, which provides a complete day-by-day log of activities and summaries of Distance traveled under live conditions, distance of pipe scanned live with the RFEC sensor, and also the number of launches/recoveries made during the 1-week trial.

EXPLORER-II FIELD-TRIAL SUMMARY LOG WITH ASSESSMENTS & SOLUTIONS

DATE	DAY	ACTIVITY	Robot Log	Sensor Log	DURATION [hrs]	SUCCESSES	FAILURES	SOLUTIONS	
								On-Site	Future
	THU-PM	Excavation - Ends			2		N/A		
11-Sep	FRI-AM	Tapping - Launcher & Antenna			4	Angled launcher tapping by TDW-Kerr is possible	Launch coupon fell into pipe	Get special site-glass fittings to go fishing	Get it right the first time..?
	FRI-PM	Fishing for Coupon			4		Launch-coupon retrieved	Kirilla used hook to fish out coupon	
14-Sep	MON - AM	Arrival & Site-Setup	N/A		2				
		Unloading & Prep	Power-up		2				
	MON-PM	Launch & Drive	Drove 460 ft. RT	Scanned ~ 200 ft.	4	Launch/Scan & Retrieval	Wrong antenna valve & milled-thread by Kerr Not able to install antenna - had to use antenna in launcher Reduced antenna range	Planning for new antenna installation by NF	
		Retrieval	Manual/Scripted removal			First time in and out of a live pipe			
15-Sep	TUE-AM	Weld-on new weldolet			1			CMU brought several spare weldoletes, plugs and caps	
		Tap Weldolet			2		Hole-saw failed	Bought new saws for NF	Get it right..??
		Launch & drive robot	Drove 260 ft. RT	Scanned ~ 100 ft.	2	Launch & Scan in Real Time	Front drive module gear shattered		Anneal spiral gear
		Setup for retrieval	Drove to launcher and inched nose into it		1	Got front drive module into launcher so it could get hooked			
	TUE-PM	Fabrication of rescue hook			2	Procured sight-fitting and 12-ft. long hook 5/16" rod with hook		NF had a 12-ft long rod with T-bar fabricated; CMU added hook and did salvage dry-runs using spare half-train setup	
		manual hook & retrieval with X-II video-assist	Used X-II video for feedback and straightened joints while manually pulling		2	Hooked front drive module leg and fully pulled robot into launcher tubr			
		Assessment & repair						Replaced drive module with spare; repaired failed gear next day Reduce pre-load on drive-modules to MED, and keep support modules on HIGH to keep sensor centered	Consider the addition of more drive-modules (replacing 2 support-modules with drive-modules?)
		Tap suceeded			1		Coupon fell into pipe - no luck fishin for it with TDW-magnet	Try alternate method?	
16-Sep	WED-AM	Fishing for coupon			2	Coupon retrieved, incl. shavings	Shavings lodged in gate-valve - unable to fully close it	By-pass or blow-by?	
		Cleaning out valve			3	Valve was cleared of debris		Continuous blow-bys with enlarged vent-valve	Valve-seal will need to be replaced
		NGA/DoT/DoE PMs call off demo but decide to do runs on THU							
	WED-PM	Removal of shavings (curled and large one)			1	Many small shavings and large shaving removed		TDW magnet needs to be stronger	passive-knuckle hinged magnet tool to get shaving(s) right aunder starting lip-edge of cutout
		Close-up for the day	None - too little time left in the day to do anything		1				
17-Sep	THU-AM	Launch & drive robot	Setup & launch		1.5		Watchdpog program enacted by operator that was NOT in the procedure	Unlaunch, reset robot & re-launch	
			Re-launch		1	Robot launched to view antenna port		Operator did not run watchdog	
		Install antenna			0.5	Antenna installed	Antenna fell of TDW adapter tool into weldolet - still able to screw it in and seal though		
			Drive in pipe NE		1.5	Drove 1,115 ft. to half-battery limit; RF still at 55-65%	Reduced range due to SW mess-up during launch (lost 1 hr.)		
	THU-PM			Scan on the way back		Scanned ~100 ft.	Not able to drive over stick-wleded weld-penetrations	Reduce all drive/support arm preloads to medium so as to not bottom-out arm-suspension	Design, fab & retrofit custom spring with higher spring-constant for less travel while leaving more compression

(Table continued on next page)

EXPLORER-II FIELD-TRIAL SUMMARY LOG WITH ASSESSMENTS & SOLUTIONS									
DATE	DAY	ACTIVITY	Robot Log	Sensor Log	DURATION [hrs]	SUCCESSES	FAILURES	SOLUTIONS On-Site	SOLUTIONS Future
									MUST get stick-weleded pipe-samples with weld-root penetrations to validate design changes
									Might need to consider stronger drive-motors, OR additional drive-modules
							Unable to continue scanning due to excessive sensor-sag making data unreliable	Collapse sensor and abort data-gathering	
			Drive back to launch point			Return trip of 1,115 ft.			
				Scanned short sections (< 40 ft.) with cathodic protection on/off			Data to be used to assess impact of external pipe-wall corrosion-protection currents on data		
		Retrieve antenna	Watch retrieval on live X-II video-cam		0.5		Pushed out antenna core from weldolet		
							Only able to retrieve weldolet; Antenna core remained in pipe		Use a different TDW tool unable to push adapter pas weldolet plug-face
			Assembled blow-by piping		0.5	Installed onto pipe & retieved antenna		Rapid blow-by valve-opening to get back-pressure to blow out antenna into fitting & close gate-valve	Increase # of setscrews and -groove wall-thickness
		Unlaunch robot	Operator controlled retrieval with scripts		0.15	Drove out under manual control with scripts in < 10 min.			
18-Sep	FRI-AM	Packing up Return to PGH Preliminary Unpack			2 2 1				
Drove total of [ft.]	2950	Scanned [ft.]	400	6	Launches/Recoveries	6	Antenna Install/Removal		

Table 1-11 : Statistics of activities during the live gas pipeline field-trial runs

Note that the robot covered a distance in excess of $^1/_2$-mile in multiple runs, and that the longest run took it at least 1,100 feet away from the launch- and antenna-point, proving that wireless communications is a viable alternative for live pipe inspection. A total of six (6) live launches and recoveries were performed, as well as six (6) successful live antenna installation/removal procedures. Due to unfavorable interactions between the sensor and drive-modules with the joints of the pipe, the team was only able to collect a total of ~ 400 feet of live RFEC data. Said data-set is in the hands of SwRI and is intended to be made part of a separate report from SwRI to the Department of Transportation (DoT).

Note that the above table also contains what steps the field-team undertook to resolve problems as they arose, as well as suggestions for future improvements to avoid the encountered problems in the field.

5.0 X-II-MFL Laboratory Experimentation

This section presents experiments designed to evaluate the system performance under simulated field conditions, particularly as they applied to the extended platform carrying a mock-up MFL sensor.

5.1 Setup

The CMU test-setup used to evaluate the new MFL sensor train, revolved around the use of (i) the launcher tube-and-fitting (to test launch & recovery), (ii) straight pipe-sections (with and without viewing cutouts to test magnetic hysteresis losses = drag) and (iii) standard 90-degree elbows and Ts for turn-script evaluations. This setup is depicted below in Figure LXXVIII:

Figure LXXVIII : Typical test-setup for the MFL sensor train, including launcher, pipes (whole & cut-outs) and elbows/Ts

This setup was used to allow CMU to study magnetic hysteresis losses and ‘anchoring’ phenomena during turns, which ultimately affect the power-consumption and thus also design-decisions related to articulation and shunting of magnets (if required).

5.2 Experimental Protocol

This section presents experiments designed to test the capabilities and operational parameters of the expanded configuration of Explorer II with an MFL sensor (X-II-MFL). Three categories of experiments were performed, which will be detailed further herein:

1. **Linear Pipe Traversal:** The task was to collect speed and current consumption data from driving inside a 21-foot long 8-inch diameter pipe with retracted and deployed MFL, with 0-4 magnet(s) per shoe, to study the effects of magnetic losses on traction and current consumption.

2. **90 Degree Pipe-Elbow/T turns:** The goal was to use the new generic scripts to perform 90 degree turns in 8" T and elbow pipe joints with 0-4 magnet(s) per shoe, in order to understand the impact of 'magnetic-anchoring' effects during sharp turns.

3. **Pull Bar Tests:** The experiment was set up to measure the draw-bar pull force of 4, 2 and 1 drive modules in the extended (with MFL sensor and additional modules) and the original (shorter train with an RFEC dummy-sensor module) configurations, to provide guidance for tolerable drag forces for the different X-II configurations.

5.3 Experimentation

5.3.1 Linear Pipe Traversal

- **METHOD**

  CMU iterated through six (6) different MFL configurations of deployed and retracted states with magnet population in the shoes of 0, 2, and 4 magnets. The testing hardware consisted of a 21 foot long straight steel 8" diameter pipe and the X-II MFL robot train. For each MFL configuration, the experiment contained five (5) trials. Each trial was set up as follows:

  - *X-II-MFL would enter in one end of the pipe, undergo the deploy procedure of all drive and support modules to medium strength and linearly traverse the pipe to the opposite end, with all 4 drive modules being driven at a constant power-width modulated current.*
  - *At the end of the pipe the robot would reverse direction and traverse the pipe while driven at a different current.*
  - *This process would be repeated at seven (7) distinct PWM current levels. Between trials support and drive modules were redeployed to avoid any preload hysteresis effects.*

  Current consumption as reported by the battery modules and speed as reported by the drive modules were recorded at 1Hz throughout the trials. Since only electronics and drive systems were active during the trials, current consumption by the drive system can be computed from total current consumption and hotel load.

  Illustrating effects of magnetic drag due to the presence of the MFL, plots for two data-sets were generated. In the first plot, the current consumption by the drive systems during each trial was plotted against time (note that the absolute value is representative/ proportional to power and that the area under the graph represents energy consumption). For the second plot, the reported speed averaged over the four drive

modules was plotted as a function of time. Since each trial varied slightly in time, lengths of trials were normalized by removing extra data rows. Both of these plots, are depicted in Figure LXXIX and Figure LXXX on page 60 (note the legend to discern magnet-strength influence).

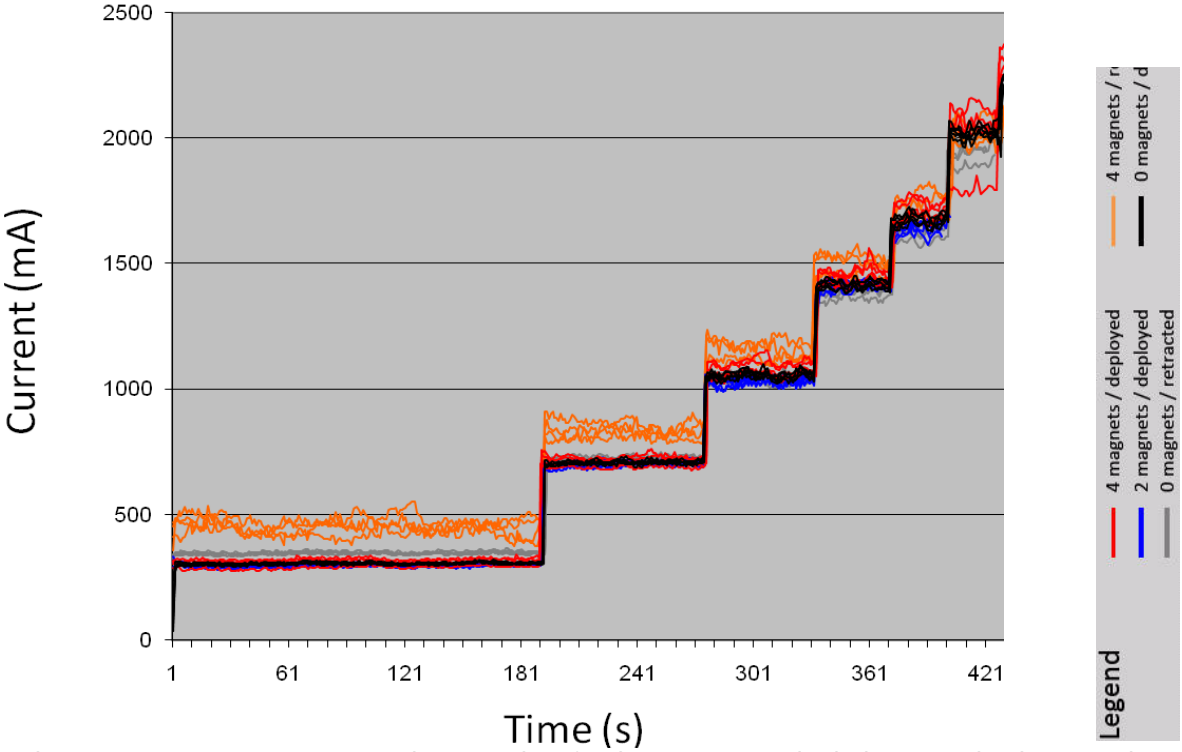

Figure LXXIX : Current consumption over time for the X-II-MFL train during stepwise-increased speed-commands in pipe-traversal experiment with varying pole-magnet strengths

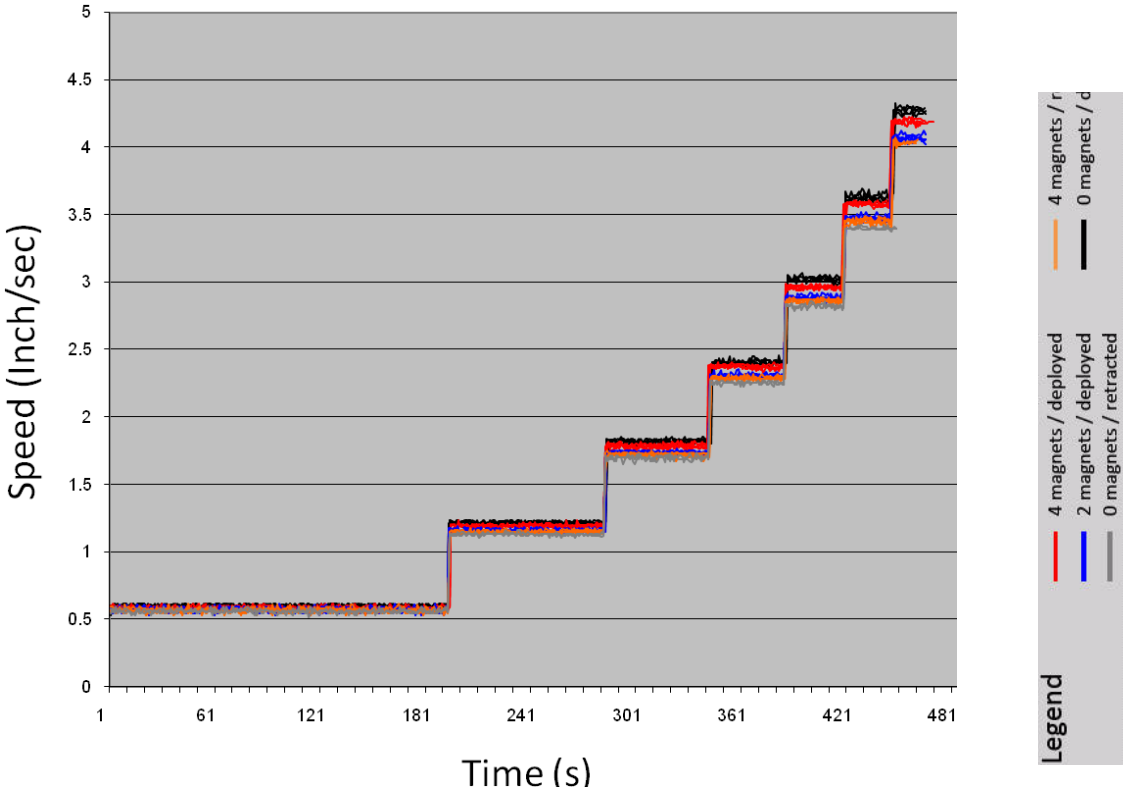

Figure LXXX : Train speed as a function of time (at const. PWM) for different magnet-strengths in linear pipe-traversal experiment

- **DISCUSSION OF RESULTS**

  The original expectation was that the MFL would have a substantial drag force affecting both the speed of the robot and its drive current consumption during linear traversal.

  However, the speed plot shows a consistent difference in speed between distinct configurations across all trials, with the difference becoming more pronounced as PWM increases. In decreasing order, these configurations are:

1. Retracted, 0 magnets
2. Deployed, 4 magnets
3. Deployed, 2 magnets
4. Retracted, 4 magnets
5. Retracted, 0 magnets

If magnetic and frictional drag forces were to account for this difference, we would expect that the 4 magnets deployed (**red-trace**) would reduce speed most significantly. Instead, 0 magnet configuration in the retracted state resulted in the most significant reduction in speed. These data suggest that the main factor behind speed variation has little to do with the magnetic drag, but another dominant factor.

Interestingly, however, the list above is also sorted in chronological order of the experimental investigation. Since the batteries were not recharged between configuration changes, it was determined (and experimentally verified), that the bus voltage was consistently dropping, and there is a 1-1 correspondence between higher voltage and higher speed performance. To control for voltage drop, the experiments were repeated with battery recharges whenever a configuration was changed.

5.3.2 Linear Traversal with Recharges

Experiments were thus repeated with recharged batteries between trials. The identical data, as detailed above, was again collected and plotted, and is reflected in Figure LXXXI on page 62 and Figure LXXXII on page 62.

- **RESULTS**

  As expected, now the speed seemed to be largely unaffected by the MFL configuration. Furthermore, as was expected, the MFL configuration had a noticeable impact on the current draw. In fact, the deployed configuration with all four (4) magnets per shoe resulted in the highest current draw, while the retracted configuration with no (0) magnets per shoe resulted in the lowest. Increases in current were minimal at slow speeds, increasing (seemingly linearly) to up to 25% of no-magnet currents when all magnets were loaded into the MFL-shoes. This indicates (as expected) a speed-related hysteresis loss, but also indicates that the rolling contact-point design for the MFL-shoes was negating any contact friction, limiting losses to hysteretic ones (almost exclusively). Small ripples in current-draw are attributed to surface bumps and imperfections in the pipe wall, resulting in higher/lower pull drive-currents to maintain a specified speed.

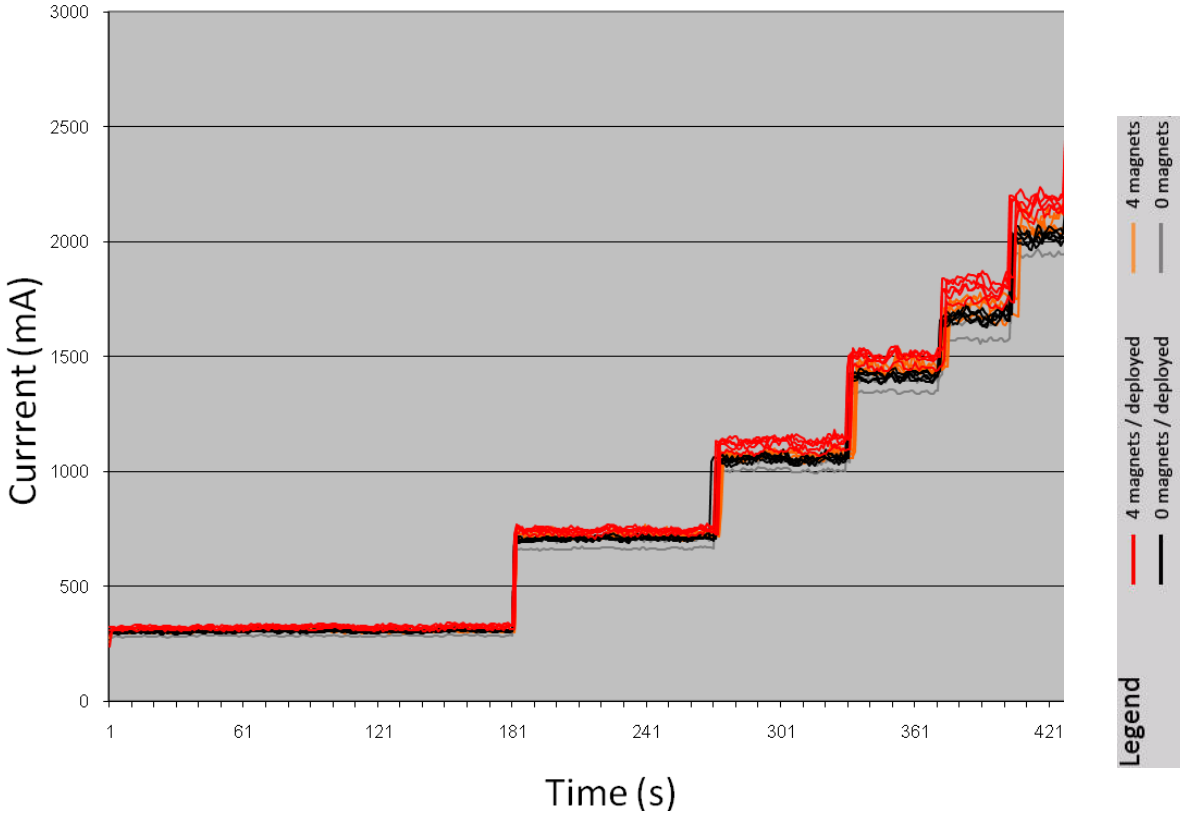

Figure LXXXI : Current consumption over time for the X-II-MFL train during stepwise-increased speed-commands in pipe-traversal experiment with varying pole-magnet strengths - charged batteries.

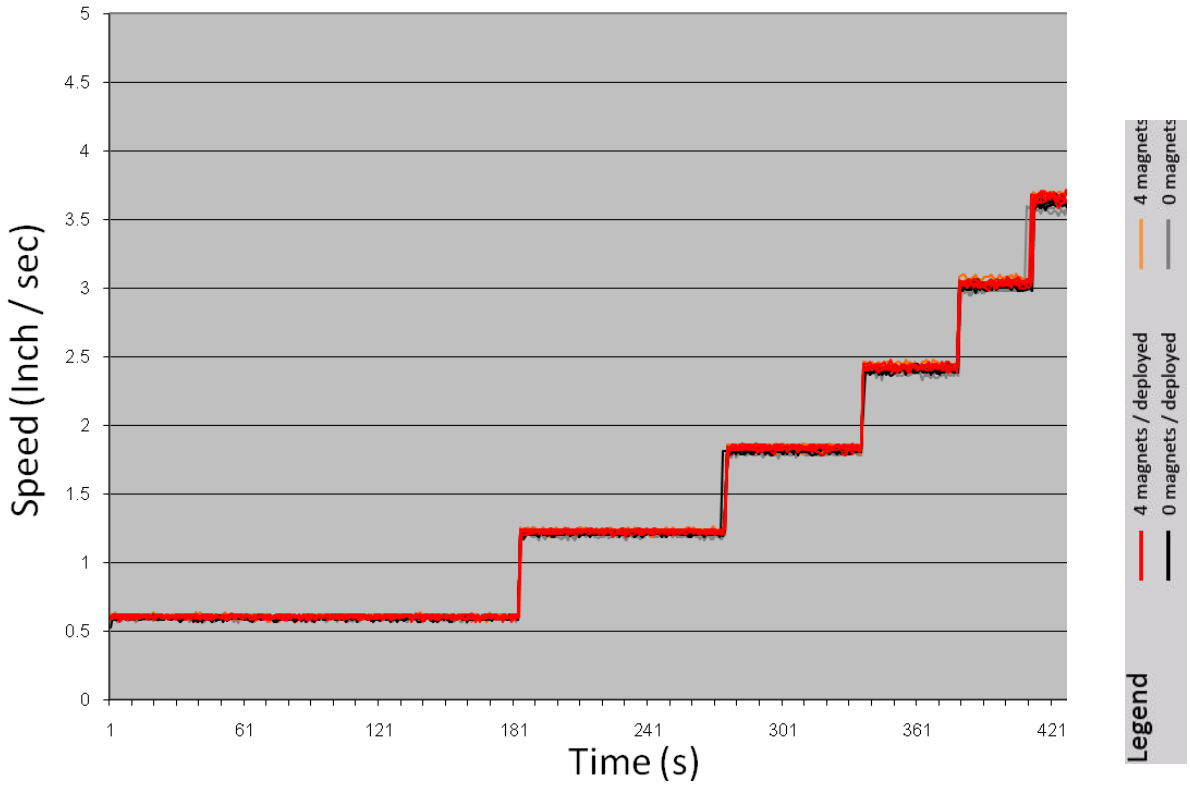

Figure LXXXII : Train speed as a function of time (at const. PWM) for different magnet-strengths in linear pipe-traversal experiment - fully charged batteries for each configuration experiment

5.3.3 Elbow and T (90-Degree) Turns

- **DESCRIPTION AND DISCUSSION**

The purpose of this test was to ensure that extended X-II-MFL train with the retracted MFL could negotiate a 90-degree turn in an 8-inch pipe network. At any given point during the turn there were at most two (2) points of contact with the MFL and the pipe. Of these contacts, one was normal to the pipe, while one shoe on either side of the normal contact-point was offset by no more than 30 degrees. This suggested that the MFL would have little effect on proceeding through the turn, which was indeed confirmed by multiple runs through the 90-degree T and elbow turns.

During normal operation of the turn with the MFL installed and fully populated with neodymium magnets, CMU had two instances of motor joint failure located in the trailing joint of the MFL. Even though the MFL maintained, at most, two points of contact with the interior pipe wall throughout the turn, it was suspected that the motor in this joint is under near critical torsional stress at a point in the turn that the added component of the force from the MFL is enough to cause drivetrain failure. A suggestion for commercial improvement would include an upgraded motor-gearbox combination suitable to higher driving loads[1].

Figure LXXXIII : X-II-MFL performing a 90-degree T- and elbow turn with (collapsed) MFL attached

The observation of this phenomenon provoked a side experiment to quantify the additional normal force exerted by the magnetic shoes in the MFL. The MFL was removed for the purposes of this test, isolated, and tested in the following way:

- *An axial force necessary to overcome friction (slip condition) was exerted and measured. Without the magnets this force was measured at 0.5 lbs, while with the magnets installed this force was measured at 1.5 lbs.*
- *Secondly, the test involved measuring the normal force needed to break the magnetic attraction from the pipe. The MFL module weighs 8 lbs, and it required double this force, namely 16 lbs, to overcome the magnetic attraction forces to the inside pipe-wall (per shoe).*

It is this 8 lb. force at the shoe in contact with the pipe wall during the turn, exerted at

1. Note that the X-II-MFL was assembled using modules originally designed for the X-II configuration only. It is recommended that the next generation X-II drive- and steering-modules be designed with a motor-gearbox combination rated for higher torques to allow more reliable transition to an MFL-sensor setup.

a point roughly 4 inches away from the pivot axis, that results in an additional 32 lb.-in of torque transmitted to the MFL's trailing joint at the point where the MFL shoe makes contact with the interior wall of the pipe. This additional load will have to be accounted for in future designs. Note that this calculation will need to be repeated once the final magnetic strength of a commercial MFL-sensor is known, and adjusted to the number of shoes expected to be in contact with the pipe, depending on the shoe- and pipe geometry.

Also, the launch and recovery capability of X-II-MFL in the extended configuration was tested in the 45 degree 6"-8" launch-fitting fixture. Figure LXXXIV shows the MFL dummy module in the middle of X-II-MFL's ascent into the launch tube.

Figure LXXXIV : X-II-MFL ascending the 45-degree inclined launcher-fitting with (collapsed) MFL attached

The revised scripts were capable of properly guiding the X-II-MFL in and out of the launcher cutout, with the magnet-shoes fully collapsed, but still active (not shunted or magnets removed). There was no measurable or discernible 'magnetic-anchoring' observed, because again, (i) only a single point of contact is possible at any point in time with any of the shoe-poles, and (ii) the contact is one of rolling friction, and (iii) at most two shoes touch any edge of the cutout at this point in the transition, and (iv) the magnetic flux lines are very weak in the interstitial (free) space between the rolling shoe-poles. It is thus believed that the proposed shoe design, regardless of magnet-strength, is critical to avoiding 'magnetic-anchoring' for any obstacle-handling configuration.

5.3.4 Drawbar Pull Tests

- **METHOD**

  The drawbar pull tests were designed to test effects of the MFL configuration on the robot's towing strength. Four (4) configurations were tested: the expanded MFL configuration with (1) four drive modules active, (2) two drive modules active and (3) one drive module active, and the original X-II configuration with both of its drive modules active. The four (#1) and two (#2 and #4)) drive module trials took place in a 21-foot long 8-inch diameter pipe, while the single drive trial (#3) was tested in a 4-foot long 8-inch diameter pipe. In the single drive module test, the wheels were X-II's only points of contact with the pipe (no sensor).

  For each configuration, four deploy preloads were tested:
  - *relaxed preload, where not all wheels are in contact with the pipe, and*
  - *minimum,*
  - *medium and*
  - *maximum preloads.*

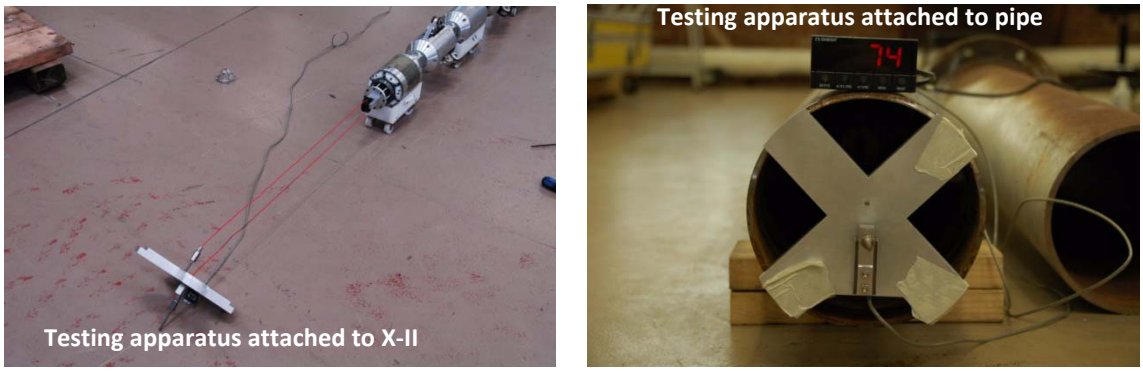

Figure LXXXV : Draw-bar pull test setup using a load-cell with a floating pulley and calibrated pull-force display

- **SETUP (SEE FIGURE LXXXV)**

  A harness was used to attach a pulley system to the rear of the robot (left image). This pulley system was then mounted to the pipe and a force transducer that read the force being exerted by the system (right image). Each trial would start with the force reading at 0. The relevant drive modules would then be commanded to drive at a given PWM current and the maximum stable force reading would be recorded. The process was repeated for each of the tested PWM settings, including 3%, 6%, 12%, 25%, 50% and 100% PWM (or percentage of full current command).

- **RESULTS**

  All testing showed that the presence of the MFL does not affect the achievable/required pull force. This is logical, since magnetic drag (electromotive or hysteretic loss) force increases with velocity. Since the MFL is stationary at the apex of the drawbar pull test, associated magnetic drag is expected to not be a factor.

  Comparison of maximum pull-force numerical results showed an expected correspondence of pull strength with preload and drive current. Increasing the preload force increased the friction force between wheels and the pipe wall, and so the robot could tow harder at the same PWM signal.

  For the entire system, with four drive modules engaged, a peak force of 368 lbs (@ maximum preload) was measured - see Figure LXXXVI on page 66. For two drive modules engaged, the peak measured force was 206 lbs (again @ maximum preload) -

Figure LXXXVII on page 66. The relationship is not quite linear, but is within 10% of the maximum measured tow-force.

These numbers are important in that they illustrate the tow-capacity of a two-/four-drive X-II platform as it relates to dragging a resisting-body through a pipe or around a corner. Hence MFL sensor-designers need to be aware of the limitations of single/dual/quad drive module configurations when designing the magnetic stages of their MFL sensor.

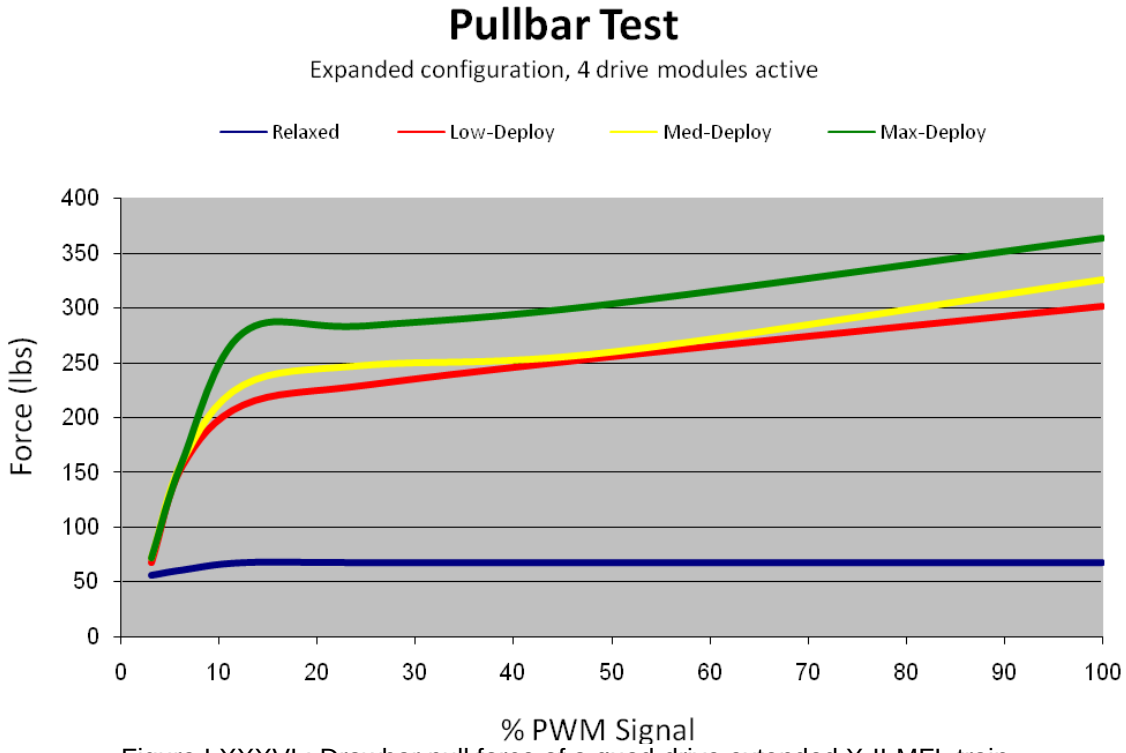

Figure LXXXVI : Drawbar pull force of a quad-drive extended X-II-MFL train

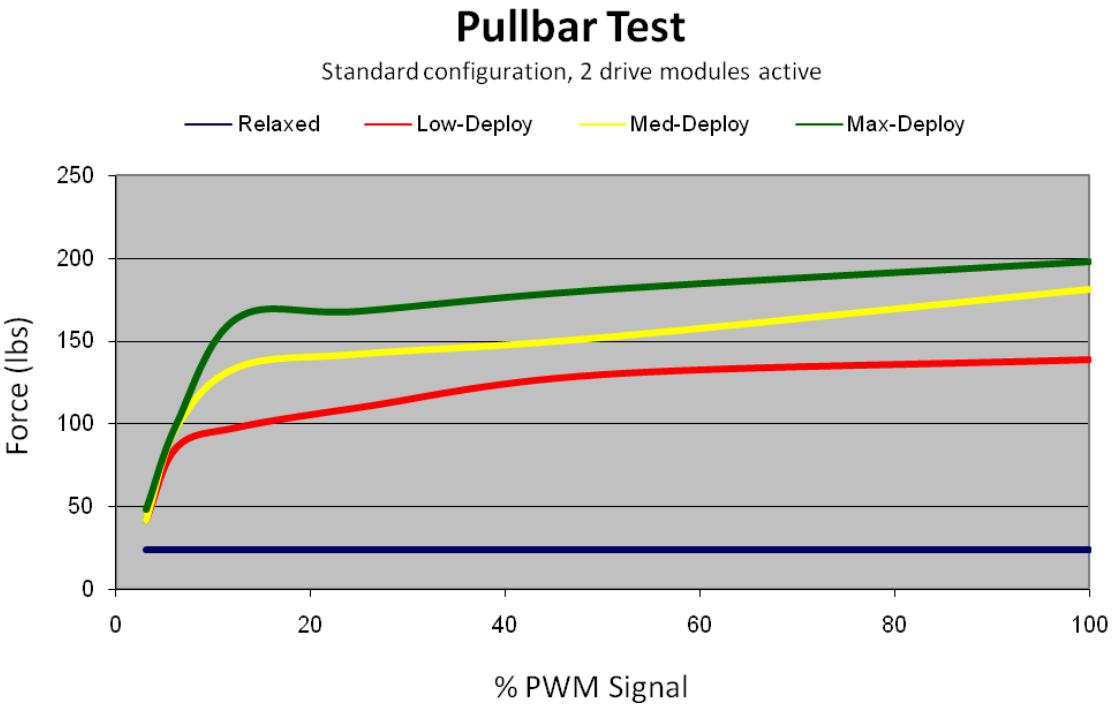

Figure LXXXVII : Drawbar pull force of a standard configuration dual-drive X-II train

A closer inspection of the data seems to indicate that driving the motors at 15% of full PWM command, results in roughly 75% of the ultimate tow-capacity for a given deployment. Beyond the 15% PWM threshold, the data trends are also linear but at a much less steep slope (see Figure LXXXVII).

For single drive drawbar pull tests, due to specifics of the test fixture used, relaxed deploy state did not produce enough traction with the pipe to yield meaningful data. Thus, only low, medium and max deploy states were tested. Results for this test were as expected, with the exception of max deploy test at ~100% PWM. Recall that the max pull strength collectively is 368 lbs. It is reasonable to expect an equal distribution among the drive modules contributing to yield roughly 90 lbs of linear pull force per module. However, 110 lbs was measured as the maximum pull strength for an individual drive module. These data are shown in Figure LXXXVIII.

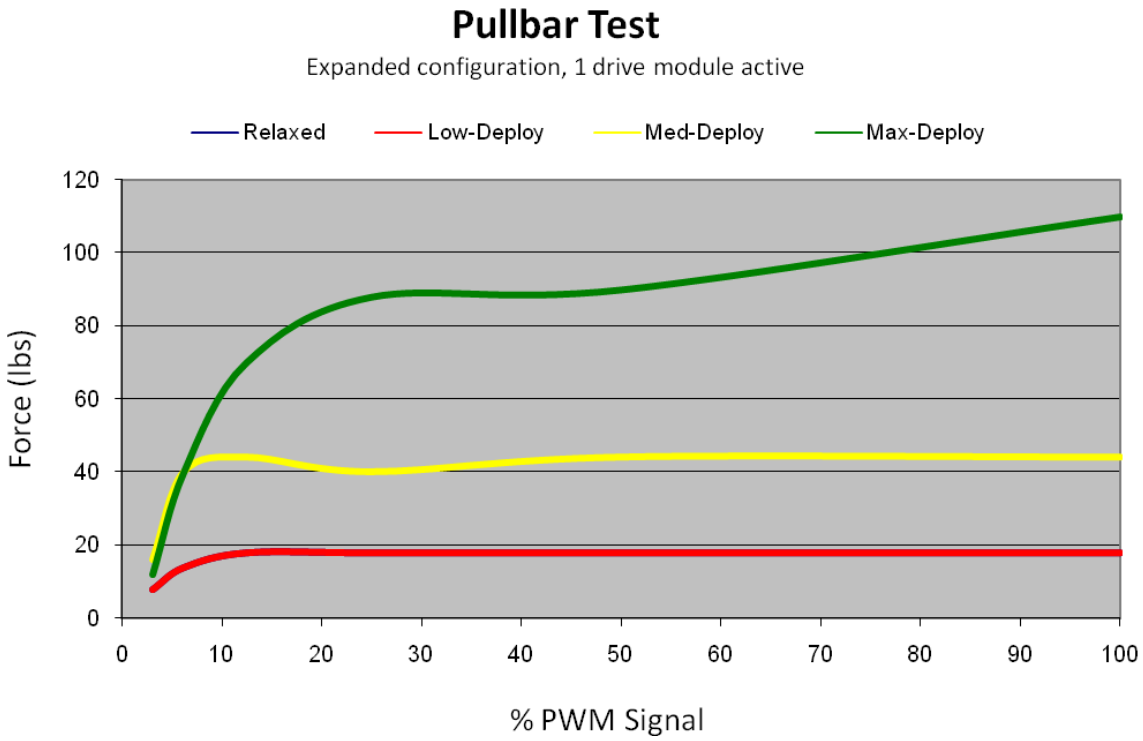

Figure LXXXVIII : Single-drive drawbar pull test-data for extended X-II-MFL train

Results for the expanded X-II-MFL configuration were also as expected. Peak pull force for the standard configuration was within 5% of that over the extended configuration with 2 modules driving.

An all encompassing plot for both the extended configuration (X-II-MFL) and the standard configuration (X-II) using two (2) drive-modules only, depicting drawbar-pull forces as a function of low-, medium- and maximum deploy forces, is shown in. Figure LXXXIX on page 68. This plot underscores the relationship of additional drive-modules to the achievable tow-force.

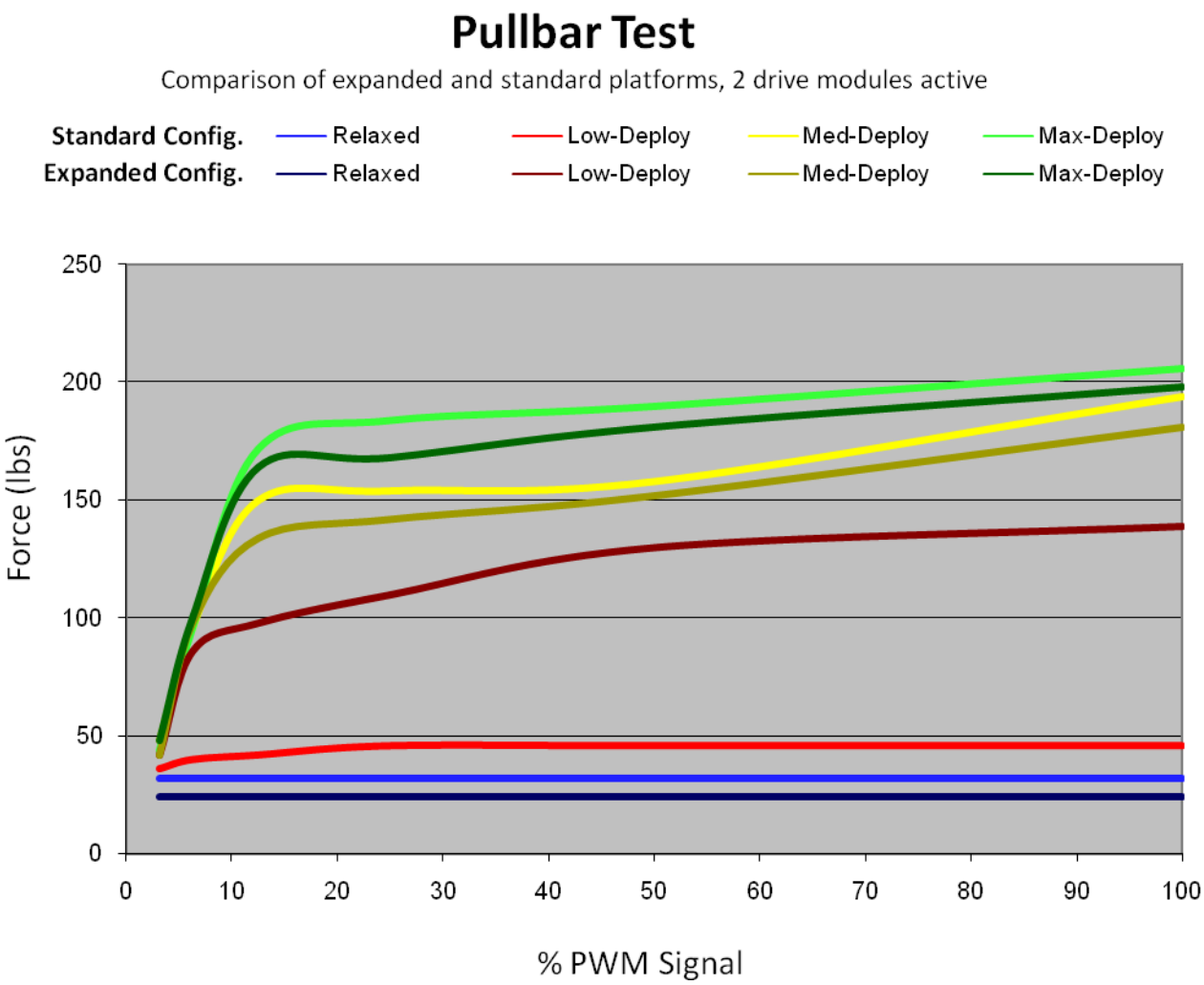

Figure LXXXIX : Drawbar pull forces generated by the standard/extended X-II/X-II-MFL train configurations as a function of low/medium/maximum drive-arm preload settings

5.4 Related experimental observation

The sensor shoe suspension mechanism was observed to sometimes get ‘stuck’ in a gap between bolted-together pipes, also known as a “negative” pipe seam. The shoe spring mechanism is pivoted so as to “follow” the pipe wall as the robot drives along. The leading end of the shoe will follow the pipe into the gap, and the shoe will pivot outward, hitting the next pipe edge-on. This is not expected to be an issue in seamlessly welded pipe, as there is typically a flat or even a pronounced weld-root due to weld-penetration. In lower-pressure (bolted) pipe-networks, the sensor-shoes have to be augmented with a simple skid on either side of the wheel to help the wheel straddle the gap and not dip into it beyond the theoretical wheel radius (well-known technique used in many other rolling sensor-designs).

5.5 Summary and Conclusions

based on the experimental program carried out and detailed in the previous subsections, CMU feels that the following conclusions can be drawn, as they relate to the different aspects of the sensor, train and performance that were being evaluated:

- **X-II SENSOR MODALITY MODULARITY**
  MFL sensor for X-II - Based on the X-II-MFL train design and prototype and the experimental data collected, it would seem readily feasible to state that an MFL sensor modality can be supported as a modular sensor in addition to the RFEC sensor, requiring additional drive/power (and associated steering/support modules) to achieve the desired performance. Careful attention will need to be paid to the sensor-design (see below) to achieve optimal operational performance.

- **SENSOR-DESIGN**
  Dual-module - The dual- module sensor design was maintained, allowing for a single module to house the sensing elements, and the second module to house all the data-collection and processing electronics. In the case of the MFL, the magnetic elements and the required articulation mechanism (incl. suspension) would need to be housed in a single module. The electronics for data-collection, post-processing, storage and interface to the on-board vehicle data-bus for wireless data-transmission would all be contained in the second module.
  Passive vs. shunted configuration - Based on the experimental data collected with the dummy MFL sensor-module, it would seem that the magnetic sensor-shoes would definitely need to be articulated to compress down for launch/recovery and obstacle passing maneuvers, but no magnet-shunting is necessary. This discovery is crucial, as it makes a small sensor-module design with magnets housed in shoes, and the needed articulation and suspension an achievable engineering effort, obviating the need for any additional shunting mechanisms[1].
  Shoe-design (wheels, yoke and flux-lines) - Additionally, it is critical for the magnetic shoe-design to force flux-lines through the magnet-stack and through the poles and into the pipe-walls, leaving only minimal flux between the carrier of the magnets and the opposing poles of the shoe. This is critical to avoid 'magnetic anchoring' during obstacle-handling maneuvers. Furthermore, we recommend that each of the poles be split and incorporate a knife-edged roller-wheel to guarantee standoff (minimal flux-gap), and include a ski to avoid the shoe from getting caught in negative gaps (pipe-joint seams, etc.).
  Shoe Articulation Design - The shoes should be mounted on a single-DoF (radial) suspension to allow them to freely follow the pipe (compliant in compression towards the center of the pipe. The articulation mechanism will need to be compact and strong enough to 'pry' the sensor-shoes off the wall during retraction motions. This will require the suspension system to be uni-directional, without any outward (only onward) radial compliance.
  Caveats (magnetic strength for full saturation) - CMU does not purport to be an expert (MFL-) sensor-design house. Hence we strongly recommend that whoever develops any future MFL-based sensor, repeat key experiments to characterize normal and linear

1. Such as those used in magnetic machinists dial-gauge stands and implemented for the larger MFL sensing head developed by Invodane, Inc. in Toronto in support of the TIGRE project jointly funded by the DoT (PHMSA) and NGA at Automatika, Inc. - see ***http://primis.phmsa.dot.gov/matrix/PrjHome.rdm?prj=160*** [37]

forces for the sensor and each of its articulated shoes, especially during expansion/ collapse, and testing of obstacle (launcher, elbow, T, mitre) passage performance.

- **TRAIN CONFIGURATION**

  Symmetry - The X-II design (see Figure XIX on page 11) has proven itself to be well suited to expansion to both reduce the length of the train (purely visual sensing scout platform - see bottom image in Figure XX on page 12), and/or increase the length of the train to allow for the addition of more traction-intensive sensing devices (MFL sensor carrier - see Figure XXXVI on page 25).

  Dual-module spread configuration - The symmetry of the platform allows for a dual module setup and should provide sufficient space for the sensing/activator and the electronics/processing/storage electronics dedicated to the sensor itself.

- **OBSTACLE-PASSING SCRIPTS**

  Launching/Recovery - The expanded and generic launch/recovery scripts have been adapted to allow for various-lengths/configurations of X-II and the X-II-MFL configuration. The approach and method remained the same and the validity and utility of the scripts was proven based on the multiple (12+) launch/recoveries that were performed without incident.

  Elbow-/T-passage - The expanded and generic launch/recovery scripts were also adapted to allow for various-lengths/configurations of X-II and the X-II-MFL configuration. The approach and method remained the same and the validity and utility of the scripts was proven based on the 20+ T/elbow passages that were successfully performed.

- **POWER CONSUMPTION**

  Correlation to speed and influence of contact-type - The MFL's influence on power-consumption was clearly correlated to travel-speed, which correlates to the hysteretic loss incurred due to the transverse magnetic resistance forces opposing train-travel, due to the induced changing (translating) magnetic field in the pipe-wall. Depending on the final magnet-strength, it will be important to verify that the battery-chemistry will be able to provide the current-draw (at a specified/maintainable voltage) required.

  Caveats (magnetic strength for full saturation related to power-draw) - The data that CMU collected was base don the strongest magnetic fields that were possible based on available OEM magnets and packaging volume. It will be important to verify the magnetic field requirements and perform a translational experiment at various speeds to verify the actual parasitic magnetic resistance forces, and their relationship to speed and dynamic longitudinal (along the along axis of the pipe in the direction of train-travel) forces.

VII. CONCLUSIONS

The X-II development and field-trial evaluation program has been completed and resulted in the development of a field-worthy prototype for use in visual and NDE inspection of live natural gas mains with pressures up to 750 psig. In order to provide a comprehensive summary of the programs' accomplishments and the conclusions drawn from the same, a bulleted list of topical areas and focus-elements has been provided below.

- **X-II SYSTEM DESIGN**

  Modularity - The X-II train design succeeded in implementing the by-module modularity required for effective reconfiguration and field-servicing. Any connectorized harnesses were replaced with contactor PCBs and modules keyed and held with 4 to 6 self-locking screws.

  Sensor Integration - The interfaces and pass-thru requirements as well as physical envelopes and weight restrictions were formulated and specified in an ICD, which was used by SwRI to develop the RFEC which was successfully built and interfaced into the platform for field-testing.

  Upgrades (CM, DM) - The drive-modules (DM) were designed as stand-alones and separated from the camera-modules (CM). The former have more rugged drive and deployment elements, allowing for towing longer and heavier trains. The latter is now a stand-alone camera- and dual (redundant) control computer unit, allowing it to collect video and transmit data wirelessly from either end. Both of the CMs are interconnected with wired ethernet (802.3) and talk to all microprocessors over an industry-standard CAN bus.

- **PROTOTYPE**

  Integration - The prototype was able to be readily integrated, given the ease with which each module could be assembled and tested in stand-alone mode. Given the presence, review and accuracy of the ICD, the sensor-modules were also successfully mated, electrically interconnected and respondent to the new software protocol and configuration software.

  Ruggedness (Drive, L&R, Obst.) - The X-II platform was tested exhaustively in outdoor test-loops and indoor obstacle mazes, including a launch/recovery fitting. X-II successfully completed several miles of driving and dozens of launches and recoveries (L&R), as well as dozens of successful elbow/T-turns. This endurance and ruggedness was essential to fine-tune scripts and prove readiness before going to field-trials.

  Software (Comms & Scripts) - The X-II platform proved to have far more reliable communications based on improved RF-gear (transceiver, antennae) and upgraded protocols, allowing it to achieve higher-gain communications. The scripts developed for the X-II platform were far more generic and easier to run and modify by the operator in real time, than was possible with X-I. The operator can now run them forward and reverse at will and jump to/from any point in the script, and adjust key variables, all on the fly, in order to deal with non-standard conditions in the pipe.

  Functionality (Acceptance) - The prototype was thoroughly tested and demonstrated to the corps of sponsors from DoE, NGA and also DoT (funders of the SwRI RFEC sensor). The system was demonstrated to perform all the launch/recovery, driving and real-time control and sensor-collection and -display functions as required in the performance requirements. The sponsor-team deemed the system ready and capable of field-use, which is an important milestone in any full-scale R&D program.

- **FIELD TESTING**

  Safety testing (Air, NG) - The X-II platform, launcher and controller were designed to be operable at 750 psig and in full immersion in natural gas (NG). The prototype was successfully tested in an air pressure-chamber to 750 psig, with all electronics operating properly and over prolonged periods, at this pressure. The safety procedures (evacuation, purging, etc.) in the launcher and the ability of the system to operate in NG environments to the same pressure was also tested and demonstrated successfully as part of the staircase testing efforts leading up to the field-trial.

  Field Trial - The X-II platform and launcher were demonstrated in a week-long field-trial on a pressurized live gas main in NW Pennsylvania. Despite some setbacks in installing the launcher and antenna weldolets, and a drive-failure on the robot, the system was rapidly repaired and logged multiple launches/recoveries (L&R) as well as ~1/2 mile of pipe-travel. Sensor data was collected successfully, but unforeseen pipe-joint obstacles made collection intermittent and incomplete, but successfully demonstrated the NDE capabilities of X-II.

- **SENSOR UPGRADE**

  MFL Sensor Design - The challenge of designing a mock-up MFL sensor was successfully carried out, by designing a sensor-module with articulating magnetic sensor-shoes with rolling contact and controlled flux-field. A suspension system was included to allow for pipe-following despite uneven surfaces and obstacles.

  Train Integration - The (non-powered) MFL sensor-module integrated seamlessly into the train and was successfully demonstrated to not impair the elongated trains ability to drive, launch/recover and the ability to handle elbows and Ts. The additional drive/ battery/steering/support modules required to lengthen the train to provide additional tow-force and battery endurance to not limit mission time given the parasitic magnetic forces, were also successfully integrated and tied into the control and communications backbone of the train and successfully controlled remotely and in real time off the improved GUI.

  Testing - The MFL sensing modality was shown to be feasible as an add-in sensor type for X-II. The concept of a carefully designed sensor-shoe and articulation, without the need for shunting to do launching and recoveries and elbow/T transitions, were the key outcomes of the test effort. The extended train configuration and preliminary mock MFL sensor were deemed critical in highlighting the key design-areas to watch for any commercial and expert (MFL) sensor design outfit, as part of the development effort for commercial sensor prototypes.

VIII. RECOMMENDATIONS

The design, laboratory experimentation and field-trial prototype evaluations for the X-II program were extremely successful. And as with any R&D program, there are always a set of recommendations and suggestions that are worth capturing for future refinement and development/ commercialization efforts. These have been drawn up in a comprehensive and structured manner, and are represented below in a bulleted and sub-itemized list.

- **X-II SYSTEM DESIGN & PROTOTYPE**

  Drivetrain (DM Gearing) - X-II was built as a single prototype, and as such gearing for the articulation and drive systems was based on OEM components that were pinned/ keyed to shafts, resulting in reduced strength and reliability. Any commercial effort should build all gearing with a user-specified material (rather than what can be gotten with precut OEM gears), and single-piece gear/shaft combinations cut from said material (avoiding all joining steps and issues associated with them). This step is considered essential and the increased price will be negligible if amortized over multiple robot units (in the case of a service company) and over time based on income from inspection jobs from (inter)national gas utility customers.

  Drive-Skis (Negative Pipe-Joint Seams) - We recommend adding some form of side-ski to the drive-wheels of the DM, in order to reduce the potential of them 'falling' into a pipe-joint gap such as is typical in bolted steel or jointed cast-iron pipes. X-II performed well in these case, as those are the conditions of the pipe-loop that NGA built and provided to CMU for testing, but field conditions may be more severe than those encountered in laboratory and field testing to date.

  Suspension Compliance (adjustable spring rate) - We recommend a longer suspension throw for the articulated triad arms for the Drive- and Support-Modules, as well as stiffer springs. The reason for this is the ability to overcome sizeable positive obstacles inside pipes, such as the weld-penetration weld-roots encountered in field-welded pipe installations, that may stall the train if high compression is applied and no throw remains in the suspension. This was the main cause of reduced NDE data gathering in the X-II field-trial, but represents a straightforward engineering solution to overcome these untested and unforeseen field conditions.

  External Programming Port - For the ease of upgrades and even development, it would be advisable to (i) provide an external programming port for the 32-bit CPUs in the Camera Module, and develop a robust CAN-based boot-loader to allow the wired (non-wireless) upgrade (and testing) of embedded 8- and 32-bit software on the robot train.

  Extended Launcher - In order to handle the extended X-II-MFL platform, it would be helpful if either (i) a longer launcher is developed for this configuration alone, or (ii) a generic longer launcher is built to handle any of the X-II configurations currently envisioned. This will be a decision the service-company will be making based on logistical concerns and financial investment.

- **ADDITIONAL TESTING**

  Welded Pipe-Loop Testing (Negative pipe-joint seams) - We recommend that a stand-alone loop of field-welded pipe be built to allow the testing of the ruggedized drivetrain and the increased suspension capability in the presence of positive (weld-seam) obstacles internal to the pipe.

  Upgraded Antenna Retention Mechanism (to suit TDW-tool) - The weldolet antenna needs to be slightly modified to allow for higher force exerted by the TDW installation/

retrieval tool, so as to successfully and positively set and recover the antenna using OEM tools and requiring little to no finesse by the operators.

Alternate (primarily shorter) train configurations - It would also be advisable to configure X-II in the different configurations alluded to in this report and test it for use in the field such as a video-scout for inspection of the pipe-run prior to performing the NDE run to be aware of any abnormal conditions within the pipe that might be concerning to the operator and/or service or utility company.

- **FIELD DEPLOYMENTS**

  Logistics and Pipe-Installations - It is recommended that field-crews receive more ample training in the installation and operation of the weld-on launcher and weldolet fittings, including drilling, cleanup and installation. The X-II field-trial was carried out with a standard field-crew which was not fully aware of all the intricacies of fitting installation and drilling when faced with launching and recovery of a robot train and antennae. It is presumed that the sublicensing commercial service provider would be well trained and capable of handling this task completely and properly.

  Cuttings Removal Tool - It is recommended that the cuttings left after the angled launcher- and vertical weldolet holes are drilled, be removed as best practically possible. Magnet-end rod-tools exist for the vertical fitting application, but it may be necessary to develop a simple articulated tool for the angled launcher fitting, to ensure as complete a cuttings-removal as possible. This will greatly reduce the chances of entrainment of metal-chips that could certainly impair any moving parts on the robot train and the sensor-module(s).

- **ALTERNATE MFL SENSOR DEVELOPMENT & TESTING**

  Sensor Design Considerations (Flux-shoe, Rolling contact, Articulation) - CMU recommends that careful attention be given to the design of any commercial MFL sensor, as it relates to the magnetic shoe design in terms of flux-field, the rolling-contact shoe-poles, its articulation and suspension.

  Pipe-Loop and -Obstacle Testing (Tow-, Elbow-/T-turn and L&R behaviors) - Any commercial MFL sensor prototype will need to be evaluated in terms of its measured magnetic tow-force (longitudinal) as well as its break-away force requirements for collapsing/expanding the shoes, and the passage of obstacles (elbows, Ts, launcher-holes), to ensure the avoidance/minimization of ‘magnetic anchoring’.

Overall we believe that the X-II platform design and prototype represent a commercially viable and innovative tool for the inline inspection requirements drafted by the DoT, that the gas utilities will have to abide by over the coming years. Given that the technology has been exclusively licensed to NGA, is a testament to the success of this development program, the maturity achieved for the technology incorporated in this system, and proof that government/industry partnerships are a successful means to drive technology to meet the needs of industry and abide by government imposed regulations aimed at public safety.

IX. ACKNOWLEDGEMENTS

The design of Explorer-II has been made possible via a cooperative research agreement to CMU, funded by NETL/DoE (DE-FC26-04-NT42264) and co-funded by NGA (Contract # M2003-009).

X. REFERENCES

[1] Ives, G., Jr., "Pipe Ruptures", PipeLine & Gas Industry Journal, Vol. 83, No.9, Houston, TX

[2] Staff Report, "New Optical methane detector improves gas leak surveys", PipeLine & Gas Industry Journal, September 2000

[3] Porter, C., Pittard, G., "Magnetic Flux Leakage Technology for Inspecting 'Live' Gas-Distribution Mains", GTI Technical Report # GRI-99/0199, Oct. 1999, Chicago, IL

[4] Schempf, et al., "Robotic Repair System for Live Distribution Gasmains", Field and Service Robotics Conference., FSR 2001, June 11 - 13, Helsinki, Finland.

[5] *Guidance Manual for Operators of Small Natural Gas Systems*, US Department of Transportation, Research and Special Programs Administration, August 1997.

[6] Schempf, et al., "*GRISLEE*: Gasmain Repair and Inspection System for Live Entry Environments", IEEE International Journal of Robotic Research, pending publication in 2004.

[7] Schempf, H. and Vradis, G., "*Explorer: Long-Range Untethered Real-Time Live Gas Main Inspection System"*, Natural Gas Technologies II Conference, Feb. 8 - 11, 2004, Phoenix, AZ

[8] Cremer, C. D., and D.T. Kendrick. "*Case Studies of Uses of the Pipe Explorer™ System*", Spectrum '98, International Conference on Decommissioning and Decontamination and on Nuclear and Hazardous Waste Management, Denver, CO, September 13-18, 1998.

[9] www.pearpoint.com

[10] KaTe System AG; http://www.ka-te-system.com/html/homee.html

[11] http://www.foster-miller.com/t_robotics.htm

[12] "*GRISLEE: Gasmain Repair & Inspection System for Live Entry Environments*", CLAWAR'01 Special Issue of the International Journal of Robotics Research, March-April, 2003, Vol. 22, Nos 3 and 4.

[13] "*Explorer: Untethered Real-time Gas Main Assessment Robot System*", 1st International Workshop on Advances in Service Robotics, ASER'03, Bardolino, Italy, March 13-15, 2003

[14] http://www.ariesind.com/gascam.html

[15] http://itrobotics.ath.cx/Products/Products.htm

[16] http://www.advantica.biz/

[17] http://www.ulcrobotics.com/

[18] http://www.maurertechnology.com/Engr/Products/MFL.asp

[19] www.netl.doe.gov/scngo/Reference%20Shelf/ tsa/tsa-videoinspect-0202_1.PDF

[20] www.bakerhughes.com/pmg

[21] CISBOT - Company: ConEd – Enbridge Product: Cisbot: Contact: Terry Whitehead, Enbridge Contact Phone Number: 416-496-7147

[22] http://www.nygas.org/M-2002-015.htm

[23] http://www.welltractor.com/

[24] "Method and System for moving equipment into and through an underground well", Pat.# 6,675,888

[25] http://www.bakerhughes.com/bot/service_tools/index.htm

[26] www.tdwilliamson.com

[27] www.roseninspection.net

[28] http://www.gepower.com/prod_serv/serv/pipeline/en/index.htm

[29] www.blackhawk-pas.com

[30] http://www.ais.fraunhofer.de/BAR/kurt.htm

[31] http://www.netl.doe.gov/publications/press/2004/tl_oilgas_bbfa.html

[32] http://www.netl.doe.gov/scngo/Natural%20Gas/Projects_n/TD&S/T&D/T&D_C_41645RobotPlatform.html

[33] Gary L. Burkhardt and Alfred E. Crouch, "Remote-Field Eddy Current Sensing for Inspection of Gas Distribution Piping," *ASNT 15th Annual Research Symposium2006 Paper Summaries CD-ROM*, Orlando, Florida, March 13-17, 2006.

[34] Gary L. Burkhardt and Alfred E. Crouch, "Remote-Field Eddy Current Inspection System for Small-Diameter Unpiggable Pipelines," *Proceedings of The Pipeline Pigging and Integrity Management Conference*, Houston, Texas, February 14-15, 2007.

[35] Gary L. Burkhardt, Albert J. Parvin, Ronald H. Peterson, Richard F. Tennis, and Todd H. Goyen, "Remote-Field Eddy Current Inspection System for Small-Diameter Unpiggable Pipelines," *ASNT's International Chemical and Petroleum Industry Inspection Technology (ICPIIT) X Conference Paper Summaries Book*, Houston, Texas, June 20-23, 2007.

[36] Gary L. Burkhardt, "Remote-Field Eddy Current Inspection System for Small-Diameter Unpiggable Pipelines,"

Technology Today, SwRI Quarterly Magazine, San Antonio, Texas, Winter 2007, pp.2-5.

[37] TIGRE Research Project co-funded by DoT-PHMSA and NGA - only official public information release site: ***http://primis.phmsa.dot.gov/matrix/PrjHome.rdm?prj=160***

XXXVIII. APPENDICES

1.0 Gas Pipeline Robot State-of-the-Art Review

1.1 Introduction - Pipe Robots

Internal pipe inspection and maintenance are not new concepts in such industries as sewer and water maintenance as well as transmission pipelines for oil and gas. Such systems typically are an integration of mechanical, electrical and software subsystems, supporting one or more sensory payloads for measuring the pipe's overall state and structural integrity (corrosion, ovality, etc.). One of the main subsystems in such inspection systems is the locomotor or mobile platform that carries the sensing and explorative end of the tool. This is the area this report will focus on as part of the state-of-the-art review contained in this report, by illustrating technical advances and deficiencies, by way of seminal platform examples (whether fielded, prototypes or in the design-stage). The intent will be to help support technology-developers and decision-makers in understanding how and where to provide technology innovation and where to allocate ones resources to see technical advances realized.

1.2 Background

The above-mentioned application-areas are discussed in brief detail below by way of an overview and a few of the salient examples and a comparative table condensing the comparative descriptors that one might use into a single graspable location. There are however substantial differences and presumptions that will remain to be clarified in order to understand the gradation in terms of capabilities and applications in this arena.

1.2.1 Water and Sewer Mains

This area is not intended to be elaborated on in any depth as part of this report. It is however worth noting that in-pipe robots, mostly self-powered units, have and are seeing their largest volume applications in this arena. All of these systems rely on a power- and (push-)pull tether to provide power and communications to the robot, and return information to the user. Most of this information is raw video-data, but can also include acoustic as well as laser-caliper dimensioning data. Efforts have been made in the past to also make these systems more autonomous by providing on-board battery power and 'cutting' the tether and relying on on-board smart software and guidance/navigation/imaging sensors to handle in-pipe locomotion decisions. However, due to the bulk and shear linear footage of water- and sewer-pipes in the world, and the relatively low barrier to entry (cost, operational infrastructure and relatively low operational hazard-level), this industry has seen substantial growth in the last decade and will continue to be the largest market for in-pipe robots in terms of revenue for near foreseeable future.

Some of the more salient images of the state-of-the-art in water and sewer pipe inspection and repair systems are depicted in the figure below:

BlackHawk

Beaver

Pearpoint

KA-TE

1.2.2 Oil- and Gas Pipelines

This application area has seen substantial work in the past 20 years. Most of the past and current effort has focussed on using passive flow-powered (pigs) platforms to carry an ever-improving array of sensors for integrity evaluation. New efforts in the past few years has begun to also look at actively powered platforms to access the unpiggable sections of these transmission mains. Both of these areas are covered further below.

1.2.2.1 Transmission Mains - Pipe Pigs

There are basically two types of pipe pigs; the simple mechanical version that is used for cleaning and flow passage surveys; and the more complex version that integrates the basic platform with other sensor-based elements intended for pipe inspection. These elements range from simple mechanical calipers to advanced electronics to optical based data storage. The evolution of the sensor-based platforms has resulted in a family of inspection tools commonly referred to as *Smart Pigs*. The simple mechanical pig is basically a piston moving through the pipe, being powered by the fluid flow and the associated pressure drop across the seals. Pigs require the internal pipe diameter to remain relatively constant and the pipe runs to be straight or only gradually curving to guarantee ‘safe’ passage. Since current sensor technologies accuracy depends on surface cleanliness (mostly), cleaning is accomplished through the mounting of bristle brushes and/or the use of hardened surfaces around the circumference of the pressure seals. The use of these types of pigs does require a means for removing the debris that accumulates in front of the pig as it moves through the pipeline; that is why an inspection run is typically preceded by one or cleaning-pig runs. A modern Smart pig is quite sophisticated in both configuration and inspection capability. Smart pigs include on-board power supplies, data recorders and storage, and sophisticated NDE sensors to measure pipe wall defects. Magnetic flux leakage (MFL) has been the most popular NDE technique employed on pigs. However, ultrasonic, eddy current and acoustic sensors are also commercially available for Smart pigs. A collection of such cleaning and sensing pigs offered by the industry leaders[1], are depicted in the figure below:

There are many physical obstacles within typical transmission pipelines that have (in the past) curtailed and/or restricted the use of these Smart pigs, many of which have seen technology improvements over the years. Despite these advances though, many deficiencies (physical and flow obstacles) remain with the current technology that will prevent the use of these devices in many miles of existing transmission pipelines, especially those belonging to local gas distribution companies.

1. Integrated Full-Service Companies: Rosen, TDW, GE/PII, TuboScope, Baker-Hughes, CPIG, InvoDane, Enduro, etc.

1.2.2.2 Oil- and Gas-Wells - Tethered & Autonomous Robots

The use of robots to perform downhole operations (E&P: Exploration & Production - whether oil or gas wells) has been under consideration for about 10 years. Existing pieces of equipment are exclusively tethered by slickline (simple cable) or coiled-tubing deployed. There are hybrids such as the WellTec system that is powered over a cable, and the iTRobotics system which is autonomous but is only used for inspections of coiled-tubing itself. Prototypes such as Shell's Bore-shuttle and Baker-Hughes downhole robot do exist but have not yet seen full commercialization - these systems have no link to the surface and operate completely autonomously and using on-board power while travelling up and down the casing in an oil/gas well. Images of these systems are shown in the figure below:

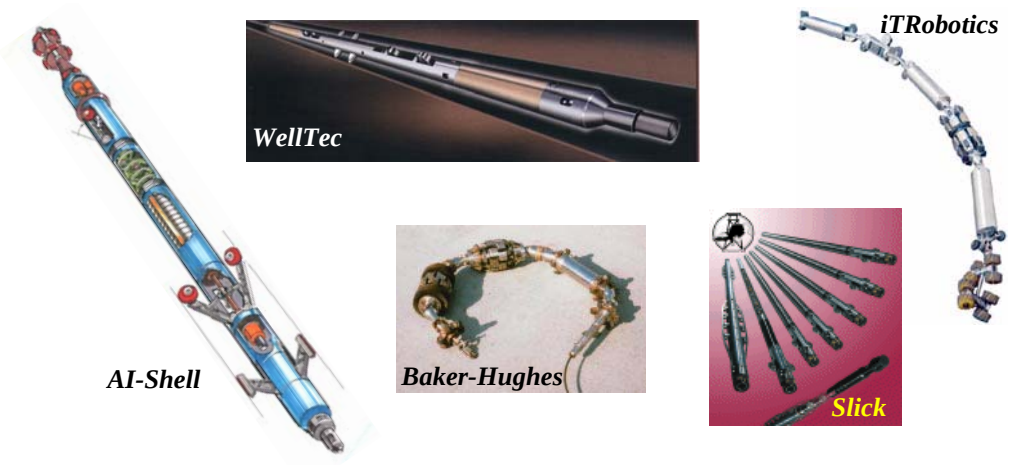

1.2.2.3 Distribution Mains - Stick-Cameras

In terms of systems that have been used in live gas mains, particularly lower-pressure (< 100 psig) distribution mains, only a few video-inspection systems have come to the commercial market. they are able to be pushed/pulled into place using a tensile/power/data cable and are launched into a live main using specialty fittings and deployment systems. They provide only video but are commonly used for rapid inspection of critical/emergency areas. They vary in size, but the inspection-diameters of the pipes in question range from 4 to 10 inches in diameter and are almost exclusively in use in the natural gas industry. Three of the main systems in use today are depicted in the image below:

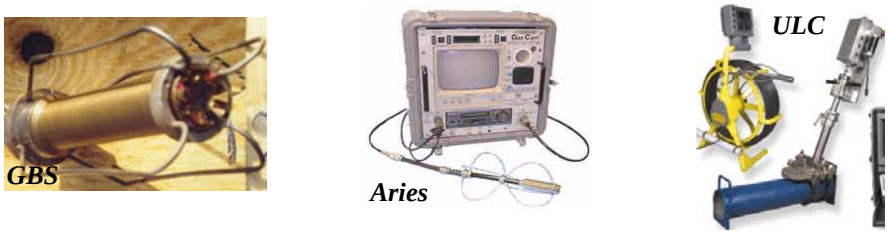

1.2.2.4 Distribution Mains - Pipe Crawlers

In the application of lower-pressure distribution mains for natural gas, several systems have been prototyped and fewer deployed for real-world inspection and repair in live natural gas mains. These

systems are characterized by both tetherless and tethered operations over substantial long distances under live conditions. Advantica (R&D division of British gas) demonstrated the ability to perform RFEC inspection of steel pipes with a segmented robot, yet it has not yet been field-hardened. The FM PipeMouse is a tethered inspection system capable of traversing sharp geometries, yet it never was field-deployed. Explorer is the first robot to perform truly untethered real-time video inspection of live gas mains in real time while also being capable of traversing bends, Ts, junctions and vertical pipe-sections. A collage of these inspection systems is given in the figure below:

Advantica

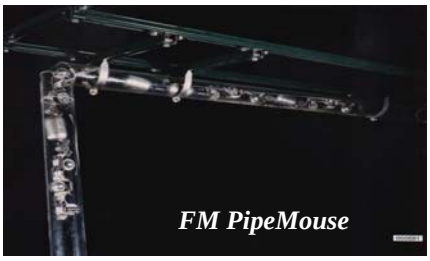

FM PipeMouse

Explorer

Other existing systems in use by the gas distribution industry revolve around pipe-inspection and repair. The two most notable ones are CISBOT and GRISLEE. The former is a tethered system capable of inspecting and repairing (via sealant-injection) cast-iron bell-and-spigot joints. The latter is a modular system to perform a visual and NDE MFL inspection, and perform an in-situ repair using composite repair sleeves - all while being deployed into and out of a main under live conditions using a coiled-tubing push-pull tether with internal power and data conductors. These two systems are depicted below:

CISBOT

GRISLEE

1.2.2.5 Other applications

Another noteworthy locomotion platform under development is the revival of the PipeMouse as the RoboScan platform for use in unpiggable transmission mains. This system will be self-powered and using autonomous control, while it scans the large-diameter transmission main for pipe-wall degradation using NDE sensor technologies.

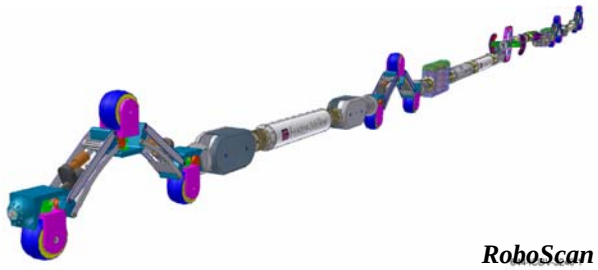

RoboScan

1.3 Platform Comparison

The comparison-table depicted on the next page, attempts to provide detail on the different platforms locomotion characteristics as well as provide common and differentiating features amongst them.

In terms of pure locomotion, it seems clear that there are fully-tethered short-range system-solutions, as well as (mostly) untethered long-range systems capable of both video as well as NDE (development only) inspection. For those systems where power is provided on-board, using rolling locomotion is a clear preference. There seem to be different approaches to provide for traction but all rely on compressive-force against the pipe. Different geometries to achieve pipe-adaptation have been implemented, as well as different types of articulation and steering joints, all the way from purely passive, to fully articulated/powered. Geometries are clearly pipe-diameter dependent, as well as what types of obstacles they need to be able to handle such as sharp bends, elbows, plug-valves, etc. With the exception of one, all systems provide for real-time data through a dedicated copper or fiber-link/-tether. Even though on the drawing-board, there seems to be a clear lack of long-range inspection capability for both small and large diameter pipe-sizes under low and high pressure conditions, utilizing more than just video inspection but also coupling it with NDE-inspection.

To achieve inspection-ranges in the miles and perform the inspection in real time and under teleoperated or supervised/autonomous fashion, will require technology advancement in key areas such as battery-power and -recharge, communications, sensor-miniaturization and reliable control/autonomy software. The platform geometries and ability to locomote provides for different solutions which are typically driven by geometrical constraints as well as innovative preference depending on the development outfit as well as any relevant real-world deployment experience they may have accumulated over time - there is however no substantially superior architecture, locomotion or integration design that has yet been proven through field-deployments to be superior to its competitors, the main reasons being a real lack of competing varieties of platforms as well as a lack of real-world deployment data for all existing platforms or those still under development.

MARKET	CATEGORY	SYSTEM	SUPPLIER OR VENDOR	Pipe Market Segment [1]	Technology Maturity [2]	Design Architecture [3]	Obstacle Handling [4]	Locomotion Mode/Type [in]	Repair Capability [Y/N]	Inspection Capability [Y/N]	Sensor Type(s) [6]	Tethered [Y/N]	Power & Comms Type [7]	Range per launch [ft]
Civil Infrastructure	*Water / Sewer Mains*	***Various*** BlackHawk, PearPoint, Beaver, KA-TE, Innuktun, etc.	Many - see previous	W/S	Comm	M, O	SPO, MC	FW, FT, PPT	Y	Y	V, UT	Y	LV, TL	< 200
Pipelines	*Pigs*	***Various*** Rosen, GE/PII, TDW, TuboScope, CPIG, B.Hughes, Halliburton, Enduro, etc.	Many - see previous	GT	Comm	M, S	SPO, MC, TSB	FP	N	Y	All; no V	N	BS, NL	Miles
Exploration & Production (E&P)	*Oil & Gas Wells*	Bore-Shuttle	AI/Shell	E&P	Prot	M	SPO, MC	FP, AW	N	Y	TBD; no V	N	BS, A	Miles
		Slick-Tool	BakerHughes	E&P	Comm	S	SPO, MC	PPT	N	Y	MFL, EC	Y	LV	Miles
		WellTractor	WellTec	E&P	Comm	M	SPO, MC	AW, PPT	N	Y	O	Y	LV, TL	Miles
		WellBot	iR/Halliburton	E&P	Field	M,S	SPO, MC	FW	N	Y	U	N	BS, A	U
	Coiled-Tube	InspectorBot	iTRobotics	E&P	Field	S	SPO, MC	FW	N	Y	MFL, EC	N	LV, NL	Mile+, U
Gas Pipelines	*Pipe-Cameras*	PipeCam	GBS	GD	Comm	M	SPO	PPT	N	Y	V	Y	LV, TL	<1000
		GasCam	Aries	GD	Comm	M	SPO, MC	PPT	N	Y	V	Y	LV, TL	<200
		HP Gas Camera	ULC	GD	Comm	M	SPO, MC	PPT	N	Y	V	Y	LV, TL	<200
	Pipe-Crawlers	RFEC Inspector	Advantica	GD	Field	S	SPO, MC	FW	N	Y	EC	N	BS, U	U
		PipeMouse	FosterMiller	GD	Prot	S	All; no V	AW	N	Y	V	Y	BS, TL	U
		Explorer	CMU/NGA	GD	Field	S	All	AW	N	Y	V	N	BS, W	>1000
		CISBOT	ConEd	GD	Comm	M	SPO, MC	PPT	Y	Y	V	Y	LV, TL	<250
		GRISLEE	CMU/MEI/GTI	GD	Field	S	SPO, MC	PPT	Y	Y	MFL, V	Y	LV, TL	<1000
		RoboScan	FM/NGA/DoE	GT	CAD	S	U	AW	N	Y	TBD	U	BS, TL	U

1 Water (**W**), Sewer (**S**), Gas Distribution (**GD**), Gas Transmission (**GT**)
2 **CAD** (Low), **Prot**otype (Lab only), **Field**ed (Real-world Proven), **Comm**ercial (Mature, Reliable & Cash-Generator)
3 Monolithic (**M**), Segmented (**S**), Other (**O**)
4 Straight-Pipe-Only (**SPO**), Minimal Curvature (**MC**), Tights Smooth Bends (**TSB**), Sharp bends Elbows and Ts (**SBET**), Verticals (**V**)
5 Flow-Pressure (**FP**), Fixed-Wheel Crawler (**FW**), Fixed-Tracked (**FT**), Articulated-Wheel (**AW**), Push-Pull-Tether (**PPT**)
6 Video (**V**), Ultrasonic (**UT**), Magnetic Flux Leakage (**MFL**), RF Eddy Current (**EC**), **EMAT,** Caliper-Tool (**CT**), Other (**O**), Unknown (**U**), **TBD**
7 POWER: Line-Voltage (**LV**), Battery Supply (**BS**) COMMS: Tether-Link (**TL**), Wireless (**W**), Autonomous (**A**), No-Link (**NL**)

1.4 References

4. **www.pearpoint.com**
5. **KaTe System AG; http://www.ka-te-system.com/html/homee.html**
6. **http://www.foster-miller.com/t_robotics.htm**
7. ***"GRISLEE: Gasmain Repair & Inspection System for Live Entry Environments", CLAWAR'01 Special Issue of the International Journal of Robotics Research, March-April, 2003, Vol. 22, Nos 3 and 4.***
8. ***"Explorer: Untethered Real_time Gas Main Assessment Robot System", 1st International Workshop on Advances in Service Robotics, ASER'03, Bardolino, Italy, March 13-15, 2003***
9. **http://www.ariesind.com/gascam.html**
10. **http://itrobotics.ath.cx/Products/Products.htm**
11. **http://www.advantica.biz/**
12. **http://www.ulcrobotics.com/**
13. **http://www.maurertechnology.com/Engr/Products/MFL.asp**
14. **www.netl.doe.gov/scngo/Reference%20Shelf/ tsa/tsa-videoinspect-0202_1.PDF**
15. **www.bakerhughes.com/pmg**
16. **CISBOT - Company: ConEd – Enbridge Product: Cisbot: Contact: Terry Whitehead, Enbridge Contact Phone Number: 416-496-7147**
17. **http://www.nygas.org/M-2002-015.htm**
18. **http://www.welltractor.com/**
19. **"Method and System for moving equipment into and through an underground well", Pat.# 6,675,888**
20. **http://www.bakerhughes.com/bot/service_tools/index.htm**
21. **www.tdwilliamson.com**
22. **www.roseninspection.net**
23. **http://www.gepower.com/prod_serv/serv/pipeline/en/index.htm**
24. **www.blackhawk-pas.com**
25. **http://www.ais.fraunhofer.de/BAR/kurt.htm**
26. **http://www.netl.doe.gov/publications/press/2004/tl_oilgas_bbfa.html**
27. **http://www.netl.doe.gov/scngo/Natural%20Gas/Projects_n/TD&S/T&D/ T&D_C_41645RobotPlatform.html**

National Energy Technology Laboratory

626 Cochrans Mill Road
P.O. Box 10940
Pittsburgh, PA 15236-0940

3610 Collins Ferry Road
P.O. Box 880
Morgantown, WV 26507-0880

One West Third Street, Suite 1400
Tulsa, OK 74103-3519

1450 Queen Avenue SW
Albany, OR 97321-2198

2175 University Ave. South
Suite 201
Fairbanks, AK 99709

Visit the NETL website at:
www.netl.doe.gov

Customer Service:
1-800-553-7681